Dissertation

zur Erlangung des Doktorgrades der Fakultät für Chemie und Pharmazie

der Ludwig-Maximilians-Universität München

The impact of transcription inhibition during maturation on the oocyte proteome

Katrin Doris Gegenfurtner

(geb. Meyer)

aus

Nürnberg, Deutschland

2019

Dissertation

zur Erlangung des Doktorgrades der Fakultät für Chemie und Pharmazie

der Ludwig-Maximilians-Universität München

The impact of transcription inhibition during maturation on the oocyte proteome

Katrin Doris Gegenfurtner

(geb. Meyer)

aus

Nürnberg, Deutschland

2019

Erklärung

Diese Dissertation wurde im Sinne von §7 der Promotionsordnung vom 28. November 2011 von Frau Prof. Dr. Angelika M. Vollmar betreut.

Eidesstattliche Versicherung

Diese Dissertation wurde eigenständig und ohne unerlaubte Hilfe erarbeitet.

München, den 29.10.2019

_____

Katrin Gegenfurtner

Dissertation eingereicht am:	04. November 2019
Erstes Gutachten:	Prof. Dr. Angelika M. Vollmar
Zweites Gutachten:	Prof. Dr. Eckhard Wolf
Mündliche Prüfung am:	03. Dezember 2019

Meinen Eltern

Table of contents

Summary

Main project: Inhibition of transcription during *in vitro* maturation of bovine oocytes

The release of a mature oocyte from the ovary is a prerequisite for successful reproduction. In the bovine, oocytes are arrested in prophase I prior to ovulation. Completion of oocyte meiosis and the first embryonic cleavages are under the control of maternal gene products. Maternal transcripts and proteins are accumulated and stored during oogenesis and gradually depleted until the embryonic genome activation

To assess the impact of transcription inhibition during maturation on the protein composition of the oocytes, a holistic proteomic analysis of GV oocytes and MII oocytes matured with or without the presence of actinomycin D (ActD) was performed. Using a label-free LC-MS/MS-based approach, substantial quantitative proteomic changes were identified between mature and immature oocytes, as well as due to inhibition of transcription. Bioinformatic analysis of this set of proteins was carried out using DAVID gene ontology (GO) and gene set enrichment analysis (GSEA) to gain insight into the related biological processes and molecular functions. Among the enriched gene sets in MII control compared to GV are GO terms related to cell cycle and RNA processing, reflecting the progression of meiosis and the importance of protein synthesis during maturation.

Proteins increased or decreased after maturation irrespective of ActD-treatment were determined and related biological processes independent of *de novo* transcription were identified. Beside cell cycle-related proteins, proteins that increase despite the absence of transcription were found to be involved in the organization of cellular components, which is crucial for cytoplasmic maturation. On the contrary, *de novo* transcription-dependent proteins were associated with cell-cell adhesion and translation. As the high degree of protein synthesis has been shown to be related with good developmental competence, this indicates the disturbed maturation in the presence of ActD. Thus, the study provides new insights into the protein profiles before and after maturation and indicates that *de novo* transcription is absolutely essential for successful maturation

Side projects: Bovine reproductive fluids in high-yielding dairy cows

Concomitant with intensive selection for increased milk yield, reproductive performance of dairy cows has declined in recent decades, in part due to an unfavorable genetic relationship between these traits. The causes of this decline in reproductive success are multi-factorial with higher milk yield being shown to have an inverse relationship with the pregnancy rates observed in dairy cows. Early embryonic loss is a major cause of this reduced pregnancy rate. Successful fertilization, implantation and establishment of pregnancy is dependent on good quality embryos, an appropriate oviductal and endometrial environment, and the successful interaction between the embryo and the endometrium. Within the FECUND project, two animal models have been created to study the effect of two conditions with adverse impact on the reproductive performance, a different genetic merit for fertility, i.e. cows with distinct reproductive traits and a different metabolic status of the animal (post-partum metabolic stress) on reproductive tissues and fluids.

A) Metabolic disturbance model

Maiden heifer **(MH)**
Postpartum lactating cow **(Lact)**
Postpartum non-lactating cow **(Dry)**
all Holstein-Friesian

B) Genetic merit model

High fertility Holstein heifers **(HFH)**
Low fertility Holstein heifers **(LFH)**

Montbéliarde heifers **(MBD)**

Side project A: Proteomic analysis of uterine luminal fluid in pregnant cows

To study the effect of genetic merit for fertility on the proteome of the uterine luminal fluid (ULF), Holstein heifers with low (LFH) and high fertility (HFH) index and heifers from the Montbéliarde breed (MBD), known to have good reproductive performance, were investigated. To focus on the maternal effect, heifers from all three groups were synchronized and received on Day 7 high-quality embryos from superovulated and artificially inseminated MBD donors. ULF from Day 19 pregnant heifers was analyzed in a holistic proteomic approach using nano-LC-MS/MS analysis combined with a label-free quantification approach. In total, 1,737 proteins were identified, of which 597 were found to differ significantly in abundance between the three groups. The majority of proteome differences in ULF samples was found comparing the HFH and MBD groups to the LFH group, showing that the genetic predisposition for fertility is prevalent regarding the ULF protein composition. Evaluation of this dataset using bioinformatic tools comprising DAVID gene ontology and gene set enrichment analysis revealed that higher abundant proteins in the LFH group are assigned to several metabolic processes as well as the immune response. Our study unveiled that the genetic merit for fertility leads to substantial quantitative differences at the level of proteins in uterine fluid of pregnant animals, thus altering the microenvironment for the early conceptus.

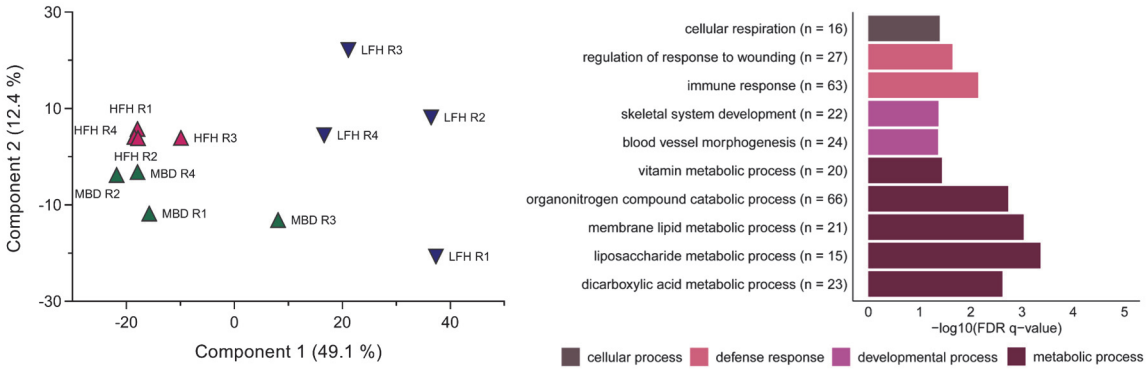

Side project B: Proteomic analysis of bovine oviduct fluid

The oviduct plays a crucial role in fertilization and early embryo development providing the microenvironment for oocyte, spermatozoa, and early embryo. Analyzing two animal models, this study aimed to investigate the impact of genetic predisposition for fertility as well as of metabolic stress on the protein composition of oviduct fluid (OF). The metabolic model comprised maiden Holstein heifers (MH) and postpartum lactating (Lact) and non-lactating (Dry) cows, while the genetic model consisted of heifers from the Montbéliarde (MBD) breed and Holstein heifers with low (LFH) and high (HFH) fertility index. Holistic proteomic analysis of OF from all groups using nano-LC-MS/MS analysis and label-free quantification led to the identification of 1637 proteins, amongst which 128 showed abundance alterations in the pairwise comparisons within both models. Most differentially abundant proteins were revealed between LFH and MBD (52) in the genetic model and between Lact and MH (19) in the metabolic model, demonstrating a substantial effect of genetic predisposition for fertility as well as of metabolic stress on the OF proteome. Functional classification of affected proteins revealed actin binding, translation and immune system processes as prominent GO clusters. Notably, actin-related protein 2/3 complex subunit 1B (ARPC1B) and the three immune system-related proteins SERPIND1, IGK protein and alpha-1-acid glycoprotein (AGP) were affected in both models, suggesting that abundance changes of immune-related proteins in OF play an important role for early embryonic loss.

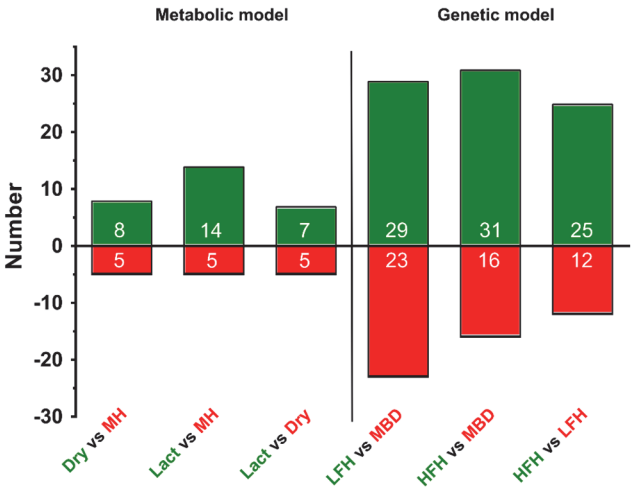

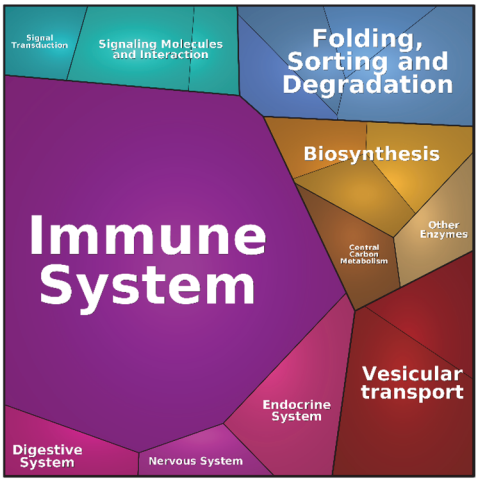

1 Introduction

1.1 Early mammalian development

One of the major drawbacks for reproductive success in mammals are disturbances in ovulation, fertilization and early embryonic development. At prenatal age, oocytes begin to develop in the ovaries until maturation is arrested at the late fetal stage and resumption of oocyte meiosis is only resumed after the first menstrual or estrus cycle, regarding humans and primates or non-primate mammals, respectively. In monovulatory species – like bovine and human - this resumption of maturation is caused in response to the gonadotropin luteinizing hormone (LH) and leads to release of the mature metaphase II (MII) oocyte into the infundibulum of the oviduct, which connects the ovary and the uterus. In humans, ovulation is induced at approximately Day 14 of the menstrual cycle, while in cattle, estrus is referred to as Day 0 and marks the receptiveness of the female. Contemporaneously with LH, follicle-stimulating hormone (FSH) levels reach their peak and exhibit a synergistic action (*1*). Elevated estrogen levels result in the hypothalamic secretion of gonadotropin-releasing hormone from the pituitary gland, subsequently triggering FSH and LH release. In humans, the ensuing luteal phase is characterized by progesterone secretions of the corpus luteum (CL), which stimulates endometrial growth in preparation of the implantation of an embryo.

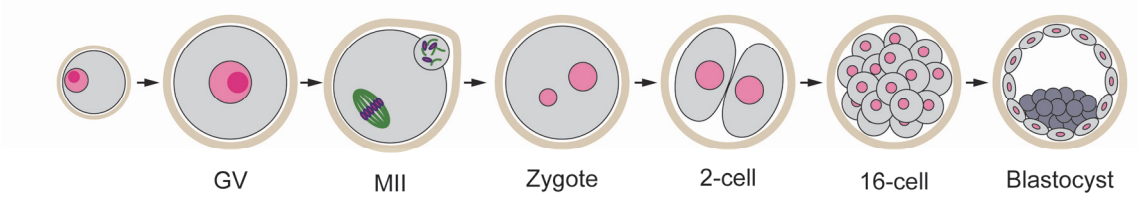

Figure 1: Development of the oocyte/embryo to the blastocyst stage. The trigger by the preovulatory LH surge induces meiotic resumption of the arrested germinal vesicle (GV) oocyte and maturation to the metaphase II (MII) stage. After ovulation, fertilization then leads to extrusion of the second polar body, followed by the first mitotic cell divisions – of which only selected stages are shown - until the blastocyst stage.

After ovulation and the concomitant release of the oocyte into the oviduct, the oocyte is ready for fertilization, the trigger for meiotic resumption leading to the extrusion of the second polar body. After entrance of a spermatozoon, the membranes of the female and male pro-nuclei dissolve and combination of the chromosomes leads to the formation of a single diploid nucleus. The so-called zygote remains in the oviduct, where the first mitotic cell divisions take place. In the following period, the early bovine embryo stays in the oviduct

until it reaches the uterus at around Day 4 to 5 post-fertilization in cows. Embryonic cleavages and compaction of the embryo results in the formation of the morula together with the first lineage decision, which marks the loss of pluripotency. At around Day 7 in cattle and Day 5 to 6 in humans, the embryo reaches the blastocyst stage, which consists of the inner cell mass – the future embryo or fetus, which stems from the compacted inner blastomeres – and the trophectoderm, which will later give rise to the placenta (*2, 3*). The early embryonic development from the GV oocyte to the blastocyst stage is schematically illustrated in Figure 1. After hatching from its outer shell, the zona pellucida (ZP), the conceptus elongates and is implanted into the uterus at approximately Day 9 post fertilization in humans and around Day 19 in cattle (*4, 5*), establishing the contact between the conceptus and the endometrium, which nourishes the conceptus in the subsequent developmental stages.

1.1.1 Oocyte maturation

As described in the preceding section, oocytes have to undergo maturation prior to fertilization. Successful oocyte maturation is a prerequisite for fertilization and subsequent embryonic development. During fetal life, the mammalian oocyte initiates meiosis and, until ovulation or atresia of the oocyte, it is arrested at the germinal vesicle (GV) stage, which is the diplotene stage of prophase I. Acquisition of the competence for resumption of meiosis takes place during the oocytes' growth phase (*6*), which is completed at a follicle diameter size of approximately 3 mm in cattle (*7*). Meiotic arrest is maintained by high cAMP levels in the oocyte, suppressing the activity of the maturation promoting factor (MPF) through stimulation of cAMP-dependent protein kinase A (PKA). *In vivo*, meiotic resumption is triggered by the pre-ovulatory gonadotropin surge that leads to decreasing cGMP levels in the follicle and oocyte, which results in an up-regulation of the activity of phosphodiesterase and finally causes a drop in intraoocyte cAMP levels (*8-10*). Resumption of meiosis then leads to germinal vesicle breakdown (GVBD), chromosomal condensation, expansion of the surrounding cumulus and progression through metaphase I to anaphase and telophase, finally leading to extrusion of the first polar body and arrest at metaphase II (MII) until fertilization and extrusion of the second polar body (*11*), as depicted in Figure 2. *In vitro*, meiotic resumption can also be induced by removal of the oocyte from the follicle, which has an inhibitory effect on the oocyte (*12*). In addition to the above-described events that occur during nuclear maturation, cytoplasmic maturation takes place, which involves major

changes in the cytoplasm such as reorganization of organelles and storage of mRNAs, proteins and transcription factors (*13-16*). Cytoplasmic maturation is comprehensively reviewed by Ferreira et al. (*15*) and can be divided into the main phases organelle redistribution, dynamics of the cytoskeleton and molecular maturation.

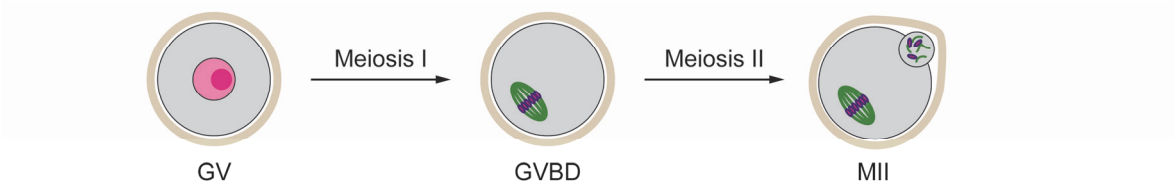

Figure 2: Oocyte maturation. During their development in the follicle of the fetal ovary, oocytes become arrested at prophase I, the GV stage. LH surge (*in vivo*) or mechanical release from the follicle (*in vitro*) results in GV breakdown (GVBD). When the oocyte reaches metaphase I, condensed chromosomes (purple) align at the metaphase plate of the spindle (green). After extrusion of one set of chromosomes in the first polar body, the mature oocyte is arrested at metaphase II (MII) until fertilization (adapted from Adhikari and Liu (*17*)).

In vitro maturation (IVM) of mammalian oocytes is an important technique for embryo technology as it directly affects the efficiencies of *in vitro* embryo production (IVP). The IVM of bovine oocytes enables the generation of larger quantities of mature oocytes than the expensive *in vivo* alternative, which requires the hormonally induced superovulation of cows. Cumulus-oocyte-complexes (COCs) for IVM and subsequent embryo production can be aspirated from the follicles of ovaries, readily available from local abattoirs. However, it has to be considered that oocytes collected this way often are of heterogeneous quality, due to differences in stage of the estrus cycle or genetic differences of the donor animals, with impact on IVP rates. Maturation can be induced by several different protocols, yet, one of the most commonly applied approaches involves the supplementation of IVM media with estrus cow serum (ECS). Moreover, addition of the gonadotropins FSH and LH has been shown to improve cumulus cell (CC) expansion, fertilization rates and subsequent embryonic development (*18-20*) and is therefore a commonly applied strategy with or without the supplementation of growth factors, e.g. epidermal growth factor.

The IVM efficacy of oocytes is influenced by many factors like oocyte quality prior to maturation or the medium composition during the maturation process. Regarding the efficacy of IVP, it has been reported that approximately 90% of immature oocytes undergo nuclear maturation, approximately 80% are fertilizable *in vitro* (*in vitro* fertilization, IVF) while less than half 50% reach the blastocyst stage in cattle (*11*). Although this suggests that the major drop in IVP efficiency is caused by problems during the *in vitro* culture, the oocyte quality seems to be the limiting factor (*21*). This is underlined by the fact that the blastocyst

rate of *in vitro* matured oocytes is at a low rate of about 35% irrespective of *in vitro* or *in vivo* embryo culture, but the blastocyst rate significantly increases for *in vivo* matured oocytes regardless of the following culture conditions (*21-23*). Therefore, understanding underlying molecular mechanisms related to impaired oocyte quality and insufficient maturation is of major importance for successful *in vitro* generation of embryos.

1.1.2 Role of transcription during *in vitro* maturation

Several studies have previously aimed to elucidate underlying mechanisms of oocyte maturation and post-fertilization development. During the oocyte growth phase in fetal life, maternal transcripts are accumulated in the oocyte, which are critical for the control of subsequent resumption of meiosis and the first embryonic cell divisions (*24, 25*). It has been shown that in bovine embryos the major embryonic genome activation (EGA), which implies the switch from maternal RNAs and proteins stored in the oocytes to transcripts generated in the embryo, takes place at the 8-cell stage (*26, 27*). It is therefore assumed that fully grown mammalian GV stage oocytes already possess most of the transcripts necessary and that stored mRNAs are gradually degraded or translated, regulating embryonic developmental processes (*28*).

Yet, the role of transcription during maturation of the oocyte is not fully understood. Transcriptional activity has been shown to occur to some extent in GV stage oocytes (*6, 29*), but there are conflicting results about the transcriptional activity after resumption of meiosis. Studies of mouse and human immature and *in vivo* matured oocytes showed an up-regulation of some transcripts during maturation (*30, 31*), while on the other hand, the absence of over-expressed transcripts has been reported in immature compared to *in vitro* matured bovine and murine oocytes (*32, 33*). In addition, another study of bovine GV stage and *in vitro* matured oocytes detected a massive reduction of the initial transcript stock, but also reported elevated levels of certain transcripts during IVM, leading to the assumption that transcription takes place to a certain degree. Radiolabeling experiments to determine the amount of transcriptional activity in GV and MII oocytes and the subsequent early cleavage stages showed that ^{35}S-UTP incorporation remains high at the GV stage but decreases to background levels at the MII stage, followed by an increase at the 2-cell stage (*34*), which is in agreement with the decrease of maturation rates from 90 to 75% in oocytes matured in the presence of the transcription inhibitor Actinomycin D (ActD) (*35*). However, these results implicate only minor transcriptional activity during maturation, whose function and

importance for maturation remains partially unclear and leaves space for further investigations.

1.1.3 The bovine as model system

Due to easier animal housing, most basic reproductive research has been conducted in mice. Yet, there are major differences in oocyte and early embryonic development between humans and mice (*36*). Regarding bovine and human, the cow is a relevant animal model for studies of reproductive biology, as it better reflects the human system. In contrast to e.g. mice and pigs, humans and cows are both single ovulating species. Moreover, they both have significantly longer estrus and menstrual cycles compared to mice, and oocyte biology and many aspects of follicular dynamics and oocyte size show a much higher degree of similarity between the bovine and the human system as compared to mice (*37*).

Thus, the results of studies of murine oocytes and embryonic development can only be partially transferred to the human system. Therefore, the analysis of bovine oocyte maturation is not solely interesting for understanding and improving bovine reproductive processes and IVM, but may to a certain extent also increase the knowledge of these processes in humans and human IVF techniques.

1.2 Targeting *in vitro* maturation on a molecular level

Due to the small amounts of sample material as compared to tissues or cell culture derived samples, the analysis of oocytes and early embryos at the transcriptome and proteome level is challenging and was limited in the past, as it requires highly sensitive procedures and instrumentation. Therefore, the technological advances in mass-spectrometry and RNA sequencing now allow a more thorough study of oocyte maturation, fertilization and embryonic development and the underlying molecular mechanisms. Thus, the following section will elaborate the results of, on the one hand, transcriptomic studies and, on the other hand, proteomic analyses of oocytes and the subsequent stages.

1.2.1 Transcriptomic studies

Bovine oocytes before and after maturation and the early embryonic developmental stages have been subject to numerous transcriptomic analyses so far. Regarding specifically

GV and MII oocytes, e.g. Fair et al. (*38*) performed a global mRNA expression analysis and detected three times more down- than up-regulated transcripts after IVM and showed that the majority of the detected genes is associated with regulatory activities including the regulation of mitogen-activated protein kinase (MAPK) activity, translation initiation and transcription. In addition, comparing *in vivo* and *in vitro* matured oocytes, affected transcripts in IVM oocytes were found to be related to metabolism, cell organization, cell growth or maintenance (*39*).

Several studies also targeted the effect of different developmental capacities on the oocyte transcriptome. Adona et al. (*40*) analyzed the impact of IVM on the transcript profile of oocytes and detected that the genes altered by IVM are mostly related to the regulation of oocyte metabolism. Moreover, in a transcriptomic study of bovine GV oocytes with different developmental competence, differentially expressed genes were shown to be involved in regulation of transcription, translation and RNA processing (*41*), which was also confirmed in a similar approach conducted by Biase et al. (*42*).

Beside the transcriptomic analysis of immature and mature oocytes, the developmental stages up to the blastocyst stage have also been investigated on the level of the transcriptome. For example Vigneault et al. (*43*) identified genes associated with the EGA and showed that a high proportion of genes at the 8-cell stage was involved in gene transcription and RNA processing. Another study by Graf et al. (*26*) performed a RNA-Seq analysis of different developmental stages, detecting on the one hand relatively few differentially abundant transcripts between GV and MII oocytes, and, on the other hand, a remarkable increase in differentially abundant transcripts between 4-cell and 8-cell stages, which marks the onset of the EGA.

1.2.2 Mass spectrometry-based proteomic studies

Although transcriptomic-based strategies have frequently been employed in oocytes and embryos, this does not give clear evidence of the corresponding protein levels, as there is no strict correlation between gene and protein expression levels, particularly in oocytes (*44, 45*). A large proportion of stored maternal mRNAs present in the oocyte is not polyadenylated and can therefore not be translated (*46*). Moreover, many proteins require post-translational modifications, such as phosphorylation, glycosylation or acetylation, for full functionality and also protein processing through proteolysis is not accessible via genome or transcriptome approaches (*47-49*). Therefore, proteomic analyses are

indispensable for understanding of molecular processes, especially during oocyte maturation.

For several years, two-dimensional gel electrophoresis (2D-PAGE) was the method of choice for proteomic experiments. However, the technical progress in both liquid chromatography and mass spectrometry systems enabled the more and more sensitive analysis of whole proteomes. Using a bottom-up proteomic approach with nano liquid chromatography – tandem mass spectrometry, referred to as nano LC-MS/MS, proteins are analyzed at the peptide level. Therefore, protein lysates are digested by a protease, typically trypsin, as trypsin cleaves peptide chains mainly at the carboxyl side of the amino acids lysine or arginine. The obtained peptides are then separated in the chromatography system and are subsequently ionized and analyzed by the tandem mass spectrometer, which captures the peptide ion and creates peptide fragments through collision with gas molecules, the so-called collision-induced dissociation (CID) (*50, 51*). As the peptides are predominantly fragmented at the peptide bond, this leads to a predictable pattern of fragments, the mass to charge ratios of which are then determined by the instrument. For protein identification, the obtained MS/MS spectra are matched with theoretical MS/MS spectra from databases of the respective organism.

In addition to the identification of proteins, there are several methods that enable a relative quantification by LC-MS/MS via labelling or through a label-free approach. Labelling is based on the introduction of chemical tags with stable isotopes either metabolically during cell culture (Stable isotope labelling by amino acids in cell culture, SILAC) (*52*), on the protein level (Isotope-coded affinity tag, ICAT) (*53*) or on the level of peptides, e.g. TMT (Tandem mass tag) and iTRAQ (Isobaric tags for relative and absolute quantitation) labelling (*54, 55*). The isotope-coded tags enable a simultaneous, multiplexed analysis of different samples for a more accurate quantification. On the other hand, label-free methods are less costly and require less sample material due to fewer work steps. Label-free methods are either based on the signal intensity of the precursor ion – the peptide ion – (*56*) or use the number of MS/MS spectra obtained for each peptide, which is referred to as "spectral counting" (*57*).

Proteomic approaches have been used in several studies of mammalian oocytes and embryos, such as mouse (*58-64*), human (*65*) and pig (*45, 66, 67*). In comparison to the mouse, there are relatively few proteomic studies of bovine oocytes and embryos. Using an iTRAQ-based approach, Deutsch et al. (*68*) analyzed the proteome of MII oocytes, zygotes, 2-cell and 4-cell embryos and found a considerable number of proteins, which increased in

abundance over these stages and detected proteins involved in the p53 pathway, in lipid metabolism and in mitosis. Berendt et al. (*69*) performed a 2D-DIGE-based (Two-dimensional difference gel electrophoresis) approach to analyze immature and *in vitro* matured bovine oocytes and detected changes in the levels of proteins related to cell cycle processes as well as redox enzymes. Another study, which aimed to analyze the interaction between oocyte and CCs at the GV stage showed that proteins with higher expression in CCs are functionally related to cell communication, generation of precursor metabolites and energy as well as transport (*70*). Of interest, Chen et al. (*71*) applied an iTRAQ-based approach to the analysis of *in vitro* matured buffalo oocytes and found 173 differentially expressed proteins between GV and competent MII oocytes, as well as 147 proteins between MII oocytes that were either classified as competent or incompetent. They detected a large number of proteins involved in mRNA processing and cell cycle, proteins related to the ubiquitin-proteasome proteolytic pathway and proteins associated with protein transport.

1.2.3 The transcription inhibitor actinomycin D

Actinomycin D (ActD) is an antibiotic and antineoplastic compound of the actinomycin family isolated from *Streptomyces* strains. ActD contains two cyclic pentapeptide lactones connected to aminophenoxazine (Figure 3).

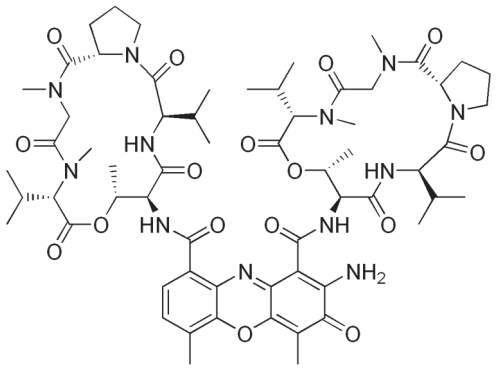

Figure 3: Chemical structure of the transcription inhibitor actinomycin D

It is used in the treatment of Wilm's tumor, a childhood cancer of the kidneys, and gestational choriocarcinoma (*72-74*). In addition to its clinical application, ActD is widely used in research as transcription inhibitor. The mechanism of action of ActD is mediated through binding DNA irreversibly by intercalation of the phenoxazone ring at pairs of guanine and cytosine, which leads to the inhibition of transcription via blockage of RNA polymerases (*75, 76*). In addition, the pentapeptides of the ActD structure have been

described to be located in the minor groove of the DNA (*77, 78*). ActD provides an useful experimental tool due to its ability to shut off transcription fast by affecting all three eukaryotic polymerases, while class one transcription has been shown to be most sensitive to ActD (*79*). In *Xenopus laevis*, inhibition of transcription with ActD blocked the release of the oocytes from the follicle but did not inhibit progesterone-induced oocyte maturation (*80*). In bovine oocytes, ActD treatment led to dose-dependent decrease of maturation, cell cleavage and Day 8 blastocyst rate, the latter being almost completely inhibited (*35*).

1.3 Aim of the thesis

Oocyte maturation is an essential step required for reproductive success, as oocyte quality impacts the subsequent developmental stages. It has been commonly accepted that bovine oocyte maturation is under the control of maternal transcripts stored in the oocyte during growth phase. Yet, several studies conducted aimed to target the role of transcription during oocyte *in vitro* maturation (IVM) and results indicated that, to a certain degree, transcription takes place.

The main focus of the present work is therefore to investigate the impact of transcription during IVM on the oocyte proteome. To achieve this, oocytes are matured in the presence of a transcription inhibitor and the protein composition of oocytes before and after maturation is analyzed in a holistic proteomic approach. Using label-free relative quantification, protein abundance alterations are detected between germinal vesicle (GV) and control and transcription-inhibited metaphase II (MII) oocytes. The central question is whether, and to which extent, the absence of transcription during maturation affects the oocyte proteome. To address this, first the quantitative proteome at the initial and final stage of non-inhibited oocyte IVM is assessed in-depth. Proteins involved in meiosis resumption until arrest at the MII stage are studied and related cellular processes are identified.

Moreover, proteomic alterations during inhibited compared to changes during non-inhibited maturation will provide additional knowledge about the effect of the absence of transcription during IVM. Single proteins dependent or independent of transcription are identified and functionally classified to determine underlying biological processes that do or do not require transcription. Thus, this work presents a comprehensive analysis of proteomic changes associated with *in vitro* maturation in bovine oocytes.

.

2 Material and Methods

2.1 Materials

2.1.1 Chemicals and reagents

Reagent	Supplier
Acetonitrile, LC-MS grade	Merck Millipore (Darmstadt, Germany)
Actinomycin D	Sigma-Aldrich (Steinheim, Germany)
Dimethyl sulfoxide (DMSO)	Sigma-Aldrich (Steinheim, Germany)
Dithiothreitol (DTT)	Roth (Karlsruhe, Germany)
Estrous cow serum (ECS)	Moorversuchsgut der LMU (Oberschleißheim, Germany)
Follicle-stimulating hormone (FSH)	Sioux Biochemical, IA, USA
Formic acid (FA)	Sigma-Aldrich (Steinheim, Germany)
Iodoacetamide (IAA)	Sigma-Aldrich (Steinheim, Germany)
Luteinizing hormone (LH)	Sioux Biochemical, IA, USA
Lysyl endopeptidase, MS grade	Fujifilm Wako Chemicals (Richmond, USA)
Polyvinylpyrrolidone (PVP)	Sigma-Aldrich (Steinheim, Germany)
Potassium chloride	Roth (Karlsruhe, Germany)
Potassium dihydrogenphosphate	Roth (Karlsruhe, Germany)
Sodium chloride	Roth (Karlsruhe, Germany)
Sodium hydrogen phosphate	Roth (Karlsruhe, Germany)
Tissue culturen medium 199 (TCM 199)	Minitüb (Tiefenbach, Germany)
Tris-(2-carboxyethyl)-phosphine (TCEP)	Roth (Karlsruhe, Germany)
Tris	Roth (Karlsruhe, Germany)
Trypsin, sequencing grade, modified	Promega (Madison, WI, USA)
Urea	Roth (Karlsruhe, Germany)
Water, LC-MS grade	Merck Millipore (Darmstadt, Germany)

Table 1: List of reagents and solvents

2.1.2 Technical equipment

Device	Manufacturer
Cell culture equipment, Nunc	Thermo Fisher Scientific, Waltham, USA
Centrifuge 5427 R	Eppendorf, Köln, Germany
Electronic aspirator pump, 3014	Labotect, Göttingen, Germany
Incubator CB 53	Binder, Tuttlingen, Germany
Q Exactive HF-X mass spectrometer	Thermo Fisher Scientific, Waltham, USA
Separation column PepMap RSLC C18, 2 µm, 100 Å, 75 µm x 50 cm	Thermo Fisher Scientific, Waltham, USA
Stereomicroscope Stemi SV6	Zeiss, Jena, Germany
Thermomixer 5436	Eppendorf, Köln, Germany
Transferpettor 5 µl	Brand, Wertheim, Germany
Trap column Acclaim PepMap RSLC 100, C18, 3 µm, 100 Å, 75 µm x 2 cm	Thermo Fisher Scientific, Waltham, USA
UltiMate 3000 RSLC nano System	Thermo Fisher Scientific, Waltham, USA
Ultrasonicator Sonopuls UW3200	Bandelin, Berlin, Germany
Vacuum concentrator	Bachofer, Reutlingen, Germany
Vortex Genie 2	Bachofer, Reutlingen, Germany

Table 2: Instruments and material for cell culture and analytics

2.1.3 Software

Software name	Supplier
BioVenn	Tim Hulsen, Computational Drug Discovery (CDD), Nijmegen, The Netherlands
Cytoscape v3.3.0	The Cytoscape Consortium, San Diego, CA, USA
Cytoscape plug-in ClueGO v2.2.0	The Cytoscape Consortium, San Diego, CA, USA
Cytoscape plug-in CluePedia v1.2.0	The Cytoscape Consortium, San Diego, CA, USA
DAVID v6.8	Laboratory of Human Retrovirology and Immunoinformatics, Frederick, USA
GraphPad Prism 8	GraphPad Software, San Diego, CA, USA
GSEA v2.0	Broad Institute, Massachusetts, USA
MaxQuant v1.6.1.0	Max-Planck-Institute of Biochemistry, Martinsried, Germany
Microsoft Office 2013	Microsoft, Redmont, WA, USA

Perseus v1.5.8.0	Max-Planck-Institute of Biochemistry, Martinsried, Germany
REVIGO	Rudjer Boskovic Institute, Zagreb, Croatia
STRING v11.0	STRING Consortium, Zurich, Switzerland

Table 3: Software and online tools used for data evaluation

2.2 Methods

2.2.1 Generation of oocytes

For collection of cumulus-oocyte complexes (COCs), post-mortem bovine ovaries were obtained from a local abattoir and transferred to the laboratory in phosphate-buffered saline (PBS; 1 mM KH_2PO_4, 2 mM KCl, 8 mM Na_2HPO_4, 0.9 mM $CaCl_2$, 0.49 mM $MgCl_2$, 0.8% NaCl). Ovaries were washed several times in PBS to remove blood and cell debris. COCs were aspirated by puncture and suction from 3−8 mm follicles with an 18-gauge needle and a vacuum pressure of approximately 60 mm Hg. Oocytes with a complete cumulus oophorus were selected from follicle fluid sediments, and were randomly assigned to one of the three groups GV, MII control and MII AD oocytes.

COCs of the GV group were mechanically denuded by vortexing for 4 min and washed three times in 1 mL PBS containing 1 mg/mL polyvinylpyrrolidone (PVP) to remove the CCs. Denuded GV oocytes were evaluated microscopically and morphologically intact oocytes were collected, frozen on dry ice after removal of PBS and stored at -80 °C.

2.2.2 *In vitro* maturation

COCs of the MII and MII AD groups were washed three times in maturation media consisting of tissue culture medium 199 (TCM 199) supplemented with 5% estrous cow serum (ECS), 0.025 IU/mL b-FSH, and 0.0125 IU/mL b-LH. The COCs were transferred to four-well plates in groups of 35 in 400 µl of maturation media per well. Transcription was inhibited by addition of 2 µg/ml actinomycin D in 5% DMSO to COCs of the MII AD group. For the control MII group, DMSO was added in a final concentration of 0.01% in the maturation media to have the same DMSO concentration in both groups. COCs were matured for 23 h at 39 °C in a humidified atmosphere with 5% v/v CO2 in air.

2.2.3 Collection of oocytes

After maturation, oocytes were evaluated microscopically and were manually denuded separately for each batch by vortexing for 4 min in 1 mL PBS containing 1 mg/mL PVP. Denuded mature oocytes were washed three times in PBS/1 mg/mL PVP. After removal of PBS, MII control and MII AD oocytes were separately frozen on dry ice and stored at −80 °C until analysis.

2.2.4 Protein lysis and tryptic digest

Samples were lysed in denaturation buffer (8 M urea, 50 mM Tris-HCl, pH 8.0) and ultrasonicated twelve times for 10 s. Cysteine residues were reduced during 30 min of incubation in 4 mM dithiothreitol (DTT) /2 mM tris(2-carboxyethyl)phosphine (TCEP) at 56 °C followed by alkylation in 8 mM iodoacetamide (IAA) for 30 min at room temperature in darkness. Excess IAA was quenched by addition of DTT to a final concentration of 10 mM. For digestion, samples were first incubated with Lys-C with a protease:protein mass ratio of 1:100 for 4 h at 37 °C and were then diluted to < 1 M Urea, followed by addition of trypsin with a protease:protein mass ratio of 1:50. Incubation was performed overnight at 37 °C, and the peptide solution was subsequently dried using a vacuum concentrator and stored at -80 °C.

2.2.5 LC-MS/MS analysis

Digested samples were re-dissolved in 0.1% formic acid (FA) and separated using an UltiMate 3000 RSLC nano system with a PepMap C18 column (500 mm x 75 µm, 2 µm) at a constant flow rate of 250 nL/min. Peptides were separated using linear gradients that consisted of a first ramp from 3 to 25%B (100% acetonitrile, 0.1% FA) within 160 min, followed by a ramp to 40% B within 10 min and a third ramp to 85% B in 5 min. The liquid chromatography was coupled online to a Q Exactive HF-X mass spectrometer via liquid junction. For data acquisition, collision induced dissociation (CID) spectra were acquired, and acquisition cycles consisted of one full MS scan at a resolution of 60,000 and a mass range of 350 to 1600 m/z followed by 15 data dependent MS/MS scans at a resolution of 15,000.

2.2.6 Data processing and statistical analysis

Spectral data (Thermo RAW files) were processed using MaxQuant version 1.6.1.0 and the implemented label-free quantification (LFQ) option (*56, 81*). For protein identification, MS/MS spectra were searched against the bovine Uniprot database (April 2018) using the Andromeda search engine. The ‘match between runs’ option was enabled with a match time window of 0.7 min and an alignment time window of 20 min. Unique and razor peptides were used for protein quantification. Trypsin and Lys-C were chosen as enzymes with a maximum of two missed cleavages allowed. Carbamidomethylation was

selected as fixed modification, and oxidation (M) was used as variable modification. All other parameters were set according to MaxQuant default settings.

Further data analysis was performed using Perseus version 1.5.8.0. Protein identifications were filtered for at least five valid values in at least one group and missing values were imputed from normal distribution. LFQ intensities of precursor ions were log2-transformed and t-tests of pairwise comparisons between the three groups were carried out. Proteins were considered as significantly altered in abundance with a t-test q-value of less than 0.05 and a log2-fold change of > |0.6|.

2.2.7 Bioinformatic analysis

Venn diagrams were created using the web application BioVenn provided on http://www.cmbi.ru.nl/cdd/biovenn/ (*82*). Database for Annotation, Visualization and Integrated Discovery (DAVID) functional annotation clustering (https://david.ncifcrf.gov) was performed separately for significantly higher or lower abundant proteins in each of the three pairwise comparisons for the GO terms “biological process”, “molecular function” and “cellular component” using the integrated *Bos taurus* dataset as background (*83-85*). Gene clusters of related biological functions showing an enrichment score above 1.3 were considered as relevant.

Gene set enrichment analysis (GSEA) was carried out using the software GSEA v2.2.2 provided by the Broad Institute (http://software. broadinstitute.org/gsea) (*86, 87*). For each pairwise comparison, LFQ intensities for all proteins were loaded into the GSEA software and the following parameters were set: Number of permutations: 1000; Collapse dataset to gene symbols: false; Permutation type: gene set; Max size: exclude larger sets: 500; Min size: exclude smaller sets: 5. Among the databases provided by the Broad Institute, the following gene sets were chosen for analysis: c2.cp.kegg.v5.1.symbols.gmt [Curated]; c5.bp.v5.1.symbols.gmt [Gene ontology]; c5.mf.v5.1.symbols.gmt [Gene ontology]. All other parameters were set to GSEA default values. Gene sets with an FDR q-value of less than 0.05 were considered as significant.

To cluster the significantly enriched gene sets obtained by the GSEA into superordinate terms, the enriched gene sets for each comparison were submitted to the online tool REVIGO (http://revigo.irb.hr/) (*88*).

For proteins showing lower or higher abundance in both MII groups compared to the GV groups, functional annotation enrichment analysis was carried out using the online tool STRING (https://string-db.org/) (*89*).

Proteins showing significant abundance alterations between control MII oocytes and GV oocytes were subjected to Cytoscape (v3.3.0) and the ClueGO (v2.2.0) and CluePedia (v1.2.0) plug-ins to create functional network analysis (*90-92*). GO tree levels 3 to 8 were displayed with a minimum number of three genes per cluster. For statistics, two-sided hypergeometric test and “Bonferroni step-down” was applied to calculate enrichment for terms and groups according to the GO biological process. For GO term connectivity the κ-score was set to 0.4.

3 Results

To study proteomic changes in bovine oocytes during *in vitro* maturation, nano-LC-MS/MS-based analysis was carried out. Hereby the following three experimental groups were analyzed: immature GV oocytes, *in vitro* matured MII oocytes and MII oocytes treated with the transcription inhibitor actinomycin D during IVM. For a statistically powerful evaluation, eight biological replicates were analyzed per group. Given that a bovine oocyte contains around 90 ng of total protein, for each of the biological replicates 25 oocytes, which were matured separately and which were morphologically evaluated for the presence of a polar body, were pooled to obtain approximately 2.3 µg total protein for LC-MS/MS analysis. Thus, for the eight replicates of each experimental group (GV, MII, MII AD), 200 oocytes were collected, i.e. 600 oocytes in total. The experimental strategy is graphically illustrated in Figure 4.

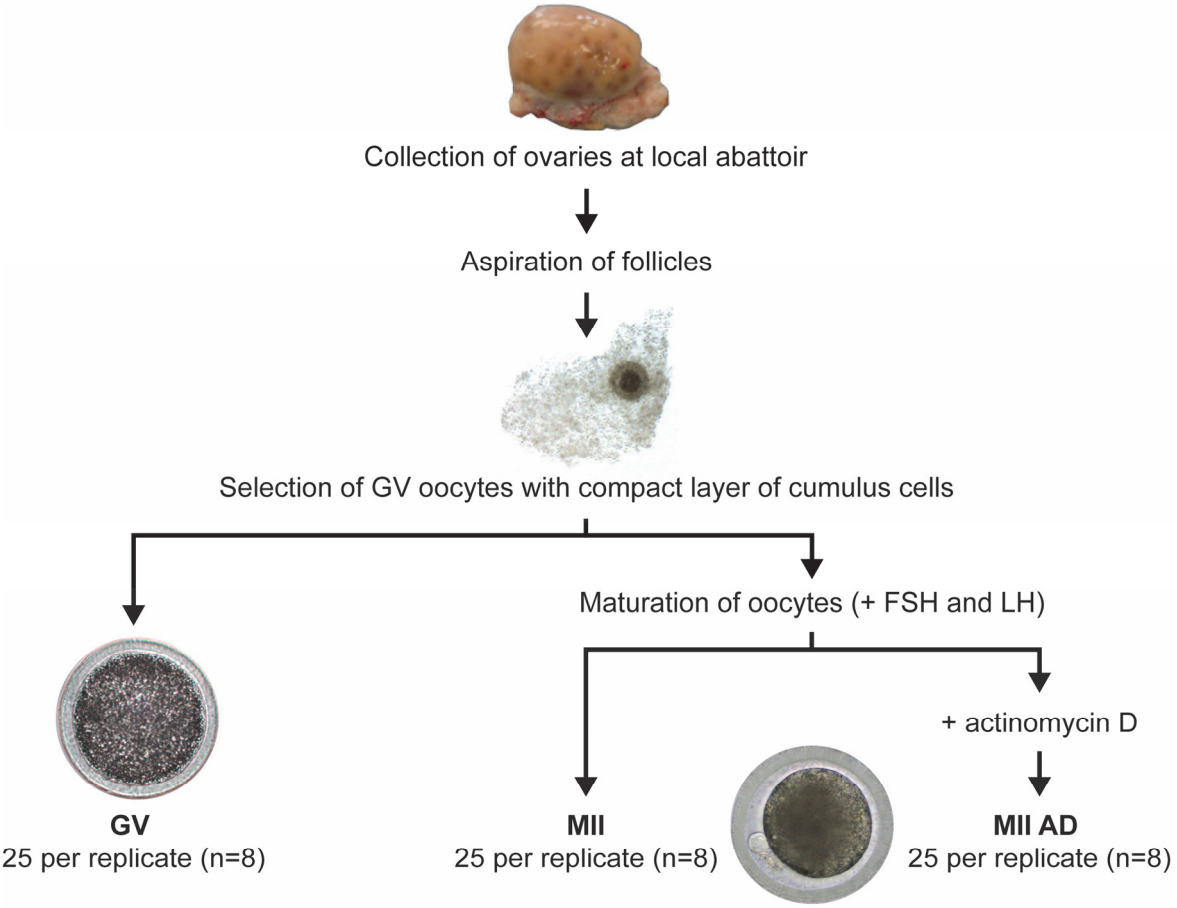

Figure 4: Experimental design. After aspiration of the follicles, oocytes are either denuded and collected prior to maturation or are matured *in vitro* with or without the transcription inhibitor actinomycin D.

3.1 Protein identifications among the developmental stages

Overall, 2018 proteins were identified in the oocytes across all three groups, including GV, MII and MII AD with 8 biological replicates per group. The Venn diagram in Figure 5A illustrates the overlap of the proteins identified in each of the different groups. A total of 1263 proteins was commonly identified in GV, MII and MII AD oocytes, corresponding to 62.6% of all protein identifications. The vast majority of proteins identified in a single group was detected in MII AD, namely 276 proteins, equal to 13.7% of all proteins, followed by MII and GV with 145 and 115 proteins, respectively, equivalent to 7.2% and 5.7% of the total set of proteins. The full list of identified proteins with the corresponding LFQ intensities is provided in Supplementary table 1.

3.2 Reproducibility of the biological replicates

To assess the reproducibility of the oocyte treatment and collection as well as of the sample processing and the LC-MS/MS-based analysis, the protein IDs in the eight replicates of each groups and their overlap were examined. Figure 5B illustrates that the replicates of the GV group showed the highest degree of similarity of the three groups with 61.0% of the protein IDs shared between all eight replicates, while approx. 30% were commonly identified in two to seven replicates and 8.9% were detected solely in a single replicate, respectively. The comparison of protein identifications within individual replicates within each group reveals higher heterogeneity between the eight replicates of the MII and the ActD-treated MII group regarding identified proteins. In MII and MII AD, 56.4% and 51.6%, respectively, were found in all eight replicates and 13.5% and 20.9% were identified only in a single biological replicate. However, the higher number of protein IDs in only one of the eight replicates correlates with the higher number of protein identifications, namely 1671 in MII AD as opposed to 1536 in MII and 1556 in GV oocytes. Regarding LFQ values of the proteins used for relative quantification, a high degree of similarity was observed among the replicates of each group. For further analysis, only LFQ values of proteins detected in at least five of the eight replicates in at least one of the three groups were used for relative quantification. Unsupervised hierarchical clustering of the respective LFQ intensities revealed a perfect separation between GV, MII and AD-treated MII oocytes, as shown in Figure 6A, while GV and MII AD oocytes are more closely related and separated from the MII group, which indicates disturbed maturation in MII AD. The principal component analysis (PCA) (Figure 6B), also demonstrates a strict separation between the

groups. Moreover, the PCA hints at a slightly higher degree of heterogeneity in the GV group, when regarding component 1, while replicates of the MII group cluster very closely together.

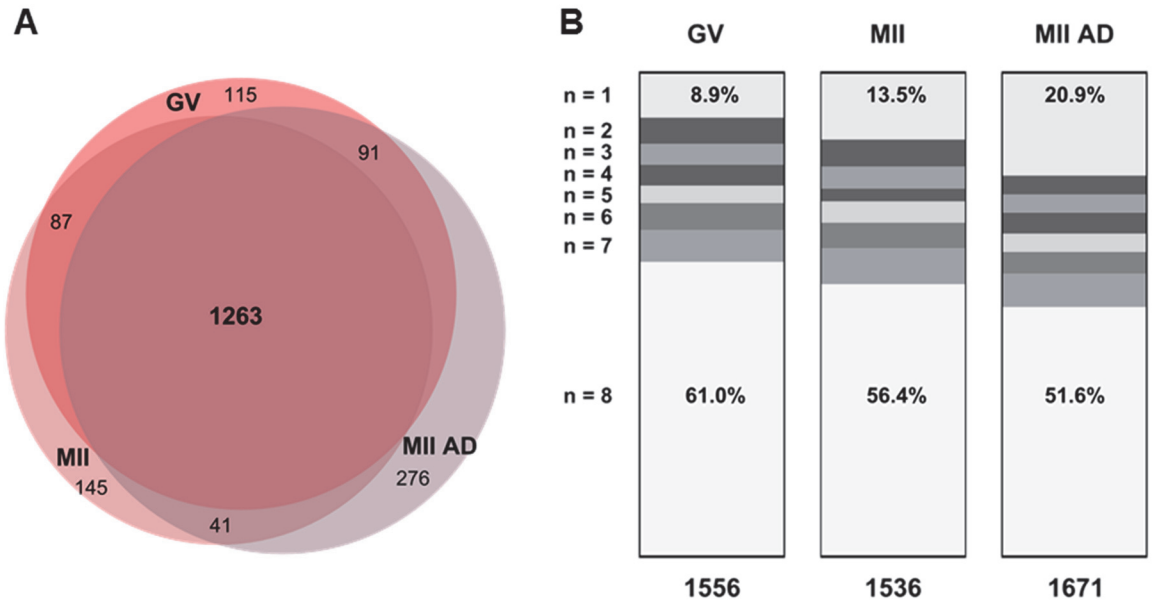

Figure 5: (A) Venn diagram of protein identifications of the three groups shows that 63% are shared between all groups. **(B) Overlap of the protein IDs among the eight biological replicates** within each group is highest in the GV group.

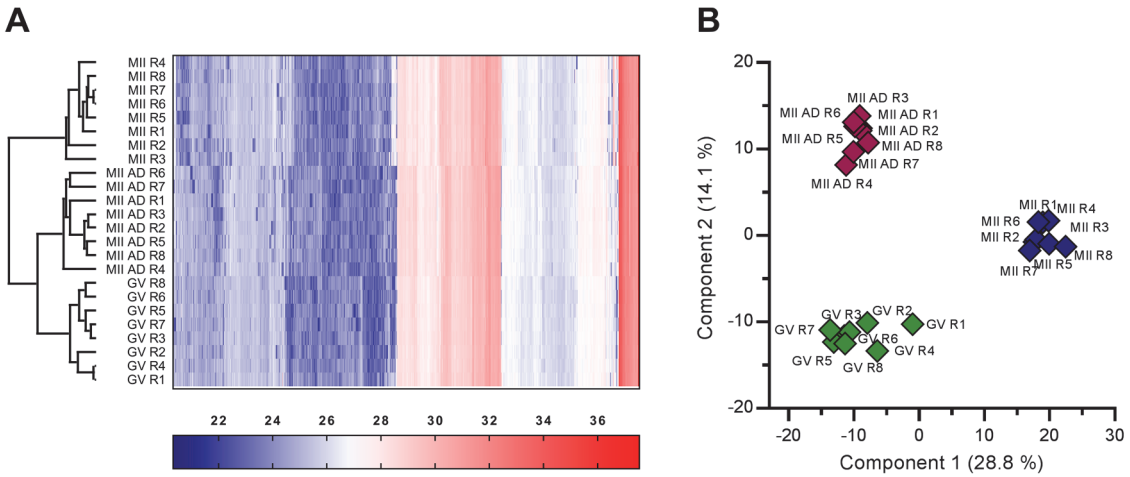

Figure 6: Unsupervised hierarchical clustering (A) and principal component analysis (B) of LFQ values of the proteins quantified in GV, MII and MII AD oocytes show a clear discrimination of the three groups.

3.3 Quantitative proteome alterations

To detect quantitative proteome alterations, pairwise comparisons were carried out between the three groups based on the LFQ intensities. In the comparisons of MII to GV oocytes, 294 proteins were abundance-altered and 225 were differentially abundant in MII AD compared to GV. The vast majority of significantly abundance-altered proteins was

detected comparing AD-treated and control MII oocytes with 393 significantly abundance-altered proteins, corresponding to approx. one fifth (19.5%) of all identified proteins. Among these, 186 were decreased in MII AD, while 207 proteins were found to be increased in MII AD.

		MII versus GV		MII AD versus GV	
Protein name	**Gene name**	**P-value**	**log2-fold change**	**P-value**	**log2-fold change**
Wee1-like protein kinase 2	WEE2	6.6E-12	5.2	1.1E-11	5.1
Bifunctional 3'-phosphoadenosine 5'-phosphosulfate synthase 2	PAPSS2	1.2E-06	3.9	4.6E-02	1.4
Hemoglobin subunit alpha	HBA	2.6E-03	3.5	1.2E-04	2.2
Cyclin-dependent kinases regulatory subunit 1	CKS1B	1.6E-05	3.0	6.0E-02	1.6
Filamin-A	FLNA	4.0E-05	2.9	8.5E-03	2.1
Securin	PTTG1	4.8E-07	2.8	4.5E-07	2.9
Cyclin-dependent kinases regulatory subunit 2	CKS2	3.5E-04	2.7	1.2E-03	2.6
Uncharacterized protein	LOC112444303	3.2E-07	2.7	4.7E-02	0.7
Serine/threonine-protein kinase VRK1	VRK1	1.8E-09	2.4	1.0E-03	1.9
Bis(5'-adenosyl)-triphosphatase	FHIT	2.6E-10	2.4	8.5E-05	0.9
Uncharacterized protein	F1MLM3	5.2E-06	2.0	8.7E-04	1.8
Nucleophosmin	NPM1	3.7E-08	1.9	7.6E-07	1.5
Pleckstrin homology domain-containing family G member 1	PLEKHG1	9.1E-06	1.9	2.4E-05	1.8
Activated RNA polymerase II transcriptional coactivator p15	SUB1	6.2E-05	1.7	1.7E-02	0.9
Integrin alpha-2	ITGA2	2.3E-04	1.7	2.0E-03	1.2

Table 4: Top 15 proteins with higher abundance in both MII control and MII AD compared to GV

The full lists of abundance-altered proteins are provided in the appendix in Supplementary tables 2 to 4. Regarding MII control, 159 proteins were increased after maturation and 135 were decreased, while in MII AD, 97 were higher abundant after IVM and 128 were found to be decreased. Of interest, 75 proteins were differentially abundant in both GV versus MII as well as in GV versus MII AD, of which 31 were commonly increased and 34 were commonly decreased after maturation, such as y-box-binding protein 2 (YBX2), wee1-like protein kinase (WEE2), transforming acidic coiled-coil-containing protein 3 (TACC3), zygote arrest 1 (ZAR1), stathmin (STMN1), filamin-A (FLNA) and securin (PTTG1). Moreover, 10 proteins were affected in opposite ways in MII AD than in MII control, e.g. histone H2B (HIST1H2BI), or 60S ribosomal protein L22 (RPL22). Proteins with lower or higher abundance, respectively, in GV compared to MII and MII AD are listed in Supplementary tables 5 to 7. The Top 15 proteins with higher abundance in MII and MII AD compared to GV are presented in Table 4.

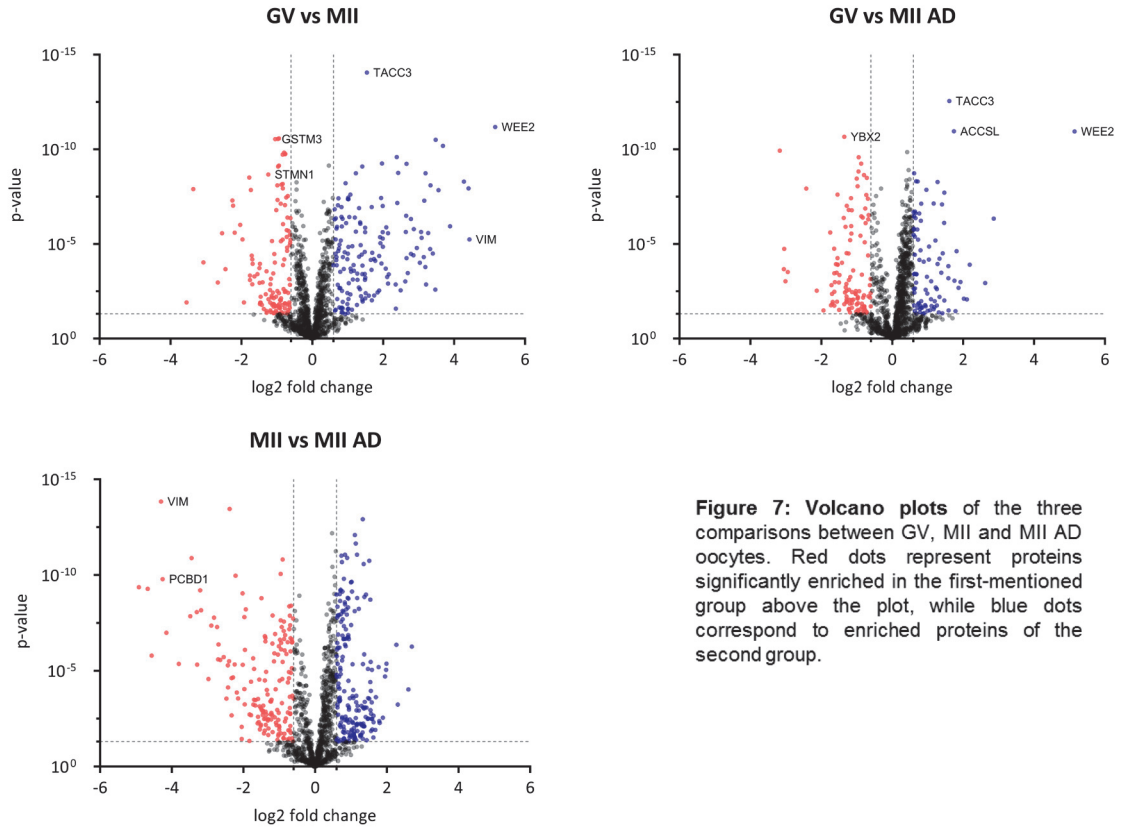

Figure 7: Volcano plots of the three comparisons between GV, MII and MII AD oocytes. Red dots represent proteins significantly enriched in the first-mentioned group above the plot, while blue dots correspond to enriched proteins of the second group.

The log2-fold changes and p-values of the proteins within each pairwise comparison are plotted in Figure 7. Proteins with a log2-fold change > $|0.6|$ and a t-test p-value < 0.05 are marked and proteins of interest are highlighted. As shown, the protein WEE2, which is well described in the context of oocyte maturation and development, is the protein with the highest abundance alteration in both MII versus GV and MII AD versus GV with a 36- and

35-fold increase (log2-fold change of 5.2 and 5.1), respectively, after maturation. Regarding the comparison of both MII groups, vimentin (VIM) and pterin-4-alpha-carbinolamine dehydratase (PCBD1) were found to be among the proteins with the highest decrease in MII AD compared to control MII oocytes: VIM and PCBD1 were 20- and 19-fold higher abundant in the control group, while, on the other hand, gamma-interferon-inducible lysosomal thiol reductase (IFI30) and importin subunit alpha (KPNA2) were 6- and 5-times higher abundant in MII AD.

3.4 Functional characterization of proteome alterations

For functional characterization of the identified proteins, DAVID gene ontology analysis was carried using the GO terms “cellular component”, “biological process”, “molecular function” and the KEGG pathways for abundance-altered proteins of the respective pairwise comparisons, regarding up- and down-regulated proteins separately.

Significantly (Enrichment score > 1.3) GO terms in GV compared to MII were “nucleotide-excision repair, DNA damage recognition”, “lysosome”, “nuclear membrane”, “carbohydrate metabolic process” and “ubiquitin mediated proteolysis”, while “RNA binding”, “cell-cell adhesion”, “translational initiation”, “carbon metabolism” and “innate immune response” were the top 5 enriched GO terms in MII compared to GV. Additionally, the ClueGO network shown in Figure 8 illustrates the processes to which the proteins that were significantly altered in the respective pairwise comparisons are related to. Proteins enriched in MII (blue nodes) were predominantly assigned to numerous nucleotide and nucleoside metabolic processes as well as mRNA-related processes. Moreover, a smaller cluster including meiosis I and oocyte maturation and development was found to be associated with the higher abundant proteins in mature oocytes.

Comparing AD-treated MII oocytes to GV, only the GO terms “RNA binding” and “cell-cell adhesion” were enriched in GV. Proteins with higher abundance in MII AD were, among others, assigned to the following GO terms: “cell-cell adhesion”, “extracellular matrix organization”, “cell division” and “focal adhesion. The GO analysis of altered proteins in MII control compared to MII AD oocytes lead to the identification of 11 cluster enriched in MII, of which “RNA binding”, “nucleotide binding”, “cell-cell adhesion”, “mitochondrial inner membrane” and “carbon metabolism” were the five GO terms with the highest enrichment score.

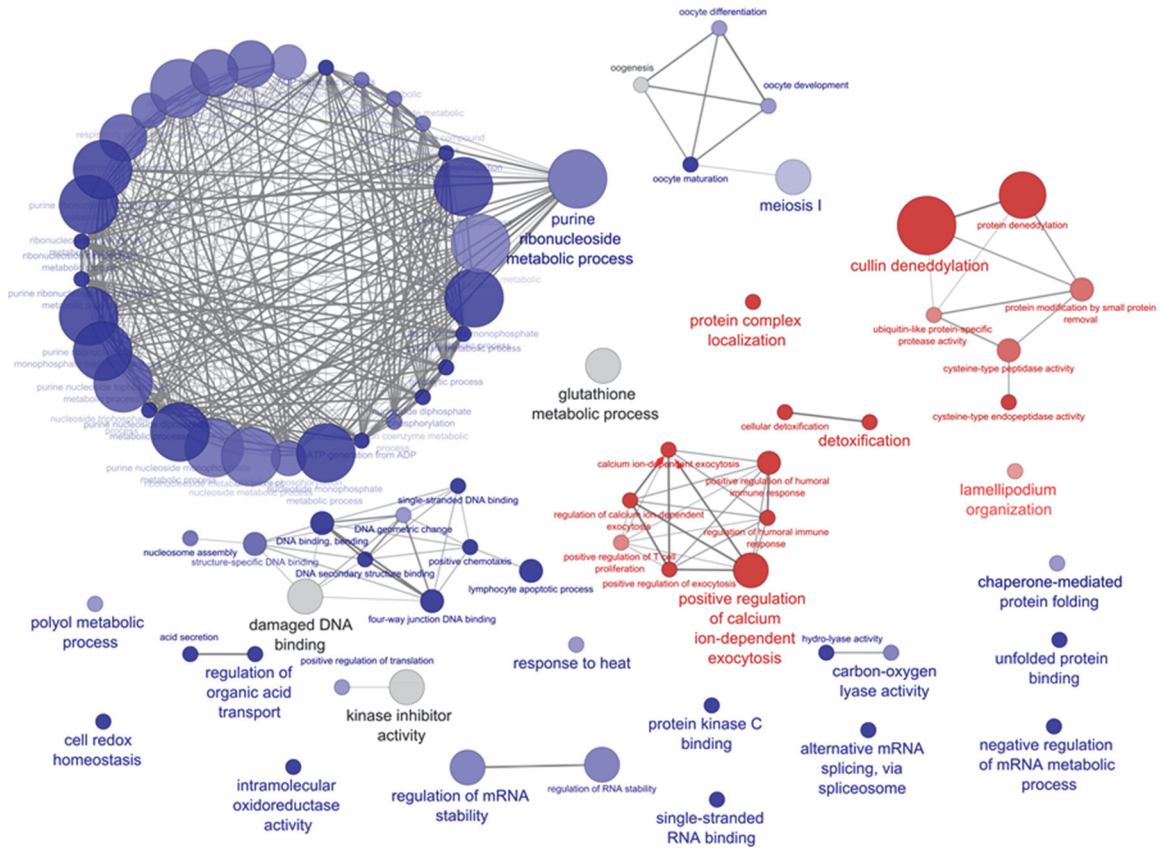

Figure 8: ClueGO of significantly altered proteins in the comparison of GV and MII. Red nodes represent GO cluster that are enriched in the GV stage compared to the MII stage, while blue nodes correspond to cluster of proteins that are more abundant in the MII group.

On the other hand, among the eight GO terms enriched in MII AD were “nucleotide excision repair, DNA damage recognition”, “ubiquitin-dependent protein catabolic process”, “translational initiation”, “cell-cell adhesion”, “lysosome” and “Golgi organization”. Supplementary tables 9 to 11 provide the full list of enriched GO terms for the respective pairwise comparisons together with the associated proteins. In addition, DAVID GO was performed for proteins with significantly higher levels in MII compared to GV, but which are not increased in MII AD over GV, resulting in eight enriched GO cluster. Among these, the cluster related to RNA binding showed the highest enrichment score, followed by “cell-cell adhesion”, “spliceosomal complex” and “nucleosome”, which are listed in Supplementary table 12.

For a comprehensive analysis of the dataset and validation of the results of the DAVID GO analysis, a gene set enrichment analysis (GSEA) was carried out for every pairwise comparison using the gene set databases KEGG pathway and the GO categories biological process and molecular function.

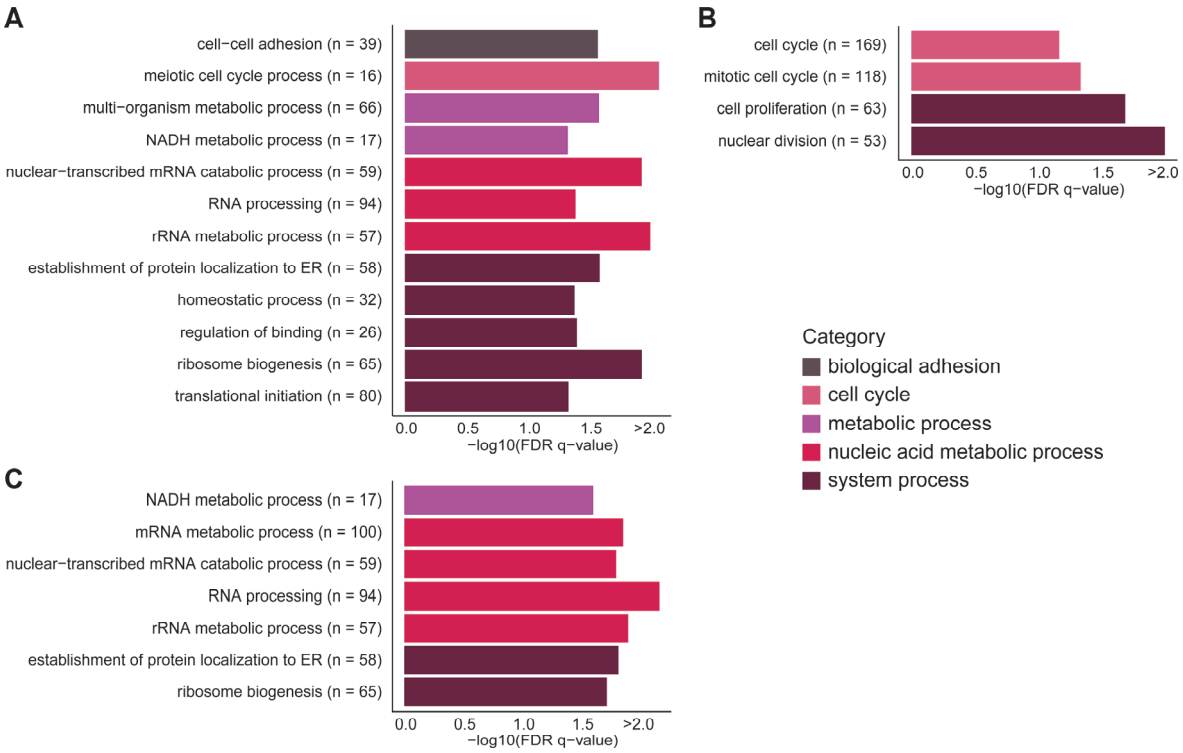

Figure 9: Summary of the results of the GSEA. Enriched gene sets in MII **(A)** and MII AD **(B)** compared to GV and MII compared to MII AD **(C)** are clustered in superordinate GO terms using REVIGO. For each set, the number of proteins is depicted in brackets. Identical bar colors correspond to the same umbrella terms stated in the legend.

Name	GO ID	size	FDR q-value
GO nucleic acid binding transcription factor activity	GO:0003700	20	0.003
GO meiotic cell cycle	GO:0051321	16	0.009
GO meiotic cell cycle process	GO:1903046	15	0.009
GO rRNA metabolic process	GO:0016072	57	0.010
GO ncRNA processing	GO:0034470	62	0.011
KEGG ribosome	-	55	0.011
GO nuclear chromatin	GO:0000790	18	0.012
GO poly a RNA binding	GO:0008143	242	0.012
GO ribosome biogenesis	GO:0042254	65	0.012
GO nuclear transcribed mRNA catabolic process nonsense mediated decay	GO:0000184	59	0.012

Table 5: Top 10 gene sets significantly enriched in MII compared to GV oocytes.

While the DAVID GO analysis shows enriched GO terms for the set of significantly abundance-altered proteins, the GSEA is based on the LFQ values of all identified proteins in the respective comparison and calculates enriched gene sets based on these intensities. Therefore, GSEA data are complementary to the DAVID analysis data. Gene sets were considered as significantly enriched with a false discovery rate (FDR) q-value of less than 0.05. All significantly enriched gene sets are listed in Supplementary tables 13 to 15. In both comparisons of MII oocyte groups – MII control and AD-treated MII – to the GV stage, no gene set was significantly enriched in GV compared to the MII groups. However, several gene sets higher in MII and MII AD than in GV were identified. Among the 38 enriched sets in MII, the top five were "nucleic acid binding transcription factor activity", "meiotic cell cycle", "meiotic cell cycle process", "rRNA metabolic process" and "ncRNA processing", of which the top ten are listed in Table 5. Six gene sets were enriched in MII AD compared to GV, namely "mitotic nuclear division", "organelle fission", "cell proliferation", "spindle", "mitotic cell cycle" and "cell cycle". Comparing MII control and MII AD, 18 gene sets were significantly enriched in MII but none was higher in MII AD. Among these set, the top five were "RNA processing". "rRNA metabolic process", "cytosolic ribosome", "mRNA metabolic process" and "ribosomal subunit". A summary of the results of the GSEA is shown in Figure 9, clustering the significantly enriched gene sets in both MII and MII AD compared to GV as well as of MII compared to MII AD under the corresponding collective term using REVIGO.

GO ID	Term	Gene count	FDR	Proteins
GO:0022402	cell cycle process	9	0.0059	CKS2, FLNA, ITGB1, NPM1, PRC1, PTTG1, TACC3, VRK1, WEE2
GO:0007049	cell cycle	10	0.0065	CKS1B, CKS2, FLNA, ITGB1, NPM1, PRC1, PTTG1, TACC3, VRK1, WEE2
GO:0000278	mitotic cell cycle	7	0.0133	CKS2, FLNA, ITGB1, PRC1, TACC3, VRK1, WEE2
GO:0000280	nuclear division	5	0.0133	CKS2, FLNA, PRC1, PTTG1, WEE2
GO:0021943	formation of radial glial scaffolds	2	0.0133	FLNA, ITGB1
GO:0050790	regulation of catalytic activity	12	0.0133	ATP1B1, CKS1B, CKS2, ITGA2, ITGB1, NPM1, PTTG1, SNCA, TCEA1, TMSB4X, TPM2, WEE2

GO:0051301	cell division	6	0.0133	CKS1B, CKS2, PRC1, PTTG1, TACC3, VRK1
GO:0051336	regulation of hydrolase activity	9	0.0133	ATP1B1, ITGA2, ITGB1, NPM1, PTTG1, SNCA, TCEA1, TMSB4X, TPM2
GO:0051726	regulation of cell cycle	9	0.0133	CKS1B, CKS2, ITGB1, NPM1, PRC1, PTTG1, RBBP7, TACC3, WEE2
GO:0060700	regulation of ribonuclease activity	2	0.0133	NPM1, TCEA1
GO:0065009	regulation of molecular function	14	0.0133	ATP1B1, CKS1B, CKS2, FLNA, ITGA2, ITGB1, NPM1, PLEKHG1, PTTG1, SNCA, TCEA1, TMSB4X, TPM2, WEE2
GO:1904064	positive regulation of cation transmembrane transport	4	0.0133	ATP1B1, FLNA, SNCA, TMSB4X
GO:1903047	mitotic cell cycle process	6	0.0156	CKS2, FLNA, ITGB1, PRC1, TACC3, VRK1
GO:0043462	regulation of ATPase activity	3	0.0187	ATP1B1, TMSB4X, TPM2
GO:0006996	organelle organization	13	0.0197	CKS2, FLNA, ITGB1, NPM1, PRC1, PTTG1, RBBP7, SNCA, TACC3, TMSB4X, TPM2, VRK1, WEE2

Table 6: STRING analysis. Top 15 enriched biological functions according to STRING analysis of proteins with higher abundance in both MII control and MII AD compared to GV.

Proteins with increased or decreased abundance in MII as well as in MII AD versus GV oocytes, were submitted to STRING analysis separately. Supplementary table 8 provides the significantly enriched biological processes the respective proteins are predominantly involved in. Additionally, the STRING network for proteins with higher abundance in the oocytes after IVM is presented in Figure 10 and the Top 15 enriched biological processes are listed in Table 6. Among the most significant terms are several cell cycle and cell division related processes, which includes e.g. WEE2, TACC3 or the cyclin-dependent kinases CKS2 and CKS1B. Moreover, enriched terms with a high number of related proteins are e.g.

"regulation of metabolic process", "regulation of gene expression" and "cellular component organization".

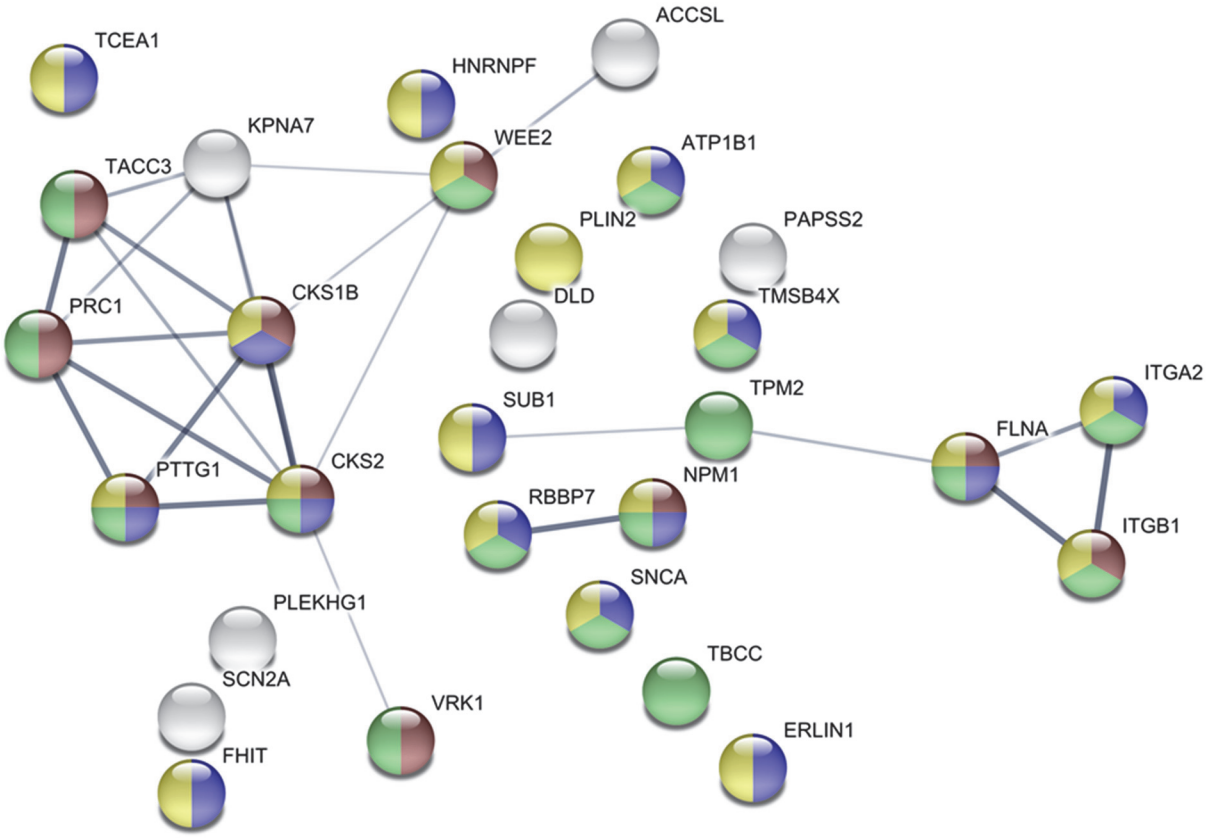

Figure 10 STRING network analysis of proteins with elevated abundance in both MII and MII AD oocytes compared to GV oocytes. Line strength indicates the level of confidence, which ranges from low (0.150) to highest (0.900). Node colors represent the related biological processes: red = cell cycle; blue = regulation of gene expression; green = cellular component organization and yellow = regulation of metabolic process.

4 Discussion

Several studies conducted to examine oocyte maturation have described a large pool of stored transcripts and proteins and a strong decrease of transcription after the GV stage, and showed that transcription is active during *in vitro* maturation (*24, 25, 28, 32*). However, due to a broad variety of post-transcriptional and post-translational processes, transcriptomic approaches can provide only limited knowledge about the functional level of proteins. Therefore proteomic approaches are indispensable for a comprehensive molecular analysis in any biological system.

While morphological and genetic aspects of oocyte maturation have been studied in detail since decades, the dynamic processes at the proteome level were not accessible until LC-MS/MS-based analytical methods and genome databases became available. The experiments described here address the question which proteins undergo quantitative changes during maturation. Given that the huge oocyte with 90 µm diameter contains a substantial amount of proteins (90 ng) and numerous stored transcripts, it is of special interest if *de novo* transcription is necessary for a successful maturation process, which individual proteins are dependent on *de novo* transcription and which are synthesized from stored mRNAs or pre-mRNAs. This discrimination can be performed by addition of the well-established transcription inhibitor actinomycin D to the maturation medium. In addition, the approach described here also aims to identify and categorize proteins altered in abundance by proteolytic processes.

4.1 Strategy and reproducibility of the proteomic analysis

To address these questions, a holistic nano LC-MS/MS-based proteomic analysis of immature and *in vitro* matured oocytes was carried out. Beside MII oocytes matured according to the standard IVM protocol, oocytes matured in the presence of the transcription inhibitor ActD were analyzed. Oocytes that underwent this procedure are referred to as MII AD in this thesis, but it has to be considered that they do not possess the developmental capacity of normal MII oocytes (*35*). The presence of a polar body was assessed microscopically for each MII and MII AD oocyte to ensure their successful nuclear maturation. Thus, only biologically well characterized germ cells were subjected to the proteome analysis, which indicates successful nuclear maturation. However, cytoplasmic maturation may be disturbed, which is not evident from morphological observation.

For statistically powerful evaluation, eight biological replicates were analyzed per group and the complexity of the sample preparation, e.g. pre-fractionation or labelling, was reduced to ensure reproducibility. To minimize operational procedures in favor of reproducibility, oocytes were not denuded from the ZP prior to lysis and protein digestion, although the presence of very high abundant proteins from the zona pellucida (ZP) limits the attainable number of protein identifications due to the common problem of undersampling in LC-MS/MS analysis of complex samples. In addition, for a high degree of reproducibility, the straight-forward label-free quantification with the MaxQuant and Perseus platform was chosen for data analysis (*56, 81*), which is one of the most commonly applied software tools for label-free quantification.

With this experimental strategy, 2018 proteins were identified across all samples. A number of proteomic studies targeting oocytes of different species with mass spectrometry-based approaches revealed a broad range of protein IDs. For example, 3699 proteins were identified by Pfeiffer et al. (*63*) from 1884 murine MII oocytes, while Wang et al. (*62*) identified 2781 proteins in GV and 2973 proteins in MII oocytes from in total 7000 GV and MII oocytes and zygotes. In human, 2154 proteins have been identified by Virant-Klun et al. (*65*) in a proteomic approach starting from 100 oocytes, which were down-scaled to the level of single cells. In addition, 3765 proteins were identified by Chen et al (*71*) in a comparative proteomic analysis of GV and MII buffalo oocytes using iTRAQ-labelling of 20 µg of protein combined with an in-gel-fractionation. In contrast, in the present study, the focus was on a reliable and reproducible analysis of proteomic changes during IVM and how these are affected by the absence of transcription, rather than on a high number of identified proteins. Nevertheless, the total number of protein IDs obtained here demonstrates that the analytical depth of the analysis was reasonably high.

To gain insight into the reproducibility of the sample collection and also the sample processing, the overlap of identified proteins within the eight replicates of each group was evaluated. Several factors during oocyte collection and maturation lead to an increase of heterogeneity among the samples, which is inevitable when ovaries are obtained from abattoirs. Among these factors is a different oocyte quality caused by different stages of the estrous cycle, as well as age and genetic variations among the donor animals. Moreover, *in vitro*, approximately 90% of the oocytes undergo nuclear maturation, approximately 80% undergo fertilization, cleaving at least once and only about one third of the original pool of GV oocytes reaches the blastocyst stage after IVF (*11*), showing that despite successful nuclear maturation, the oocyte quality strongly varies even at the MII stage.

As shown in Figure 5B, the highest similarity among the replicates was seen in the GV oocytes with more than 90% of proteins detected in at least two replicates. Among the MII control oocytes, lower similarity with approximately 86% in a minimum of two replicates was found. This reflects the diversity in GV oocyte quality, which affects maturation, leading to a more diverse pool of MII oocytes. This effect is even more pronounced in the presence of the transcription inhibitor, where the comparatively low proportion of roughly half of the proteins was detected in each sample. This statistical finding indicates that, despite successful extrusion of the polar body, the maturation process is impaired through the inhibition of transcription.

4.2 Oocyte maturation is reflected by substantial proteomic changes

To assess the impact of inhibition of transcription during maturation *in vitro* on the oocyte proteome, first changes in the protein content during maturation were evaluated. Comparing the proteome of GV and MII oocytes, the dataset presented here demonstrates that IVM is associated with numerous significant changes in the quantitative protein composition. 294 proteins were found to be altered in abundance between the two groups, corresponding to 15% of all identified proteins, of which approximately half increased or decreased during maturation, respectively. This set of proteins comprises several proteins, which have previously been well described in the context of oocyte and early embryonic development, such as zygote arrest protein 1 (ZAR1), stathmin (STMN1), wee1-like protein kinase (WEE2) and vimentin (VIM). While ZAR1 and STMN1 were decreased after maturation, WEE2 and VIM are the proteins with the highest increase in abundance with a 36-fold (WEE2) and a 22-fold increase (VIM) in the MII stage.

Beside the identification of differentially abundant proteins, their affiliation to the biological processes and molecular functions associated with maturation were assessed using DAVID GO and gene set enrichment analysis. Proteins with decreased abundance in MII compared to GV oocytes were, among others, found to be related to the term “lysosome”. Lysosomes are important for embryogenesis and have been studied in mouse embryos: they increase after fertilization, stay abundant until the morula stage, after which they decrease (*93*). One protein within this cluster, lysosome-associated membrane glycoprotein 2 (LAMP2), is 1.7-fold more abundant in GV oocytes compared to MII. It is a major component of the lysosomal membrane and essential for lysosomal biogenesis (*94*).

Knockdown of LAMP2 by injection of siRNA resulted in developmental retardation of embryos, even more pronounced when both LAMP1 and LAMP2 siRNA were injected (*93*).

In both GSEA and DAVID analysis clusters related to translational initiation and RNA processing or binding were found to be enriched. Fig. 9 shows an overview of the enriched gene sets in MII compared to GV, clustered in superordinate terms. The DAVID GO analysis revealed that "RNA binding" is the cluster with the highest enrichment score in MII compared to GV. This is in good agreement with the literature, as for example Chen et al. (*71*) compared the proteome of GV oocytes and incompetent and competent MII oocytes and found that proteins related to the ribosome were among the proteins with higher expression in competent oocytes. In addition, they found a large number of proteins involved in mRNA processing and cell cycle and hypothesized that progression of the cell cycle might be driven by regulation of protein expression. It has previously been shown that large amounts of mRNA are synthesized and stored in the cytoplasm during maturation (*25*), and protein synthesis has been described to be essential for oocyte maturation and subsequent embryo development (*15*).

Notably, the GSEA showed an enrichment of the gene sets "meiotic cell cycle process" and "meiotic cell cycle". Proteins within these gene sets comprise, among others, WEE2, securin (PTTG1) and aurora kinase A (AURKA1). The serine/threonine kinase AURKA is involved in many processes essential for mitosis. It regulates centrosome migration and separation, followed by assembly of a bipolar spindle, trigger of mitotic entry, alignment of chromosomes in metaphase, cytokinesis and the return to G1 (*95, 96*). A substrate of AURKA is transforming acidic coiled-coil-containing protein 3 (TACC3), which supports the centrosome-dependent microtubule assembly in mitosis and which has also been found to be higher abundant in MII compared to GV with a 2.9-fold increase (*97*). Furthermore, the activation of the cyclin-dependent kinase 1 (CDK1)/cyclin B complex is also supported by AURKA (*98*). Thus, the holistic proteomic analysis of oocytes before and after maturation revealed several proteins important for IVM and their related biological processes.

4.3 Maturation-associated proteins independent of *de novo* transcription

To identify proteins and related biological processes independent of *de novo* transcription, proteins which are commonly increased or decreased after maturation irrespective of the presence of the transcription inhibitor were closely examined. In total, 75

proteins were found to be significantly altered in the comparisons of GV oocytes to both groups of oocytes after maturation, of which 34 were commonly decreased and 31 were commonly increased after maturation in MII and MII AD. Due to the low number of these proteins, DAVID GO analysis would not lead to a meaningful evaluation of associated cellular processes. Thus, both sets of proteins were submitted to STRING network analysis separately, to reveal biological processes these proteins are related to. Figure 10 graphically illustrates the results of the STRING analysis, clustering functionally related proteins.

Proteins that are degraded during maturation were found to be predominantly related to reproduction-related GO terms, such as “sexual reproduction”, “reproductive process” and “single fertilization”, as shown in Supplemental Table 8. Within this cluster is YBX2, an oocyte-specific RNA-binding protein (*99*), which has been reported to have an important role in storage and translational regulation of maternal mRNAs during bovine *in vitro* embryogenesis (*100*). Its depletion results in a markedly perturbed oocyte growth and maturation (*101*) and leads to female sterility (*102*). In agreement with our data, YBX2 protein levels were shown to decrease from the GV oocyte stage throughout development to the blastocyst stage (*100*).

Besides YBX2, STMN1 and ZAR1 were also among the proteins with decreased abundance in both MII stage groups. ZAR1 and STMN1 have previously been described in the context of early embryonic development. ZAR1 is an oocyte specific maternal-effect gene involved in the oocyte-to-embryo transition and essential for female fertility (*103*). Maternal-effect genes are crucial for early cleavage regulation before the activation of the embryonic genome (*104*). STMN1, a substrate of CDK1, is a microtubule-destabilizing, cytosolic phosphoprotein involved in the construction of the mitotic spindle. A threshold level of STMN1 is required for progression through mitosis (*105*). It acts as a relay integrating diverse intracellular signaling pathways involved in regulation of cell proliferation, differentiation and function. A particular role for STMN1 at the successive steps of oocyte maturation and early embryonic development was suggested (*106*).

In addition, STRING analysis showed an enrichment of the term “regulation of metabolic process” for both higher and lower abundant proteins after maturation. Proteins involved in different metabolic processes have also been shown to be differentially abundant in the comparisons of immature and mature buffalo and pig oocytes (*45, 71*). Metabolic pathways are indispensable for successful cytoplasmic maturation as the oocytes require different metabolites during the maturation process (*15*).

On the other side, STRING analysis for the 31 proteins with an increase in abundance from GV to MII stage revealed an involvement of these proteins in cell-cycle-related processes. Within the GO term “cell cycle” are, among others, PTTG1, TACC3 and WEE2. The enrichment of these cell division-related proteins not only in the control but also in the ActD-treatment MII group indicates the transcription independent up-regulation of proteins necessary for meiotic cell division during maturation. Strikingly, WEE2, PTTG1 and TACC3 showed approximately the same ratio in MII and MII AD compared to GV. After maturation, WEE2 was 35.7 (MII control) and 35.4 (MII AD) times higher abundant in mature compared to GV oocytes, PTTG1 6.9- (MII control) and 7.3- (MII AD) fold higher and TACC3 2.9- (MII control) and 3.1- (MII AD) fold increased. Transcript levels of PTTG1, which plays a role in preventing chromosome segregation, were found to maintain high in porcine GV and MII oocytes compared to the zygote to blastocyst stages and also PTTG1 protein levels were shown to gradually decrease after fertilization (*107*). WEE2 is a downstream substrate of protein kinase A and known to be responsible for phosphorylation of the CDK1 inhibitory site, thereby maintaining meiotic arrest in oocytes (*108, 109*). High levels of WEE2 are probably needed for a tight control of the cell cycle during the upcoming cleavage cycles. In good agreement with our data, WEE2 has been found to be the protein with the highest increase in abundance during maturation in human oocytes (*65*). The very similar increase of these proteins independent of *de novo* transcription leads to the conclusion that mRNAs or pre-mRNAs for these proteins are already present in the oocyte prior to GVBD and subsequent maturation.

Moreover, “cellular component organization” is among the enriched biological processes after maturation with or without transcription inhibitor. The related proteins are e.g. the integrins ITGA2 and ITGB1, PTTG and filamin-A (FLNA). As comprehensively reviewed by Ferreira et al. (*15*), cytoplasmic maturation is associated with ultrastructural changes and the redistribution of cytoplasmic organelles, such as the mitochondria or the ribosomes. The increase of proteins involved in this process indicates a reorganization of organelles not only in MII oocytes but also in the presence of ActD and therefore in the absence of transcription.

4.4 Identification and functional classification of *de novo* transcription-dependent proteins

Of particular interest are also proteins and related biological processes that require *de novo* transcription during maturation, e.g. proteins significantly increased after normal IVM, but not in the presence of ActD or to a clearly smaller extent.

One of these proteins is vimentin (VIM), the protein with the second highest ratio after WEE2 in mature compared to immature oocytes. Although VIM is 22-fold increased after maturation without ActD, its abundance is not significantly altered in MII AD compared to GV oocytes. Therefore, the increase in abundance most likely relies on *de novo* transcription during maturation. In addition, VIM is, together with several histones, among the proteins with the highest abundance ratio in MII compared to MII AD oocytes. Vimentins are class-III intermediate filaments attached to the nucleus, endoplasmic reticulum, and mitochondria (*110*) and a role for VIM in the attainment of genomic union during fertilization in mammals was suggested (*111*).

DAVID GO analysis of the set of proteins, which were only increased in MII but not in MII AD compared to GV oocytes showed that “RNA binding” is the term with the highest enrichment score, which was also observed in the direct comparison of MII and MII AD oocytes. Moreover, a cluster containing the GO terms “translation” and “ribosome” was significantly enriched for these proteins. It has previously been shown that maternally transcribed mRNAs can be stored in the cytoplasm or in localized messenger ribonucleoprotein complexes in a translationally silent state during maturation (*112*). Until genome activation, the translational control of these transcripts is essential for properly timed oocyte development and maturation (*113, 114*). In previous publications, the high developmental capacity of oocytes was described to be related to their high rates of protein synthesis, and transcripts related to protein synthesis have been found to be higher abundant in competent oocytes (*115, 116*). Concomitantly, in their proteomic study of buffalo oocytes, Chen et al. (*71*) detected several ribosomal proteins with higher abundance in competent oocytes, indicating that the level of protein synthesis is related to the developmental competence. The higher abundance of ribosome-related proteins in MII compared to MII AD in the present study therefore leads to the hypothesis that inhibition of transcription leads to impaired protein synthesis, probably due to missing *de novo* transcripts and consequently reduced developmental competence of the resulting MII stage oocytes.

The cluster with the second highest enrichment score is “cell-cell adhesion”, a GO term that was also enriched in the direct comparisons of both MII groups to the GV group, which comprises, among others, FLNA. After maturation, FLNA was 7.2-fold higher in MII than in GV oocytes and had - despite transcription inhibition - a similar tendency, as it was found to be 4.3 times higher abundant in AD-treated MII oocytes compared to GV oocytes. This observation may lead to the hypothesis that novel transcription is partially required for the increase of FLNA levels. The different increase during maturation can be explained by the presence of transcripts for FLNA prior to the onset of maturation, supplemented by *de novo* transcription during IVM. Degradation of FLNA is promoted by filamin-A-interacting protein 1 (FILIP1), the protein with the strongest decrease in MII compared to GV oocytes. Phosphorylation of FLNA, an actin-binding protein that cross-links actin filaments, has been shown to be important for successful mitotic cell division (*117*). Moreover, it was found to control spindle migration and asymmetric division during oocyte meiosis through regulation of actin (*118*). Therefore the higher abundance of FLNA - and the lower abundance of FILIP1 - in both MII groups is likely to be related to the essential role of FLNA in cell division.

Strikingly, a set of proteins was detected, which are altered in both MII and MII AD oocytes, but which showed opposite directions in treated and untreated MII oocytes. These proteins play a role in diverse mechanisms and processes which are impaired when transcription is inhibited during *in vitro* maturation of the oocyte.

Six proteins were increased during normal, untreated *in vitro* maturation but decreased when transcription was inhibited during maturation. Alongside with the histones HIST1H2BI and HIST1H1C, these proteins include inositol-3-phosphate synthase 1 (ISYNA1), tight junction protein 1 (TJP1), 60S ribosomal protein L22 (RPL22) and pterin-4-alpha-carbinolamine dehydratase (PCBD1). The histone HIST1H2BI is the protein with the strongest abundance alteration in control versus AD-treated MII oocytes (30-fold). It is a member of the histone family H2B, which is, together with H1, H2A, H3 and H4, one of the five main histone proteins responsible for maintaining the structure of the nucleosome. In the present study, seven histones were detected among the set of abundance-altered proteins. In the comparison of GV and MII oocytes, all of them were more abundant after maturation. Strikingly, in the presence of AD only two histones – histone H1.2 and Histone H2B - were found to be altered in abundance, which showed approximately 3.5 times higher expression in GV than in MII oocytes, while they were also around 3.5-fold decreased in

MII AD compared to GV. Regarding control and AD-treated oocytes, besides HIST1H2BI seven more histones from all five histone families were significantly decreased in abundance in the treated group. As ActD is known to bind DNA at the transcription initiation complex consequently preventing elongation of the RNA chain by RNA polymerase (*76*), it apparently results in a strong degradation of certain histones during oocyte maturation.

An interesting protein among the top five proteins higher abundant in control MII than in MII AD oocytes is PCBD1. It was found to be expressed in both mouse and *Xenopus* embryos from early specification onward. It is also a co-activator for hepatocyte nuclear factor 1-alpha (HNF1A)-dependent transcription and evidence was provided that PCBD1 mutations can cause early-onset non-autoimmune diabetes (*119, 120*).

Four proteins were found to be increased around 1.6-fold after maturation compared to GV despite ActD treatment, although they are decreased approximately 1.6- to 1.9-fold after untreated maturation. These are ADP/ATP translocase 1 (SLC25A4), protein S100-B, serine/threonine-protein phosphatase 2A activator (PTPA) and PITH domain-containing protein 1 (PITHD1), all of which are 2.5 to 2.9-fold increased in MII AD compared to MII control oocytes. There is only spatial knowledge about the role of these proteins in the context of oocyte maturation. However, SLC25A4 was identified among a set of polyadenylated transcripts that decreased in abundance during oocyte maturation and was ascribed to GO processes related to energy production. For all four proteins, the question arises, why their abundance increases when it is decreased after uninhibited maturation. A possible explanation is the degradation through proteases during normal IVM: if components of the proteolytic process require *de novo* transcription and are therefore not synthesized in the MII AD group, the level of the protease target proteins remains higher in MII AD oocytes. However, for an increase in abundance compared to GV, novel translation of these proteins is also required. This hypothesis is supported by the results of a DAVID GO of proteins higher abundant in the MII AD than in the MII control group. It revealed, among others, the enriched GO terms “nucleotide excision repair, DNA damage recognition” and “ubiquitin-dependent protein catabolic process”. In eukaryotic cells, the ubiquitin proteasome system is the main route for intracellular protein degradation (*121*). In a comprehensive review, Pomerantz and Dekel (*122*) discussed that several proteins involved in the regulation of the meiotic cell cycle, such as cyclin b, cdc25 and PTTG1 are degraded by the ubiquitin-proteasome system. Cyclin B1, which is known to dimerize with CDK1, one of the key regulators of meiosis, was found to be degraded by the proteasome prior to

cell division (*17, 109, 123, 124*). In addition, proteasomal degradation of PTTG1 was shown to be crucial for segregation of homologous chromosomes at anaphase I (*125*). Furthermore, it has been shown that inhibition of the ubiquitin proteasome pathway prevents the degradation of cyclin B1 and inhibits the extrusion of the second polar body (*126*). Huo et al. (*126*) therefore suggested a major role of the ubiquitin proteasome system in oocyte meiosis, the polar body extrusion and pronuclear formation by the regulation of cyclin B1 degradation and phosphorylation of MAPK/p90rsk. In buffalo oocytes, several proteins related to the ubiquitin-proteasome proteolytic pathway were found to be higher expressed in competent compared to incompetent MII oocytes (*71*). Moreover, it has previously been shown that ubiquitin C-terminal hydrolase-L1 and the proteasome are involved in the first metaphase-to-anaphase transition of meiosis in porcine (*67*) and rat oocytes (*127*).

In conclusion, the holistic proteomic analysis of immature and mature oocytes provides a comprehensive dataset of proteins and their related molecular functions during *in vitro* maturation. The events that occur during nuclear and cytoplasmic maturation were found to be strongly reflected on the proteome level, as major changes in the protein composition were detected after maturation. During maturation, protein synthesis and cell cycle-related proteins and processes were found to be increased. Furthermore, the effect of missing transcription on the proteome during *in vitro* maturation was examined. Addition of actinomycin D during maturation enabled the discovery of proteins either reliant on or independent of *de novo* transcription during maturation. While proteins related to translation and cell-cell adhesion were found to require *de novo* transcription, proteins independent of *de novo* transcription were assigned, among others, to cell cycle and metabolic processes, providing novel insight into *in vitro* maturation on the level of proteins.

5 Side project A: Proteomic analysis of uterine luminal fluid

Original Article: Genetic merit for fertility affects the bovine uterine luminal fluid proteome

The full article is presented on the following pages. The manuscript is accepted for publication at Biology of Reproduction. Supplementary information for this publication are accessible in the supplementary information.

1. Introduction

A significant proportion of embryonic loss in dairy cows occurs quite early after conception. Some studies have indicated that up to 50% of embryos are lost prior to Day 7 (*128*). Wiltbank et al. (*129*) described four pivotal periods for pregnancy loss during the first trimester of gestation in lactating dairy cows, each corresponding to key physiological changes in the embryo, uterine environment, and ovary. These are: (i) during the first week after breeding due to fertilization failure or death of the early embryo (20%-50%), (ii) from Days 8 to 27, encompassing conceptus elongation and maternal recognition of pregnancy with losses averaging ~30%, but ranging from 25%-41%, (iii) from Days 28 to 60, with losses of ~12%, and (iv) during the third month of pregnancy (~2%).

Single trait selection for milk production was highly effective in creating the modern high-yielding dairy cow. However, negative genetic correlations between production and fertility led to a progressive decline in dairy cow fertility (*130-132*). The causes of this subfertility are typically multifactorial and can be due to impacts at the level of the follicle and oocyte, the oviduct and early embryo or the uterus and later embryo/conceptus. The elucidation of the respective contributions of these various players to the reduced fertility in dairy cows associated with intensive selection for milk yield has been the subject of intense research efforts over several decades (*133*). With changes in weightings in selection indices, particularly involving a reduction in the weighting on milk production and an increase in the weighting on fertility, the decline in fertility has begun to be reversed (*134*). In addition, the intensive use of sophisticated ovulation synchronization protocols coupled with timed artificial insemination, particularly in US dairies, has dramatically improved fertility in recent years (*135*). Whether such protocols ultimately mask underlying fertility issues which would be manifest in the absence of such protocols is unclear.

Using a model of Holstein cows with similar genetic merit for milk production traits, but with extremes of good (Fert+) or poor (Fert-) genetic merit for fertility traits, a series of recent studies analyzed the effects of genetic merit for fertility on phenotypic measures of fertility (*136, 137*). Compared with Fert- cows, those with good genetic merit for fertility had reduced incidence of clinical and subclinical endometritis (*138*), stronger expression of estrus (*139*), greater luteal phase progesterone (P4) concentrations (*139, 140*), and better coordination of corpus luteum (CL) and endometrium gene expression to support luteal P4 synthesis and endometrial receptivity (*141*).

The impact of genetic merit for fertility on the composition of uterine lumen fluid (ULF) has not been examined. After hatching from the zona pellucida, the ruminant

conceptus undergoes dramatic elongation and remains unattached in the uterine lumen for up to three weeks prior to initiation of implantation. This elongation process is driven by the maternal uterine environment as it does not occur *in vitro* or in the absence of uterine glands *in vivo* (*142*). To address the question of how the ULF promotes conceptus growth and development, analysis of ULF composition is essential. To date, the ULF proteome has been studied in several species including humans (*143*), sheep (*144-146*) and horses (*147*). In cattle, the ULF proteome has been examined in relation to P4 concentrations and the stage of the estrous cycle (*148*) as well as on Day 7 and Day 13 of the estrous cycle (*149*). Moreover, the ULF protein composition of Day 16 pregnant heifers and the proteome changes between Day 10 and 19 have been examined using a LC-MS/MS-based approach (*150*). Of interest, Faulkner et al. (*151*) compared ULF to blood plasma on Day 7 of the estrous cycle using iTRAQ-based proteomics to determine proteins with higher levels in ULF, which were, among others, related to stress and immune response as well as carbohydrate metabolism.

All of the studies above were carried out in beef heifers, which have not been selected for milk yield. To our knowledge, the effect of genetic merit for fertility on the protein composition of the ULF in dairy animals has not been analyzed. To address this question, an animal model comprising three groups of early pregnant heifers differing in their estimated breeding value (EBV) for fertility, namely Holstein with low and high fertility as well as high fertility Montbéliarde, was established. Using nano -LC-MS/MS analysis combined with a label-free quantification approach, ULF from Day 19 of pregnancy was analyzed, which corresponds to the initiation of implantation, to identify quantitative proteome alterations associated with the genetic predisposition for fertility.

2. Materials and Methods

All experimental procedures involving animals were licensed by the French Ministry for Schools, Higher Education and Research (reference number 02876.02), in accordance with the European Community Directive 2010/63/EU on the Protection of Animals used for Scientific Purposes.

Animal management and ULF sampling

Uterine luminal fluid was analyzed from three groups of heifers: Holstein heifers with low genetic merit for fertility (LFH, EBV for fertility - 0.31 ± 0.24), Holstein heifers with high genetic merit for fertility (HFH, EBV + 0.75 ± 0.18) and high fertility Montbéliarde heifers (MBD, EBV + 0.64 ± 0.20).

The estrous cycles of all heifers were synchronized by insertion of a controlled intravaginal drug-releasing device (PRID DELTA, Ceva Santé Animale, Libourne, France) containing 1.55 g of P4, which was placed in situ for eight days. One day prior to PRID removal, each animal received a 2-ml intramuscular (i.m.) injection of a prostaglandin F2α analogue (PG: Estrumate, MSD Santé Animale, Beaucouzé, France) to regress the endogenous CL. All animals received a 2.5-ml i.m. injection of Receptal (MSD Santé Animale; equivalent to 0.012 mg buserelin) on the morning of Day 0. On Day 7 of the estrous cycle, each animal received one grade 1 late morula/early blastocyst stage embryo derived from superovulated and artificially inseminated MBD donors. Animals were slaughtered on Day 19 at a commercial abattoir and the reproductive tracts were collected within 30 min of knockdown. Each individual tract was stored on ice prior to sample collection. The uterine horns ipsilateral to the CL were flushed with 10 ml of phosphate buffered saline (PBS); pregnancy was confirmed by the presence of an elongated conceptus and the recovered flush volume was noted. The ULF was then clarified by centrifugation (1000 rpm for 10 min at 4 °C) and snap frozen in 1 ml aliquots in liquid nitrogen and stored at -80 °C. For each of the three groups, four biological replicates, which stem from different animals, were analyzed.

Sample preparation

ULF samples were concentrated approximately 3 times using Amicon Centrifugal Filter Devices (Merck, Darmstadt, Germany) with a molecular weight cut-off of 3 kDa. 8 M urea / 0.4 M NH_4HCO_3 was added to the concentrated samples to a final concentration of approx. 7 M urea and samples were lysed by ultrasonicating twelve times for 10 sec

(Bandelin Sonopuls UW3200, Bandelin, Berlin, Germany). Pierce 660 nm Protein Assay (Thermo Scientific, Rockford, IL, USA) was used for protein quantification. Protein cysteine residues were reduced by addition of dithiothreitol to a final concentration of 5 mM dithiothreitol / 0.4 M NH_4HCO_3 at 37 °C for 30 min and subsequent alkylation in 15 mM iodoacetamide / 0.4 M NH_4HCO_3 for 30 min at room temperature in darkness. A trypsin/ lys-C mix (Trypsin/Lys-C Mix, Mass Spec Grade, Promega) was then added for digestion with a final protease to sample protein ratio (w/w) of 1:25 and incubated for 3 h at 37 °C followed by dilution to a final concentration of 1 M urea and overnight incubation at 37 °C. After addition of formic acid to a final concentration of 1%, the solution was dried using a vacuum concentrator and stored at -80 °C.

LC-MS/MS analysis

For analysis, samples were re-dissolved in 0.1% formic acid and separated on a PepMap C18 column (500 mm x 75 µm, 2 µm bead size, Thermo Scientific) using an EASY-nLC 1000 system (Thermo Scientific, Rockford, IL, USA). The flow rate was set to 200 nL/min and the gradient consisted of a first ramp to 25% B (100% acetonitrile, 0.1% FA) within 260 min and a second ramp to 50% B within 60 min. After separation, peptides were analyzed using a LTQ Orbitrap XL instrument (Thermo Scientific, Rockford, IL, USA), which was coupled online to the LC via liquid junction. Electrospray ionization was operated at a needle voltage of 1.9 kV and the MS was run in positive ion mode. Collision induced dissociation spectra were acquired using a collision energy of 35% and acquisition cycles consisted of one full MS scan and five subsequent data dependent MS/MS scans.

Data processing

MaxQuant (version 1.6.1.0) was used for processing the spectral data (Thermo RAW files) applying the implemented label-free quantification (LFQ) option (*56*). MS/MS spectra were searched against the bovine UniProt database (March 2018) using the Andromeda search engine to identify proteins with the ‘match between runs’ option enabled with a match time window of 0.7 min and an alignment time window of 20 min. For protein quantification, unique and razor peptides were used. Trypsin and Lys-C were chosen as enzymes with a maximum of two missed cleavages allowed. As fixed modification, carbamidomethylation was set and oxidation (M) was selected as variable modification. All other parameters were set according to MaxQuant default settings. For further analysis of the dataset, Perseus version 1.5.8.5 was used. After log2 transformation of LFQ intensities,

t-tests of pairwise comparisons between all groups were carried out. Proteins were considered as significantly altered in abundance with a t-test p-value of < 0.05 and a log2-fold change of $> |0.6|$.

Venn diagrams, gene ontology and gene set enrichment analysis

The freely accessible online tools BioVenn (http://www.cmbi.ru.nl/cdd/biovenn/) and Venny 2.1 (http://bioinfogp.cnb.csic.es/tools/venny/) were used for creation of Venn diagrams (*82*). Functional annotation clustering (https://david.ncifcrf.gov) using the Database for Annotation, Visualization and Integrated Discovery (DAVID) was performed for the gene ontology (GO) terms "biological process", "molecular function" and "cellular component" using the integrated *Homo sapiens* dataset as background (*83-85*). The human database was chosen as previously done by Faulkner et al., since it is better annotated than the *Bos taurus* database (*148, 151*).

Gene clusters were considered as significantly enriched with an enrichment score of > 1.3. Significantly higher or lower abundant proteins were analyzed separately for each of the three pairwise comparisons. In addition, using the software GSEA v2.2.2 provided by the Broad Institute (http://software.broadinstitute.org/gsea) (*86, 87*), gene set enrichment analysis (GSEA) was carried out for each comparison between the groups. Therefore, LFQ intensities were loaded into the GSEA software and the following parameters were chosen: Number of permutations: 1000; Collapse dataset to gene symbols: false; Permutation type: gene set; Max size: exclude larger sets: 500; Min size: exclude smaller sets: 5. The following gene sets were chosen for analysis, which are provided by the Broad Institute: c2.cp.kegg.v5.1.symbols.gmt [Curated]; c5.bp.v5.1.symbols.gmt [Gene ontology]; c5.mf.v5.1.symbols.gmt [Gene ontology] and c5.cc.v6.2.symbols.gmt [Gene ontology]. GSEA default values were chosen for all other parameters. Gene sets were considered as significantly enriched with a FDR q-value of less than 0.05.

For a summary and graphical illustration of the GSEA results, GSEA output for gene sets enriched in LFH compared to HFH and MBD, respectively, was submitted to REVIGO, an online tool accessible via http://revigo.irb.hr/ (*88*).

Using the online tool Proteomaps (http://bionic-vis.biologie.uni-greifswald.de/), "Proteomaps" figures were generated from log2-transformed LFQ values of all significantly higher abundant proteins in LFH compared to HFH and/or MBD (*152*).

3. Results

To investigate the influence of the genetic predisposition for fertility on the protein composition of the ULF, a holistic proteomic approach using nano-LC-MS/MS analysis was carried out. A total of 1,737 proteins were identified across the three groups (LFH, HFH, MBD), while 1,120 proteins were commonly detected in each of the three groups, corresponding to 64.5% of all identified proteins (Figure 11A). The largest number of proteins uniquely detected in a single group was found in MBD (285 = 16.4%) followed by LFH (83 = 4.8%), while only 33 proteins were detected exclusively in HFH (= 1.9%).

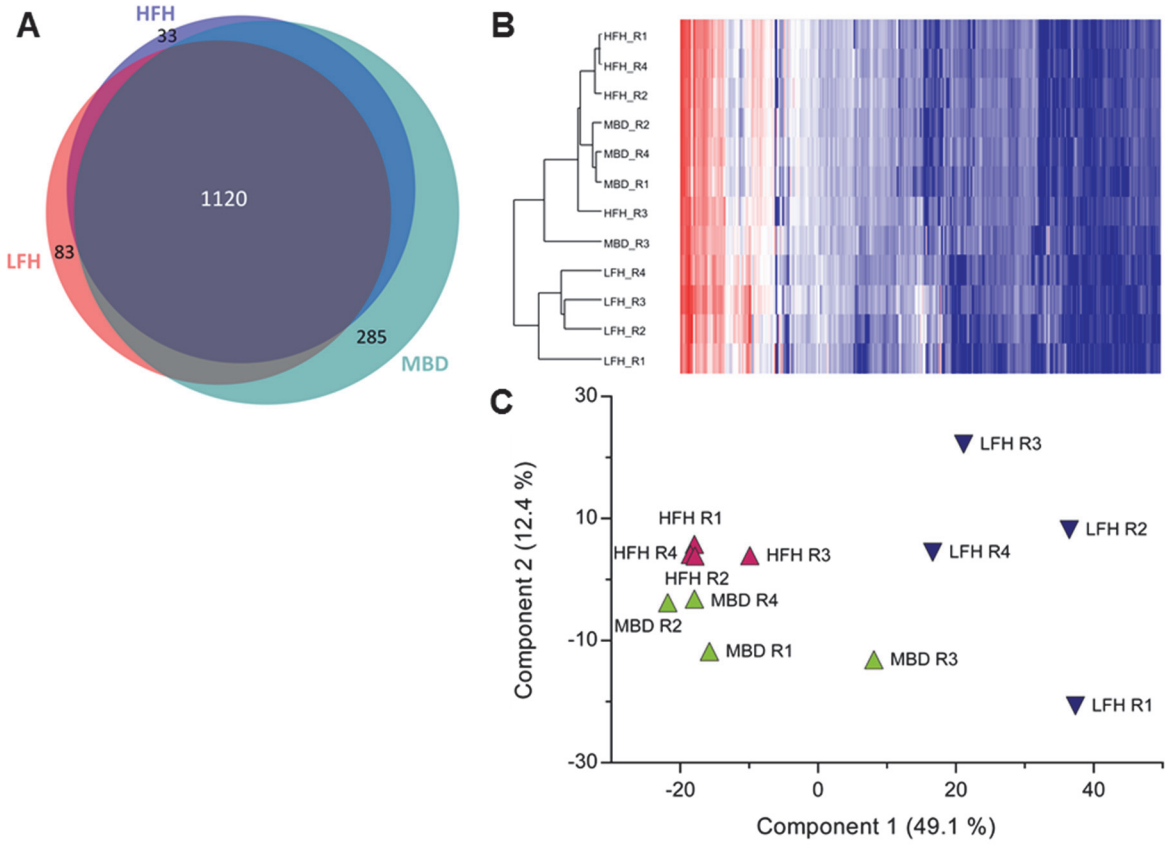

Figure 11: (A) Venn diagram illustrating the overlap of the identified proteins within the three groups LFH, HFH and MBD. 1,120 proteins were detected in all of the three groups, while the highest number of proteins identified in a single group only were found in MBD. **(B) Unsupervised hierarchical clustering and (C) principal component analysis.** PCA and Hierarchical clustering of LFQ values show a clear separation of the low fertility index group LFH from both high fertility index groups HFH and MBD.

Unsupervised clustering (Figure 11B) showed a clear discrimination of the low fertility group (LFH) from both groups with a high fertility index, whereas MBD and HFH were not clearly separated. Principal component analysis (PCA) shows a clear separation of the three groups, especially of LFH and the two groups with high genetic merit for fertility, while

MBD and HFH appeared to be more similar (Figure 11C). The variation among replicates was highest in LFH, intermediate in MBD, and smallest in the HFH group.

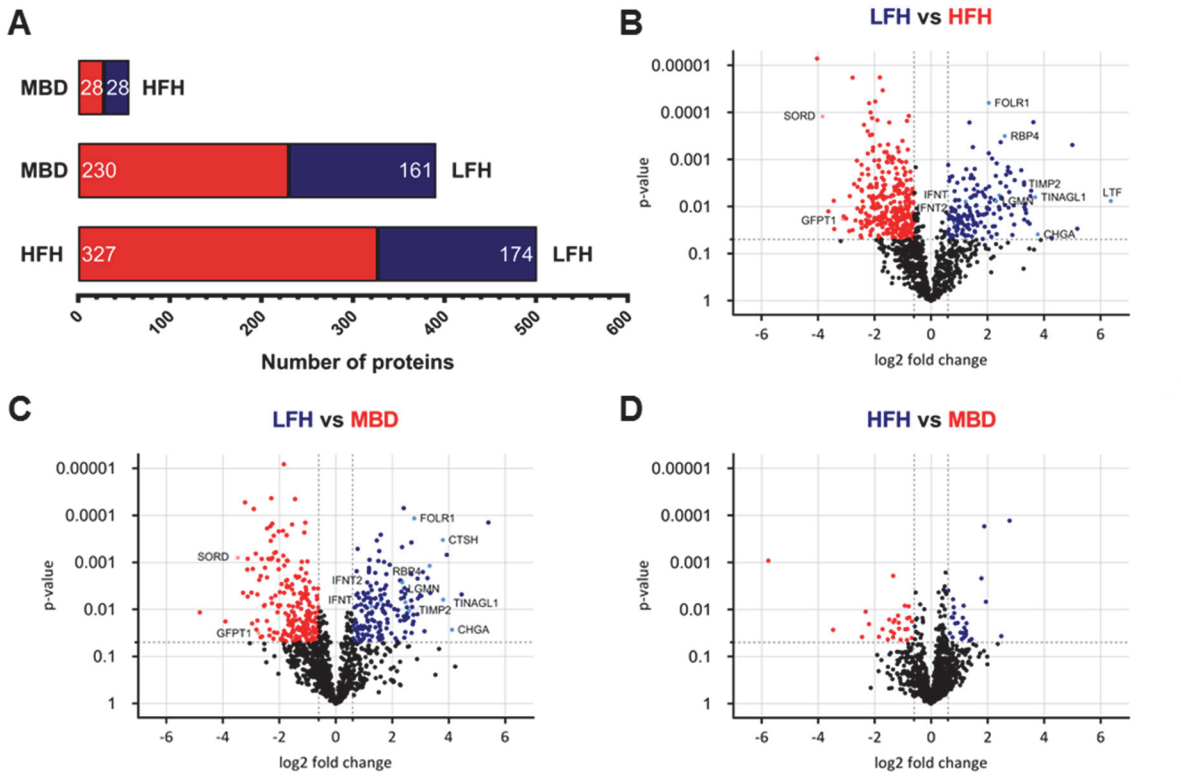

Figure 12: Differentially abundant proteins in each of the three pairwise comparisons. (A) Number of differentially abundant proteins in each comparison. Blue and red segments of the bars represent the number of proteins with higher abundance in the group stated next to the bar. The vast majority of abundance-altered proteins is found between the low (LFH) and the high (HFH and MBD) fertility groups. **(B)-(C)** Volcano plots of the pairwise comparisons. Red spots in the volcano plots represent proteins that show lower abundance in the group that is named first with a log2-fold change < -0.6 and a t-test p-value < 0.05. Blue spots are assigned to proteins with a log2-fold change > 0.6 that are more abundant in the first group compared to the second group. Indicated gene names refer to proteins elaborated in more detail in the discussion section. The respective protein spots are highlighted in the corresponding lighter colors.

Using a label-free quantification approach, quantitative differences in protein abundances in pairwise comparisons were detected. In total, 597 proteins were significantly altered in abundance in all three comparisons, counting proteins only once if they were altered in several comparisons, corresponding to 34.4% of the total number of quantified proteins. The number of abundance-altered proteins for all three pairwise comparisons is shown in Figure 12A. Most abundance alterations were found comparing both high fertility groups MBD and HFH to the LFH group. The vast majority of abundance-altered proteins was detected comparing LFH and HFH (501) followed by LFH versus MBD (391), while only 56 abundance-altered proteins were detected between HFH and MBD. The volcano

plots in Figure 12B to D show the three pairwise comparisons, highlighting proteins of interest. A full list of all identified proteins as well as of abundance-altered proteins in each of the pairwise comparisons is provided in Supplementary tables 1 to 4 of Side project A.

For functional classification of the obtained dataset, DAVID gene ontology and gene set enrichment analyses were carried out with the set of differentially abundant proteins for each of the three comparisons. Regarding the results obtained by the GSEA, gene sets were considered as significantly up-regulated with a false discovery rate (FDR) q-value of less than 0.05. For the comparison of LFH and HFH as well as LFH versus MBD, among the top 20 gene sets higher in LFH were “lysosomal lumen”, “liposaccharide metabolic process”, “dicarboxylic acid metabolic process” and “extracellular space”. A summary of the results of the GSEA is shown in Figure 13B and C, clustering the significantly enriched gene sets in LFH compared to HFH and MBD, respectively, under the corresponding collective term using REVIGO. The complete lists of significantly enriched gene sets in the GSEA results are shown in the Supplementary tables 5 to 7 of Side project A. Among others, the gene sets “ribosome”, “rRNA metabolic process” and “protein targeting to membrane” were enriched in both MBD and HFH compared to LFH. The GSEA for the comparison of HFH to MBD resulted only in enriched gene sets for MBD, including “ribosomal subunit”, “cytosolic ribosome”, “rRNA metabolic process” and “ribosome”, but no significantly enriched gene set for proteins more abundant in HFH.

The “Proteomap” shown in Figure 13A illustrates the processes to which the proteins that were significantly more abundant in LFH compared to either MBD or HFH or both are related. Using DAVID GO, the following GO terms and KEGG pathways were found to be significantly enriched (enrichment score > 1.3) for the abundance-altered proteins using the *Homo sapiens* database: In the comparison of LFH and HFH, terms with the highest enrichment scores for LFH were “lysosome”, “carbon metabolism”, “oxocarboxylic acid metabolism”, “nitrogen compound metabolic process” and “fatty acid beta-oxidation”. The enriched GO terms for the comparison of LFH and MBD were very similar to those of LFH versus HFH, except for “cysteine-type endopeptidase activity”, “glycosaminoglycan degradation”, “valine, leucine and isoleucine degradation” and “immune response”, which were higher in LFH. Regarding the comparison of HFH and LFH as well as MBD to LFH, proteins more abundant in the high fertility groups were found to be related, among others, to the GO terms “translation”, “cell-cell adhesion” and “protein transport”. DAVID GO analysis of the significantly altered proteins of the comparison of HFH and MBD resulted in

no significantly enriched term for HFH and two terms for MBD, namely “cytosol” and “nucleoplasm”. Supplementary tables 8 to 10 of Side project A show a complete list of the significantly enriched GO terms.

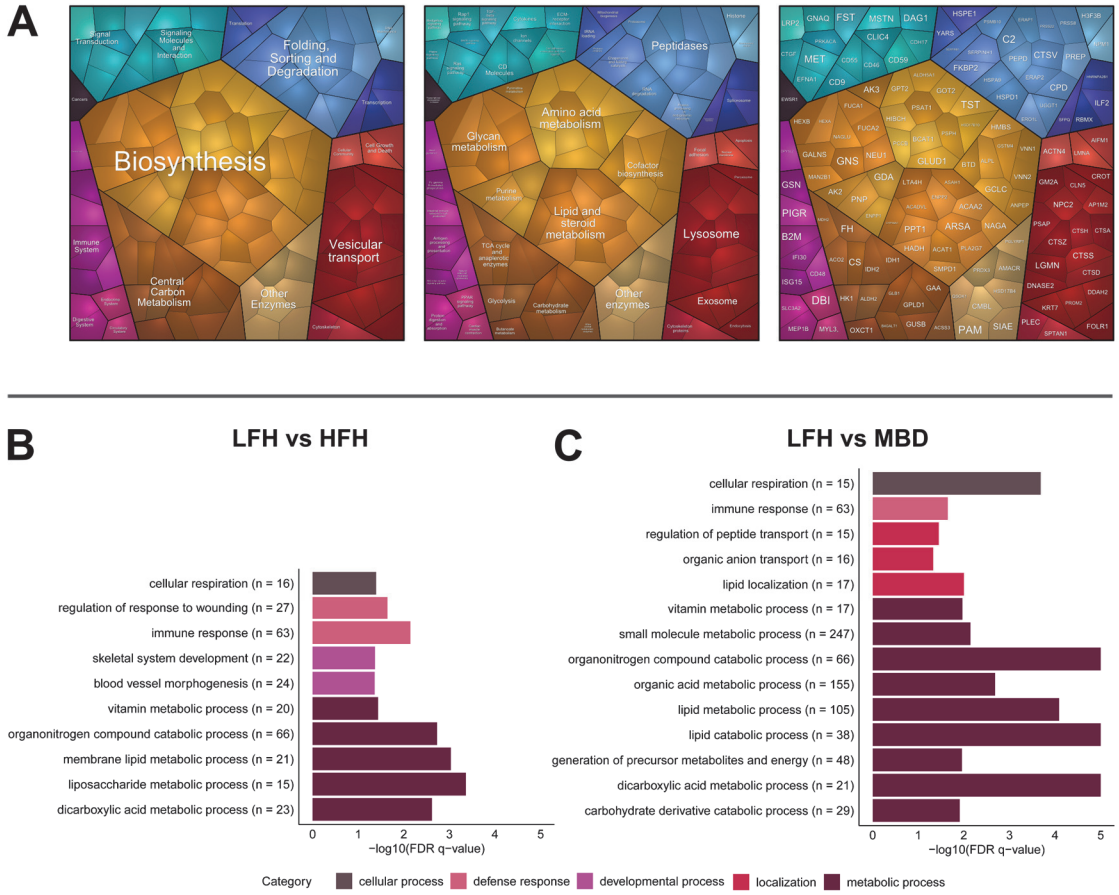

Figure 13: Visualization of affected biological processes. (A) Visualization of proteins that are higher abundant in LFH compared to HFH and MBD and their related biological processes using Proteomaps shows an involvement of these proteins in several metabolic processes. The tiles of the Proteomap are arranged according to the hierarchical KEGG pathway maps. Related functional categories are clustered in adjacent regions with similar colors. Areas of tiles represent protein abundances, weighted by protein size. **(B)-(C) Summary of the results of the GSEA.** Enriched gene sets in LFH compared to HFH **(B)** and MBD **(C)** are clustered in superordinate GO terms using the tool REVIGO. For each set, the number of proteins is depicted in brackets. Identical bar colors correspond to the same umbrella terms stated below the bar.

4. Discussion

Prior to implantation, which is initiated around Day 19 in cattle, growth of the conceptus is dependent on the constituents of the ULF. The impact of genetic merit for fertility on ULF composition has not been described. Therefore, ULF proteins from pregnant animals with different EBV for fertility were analyzed using a LC-MS/MS-based approach. As evident from other proteomic studies (*143, 148, 153*), the analysis of ULF proteome is especially challenging due to its high complexity including very high abundant proteins such as aldose reductase, cystatin or lactotransferrin. However, we identified 1,737 proteins, approximately two-thirds of which were shared between all three groups.

Genetic merit for fertility outweighs the effect of breed on the ULF proteome

To detect quantitative differences between the groups, a commonly-applied label-free quantification approach (*56, 154*) was used to determine proteins that were significantly altered in abundance. Among the set of detected proteins, 597 proteins were found to be differentially abundant in the comparisons within the different groups. As shown in Figure 12, the vast majority of abundance-altered proteins was detected in the comparison of LFH and HFH, followed by LFH compared to MBD with 29% and 23% of all identified proteins significantly altered, respectively. Interestingly, in the pairwise comparison of MBD and HFH, both groups with a positive EBV, only 3% of the identified proteins were altered in abundance. This indicates a strong effect of the genetic predisposition for fertility on the ULF protein composition, since most alterations were detected between the high and low fertility Holstein groups. Furthermore, the effect of the different genetic backgrounds of the two breeds Montbéliarde and Holstein was clearly outweighed by the influence of their genetic merit for fertility, resulting in substantial differences in the ULF proteome. A clear separation of LFH and both high fertility groups is also shown in the unsupervised hierarchical clustering (Figure 11B), as well as in the PCA (Figure 11C), while MBD and HFH were not clearly separated in the hierarchical clustering and also appeared to be more closely related in the PCA. As proteome alterations between MBD and HFH related predominantly to genetic differences between the two breeds, we will focus in the following sections on the comparison of the low fertility group LFH to both high fertility groups HFH and MBD. A similar animal model has previously been analyzed in detail by Cummins et al. (*136, 139, 155*), investigating the impact of the genetic merit for fertility in Holstein cows. Their study comprised two groups of cows with similar proportions of Holstein genetics and

similar genetic merit for milk yield, but with either negative (good genetic merit for fertility; Fert+) or positive (poor genetic merit for fertility; Fert-) EBV for calving interval. They showed that Fert+ cows had higher daily milk yield, shorter calving to conception intervals, fewer services per cow and greater concentrations of circulating insulin, demonstrating a clear influence of the genetic merit for fertility on the reproductive performance. However, none of these papers addressed the effect of the genetic merit for fertility on uterine function. In contrast, the data presented here were obtained from an animal model specifically designed to facilitate the molecular analysis of diverse key reproductive tissues and fluids, such as those in the oviduct (*156*) and, in the current study, in the uterus, in correlation with the EBV of the animals.

Genetic merit for fertility affects proteins related to metabolic processes

Regarding the results of the DAVID GO analysis, in both comparisons - MBD vs. LFH and HFH vs. LFH - proteins more abundant in the ULF of high fertility heifers were found to be associated with the enriched GO terms “translation” and “cell-cell adhesion”. Similar results were obtained by the GSEA. Although a set of ribosomal proteins was also detected in the proteomic ULF studies by others (*145-147, 149, 153, 157*), their origin and role in ULF remains unclear.

Given that the ULF in the current study was collected on Day 19 of pregnancy corresponding with the initiation of implantation in cattle, proteins involved in the GO term “cell-cell adhesion” may play a role in the attachment of the developing conceptus to the endometrium. Previously, transcriptomic studies of bovine endometrium have been conducted to elucidate mechanisms involved in the preparation of the endometrium for attachment and implantation of the embryo. The underlying processes during the preattachment period necessary for pregnancy recognition and implantation in ruminants has been comprehensively reviewed by Forde and Lonergan (*158*), Bauersachs and Wolf (*159*) and Sandra et al. (*160*). Along with several interferon-stimulated genes (ISGs), differentially expressed genes on Day 18 in endometrium of pregnant versus non-pregnant control animals were assigned to processes related to cell adhesion and endometrial remodeling (*159, 161, 162*). Moreover, in a proteomic analysis of porcine endometrial tissue, Jalali et al. (*163*) showed that endometrial proteins with altered abundance on Day 12 in pregnant and non-pregnant animals were, among others, related to growth and remodeling.

Of particular interest, in our dataset one of the proteins with very high abundance alteration between high fertility and low fertility groups was sorbitol dehydrogenase (SORD)

with a 14.3- and 11.1-fold increase in HFH and MBD compared with LFH, respectively. SORD, which is known to be located in the extracellular space, is required for the conversion of glucose to fructose by oxidation of sorbitol and has been shown to be expressed in porcine uterine glandular and luminal epithelia during the peri-implantation period (*164*). Consistent with these observations, Simintiras et al. (*165*) described a 15-fold increase in mannitol/sorbitol in the ULF of heifers from Day 12 to 14, coinciding with the initiation of elongation, and a 29-fold increase in mannitol/sorbitol in the ULF on Day 12 in heifers with supplemented with P4 – a model known to accelerate conceptus elongation (*166*). Among the proteins with the most pronounced abundance alterations in HFH and MBD in comparison to LFH (8.7 and 6.7 times higher, respectively) was glutamine-fructose-6-phosphate aminotransferase 1 (GFPT1), which also plays a role in glucose metabolism. GFPT1 is an enzyme of the hexosamine pathway catalyzing the formation of glucosamine 6-phosphate. Both proteins have previously been detected in equine uterine fluid (*167*), as well as in human (SORD) (*153*) or ovine (GFPT1) (*145*) uterine fluid. The finding is in agreement with Forde et al. (*150*) who analyzed the ULF proteome in pregnant heifers, finding that fructose and mannose metabolism was among the overrepresented pathways on Day 16.

Intriguingly, DAVID GO analysis of LFH comparisons to HFH and MBD revealed several significantly enriched GO terms associated with basic metabolic processes, such as “carbon metabolism”, “fatty acid metabolism” and “oxocarboxylic acid metabolism” (Supplementary tables 8 and 9 of Side project A). The results of the GSEA confirmed these findings, as a remarkable amount of gene sets enriched in LFH compared to MBD and HFH are related to metabolic and catabolic processes, such as “liposaccharide metabolic process”, “lipid catabolic process”, “organic acid catabolic process” and “dicarboxylic acid metabolic process” (Supplementary tables 5 and 6 of Side project A).

The results of the gene set enrichment and DAVID GO analysis were confirmed using the Proteomaps tool (Fig 13A). As already evident from the DAVID GO analysis and the GSEA, the main process represented was “biosynthesis”, with the subordinate processes “amino acid metabolism”, “lipid and steroid metabolism” and “glycan metabolism”. Notably, the GSEA also showed that a considerable number of enriched gene sets in LFH compared to MBD and HFH were catabolic processes, indicating a disturbed metabolic condition of the animals within this group. Together with the previous finding that enzymes involved in glucose metabolism are more abundant in the high fertility groups, this hints at an impaired metabolism in animals with poorer genetic merit for fertility.

The data reported here are consistent with other studies analyzing ULF proteomes. For example, Forde et al. (*150*) found metabolic processes, including the GO terms "generation of precursor metabolites and energy" and "monosaccharide metabolic process", to be overrepresented on Day 16 in pregnant vs cyclic heifers. It has also been shown that proteins involved in carbohydrate metabolism were more abundant during the early compared to the late luteal phase in beef heifers (*148*). This effect was ascribed to the adaptation of the uterus to the metabolic requirements of the embryo during the preimplantation period. The increased metabolic activity of the endometrium during pregnancy was also reflected in the findings of Ledgard et al. (*168*), who reported that proteins involved in biosynthetic pathways were more abundant in pregnant compared to non-pregnant cows. Moreover, it has been shown that proteins associated with carbohydrate metabolism are more abundant in uterine fluid compared to plasma, as embryonic growth is accompanied by changes in energy utilization and protein synthesis (*151, 169, 170*). In addition, the bovine embryo depends on the uterine environment until implantation to provide it with sufficient amounts of nutrients including amino acids, growth factors and ions (*169*).

"Vitamin metabolic process" is one of the gene sets significantly enriched in the GSEA of LFH compared to both HFH and MBD. This gene set comprises, among others, folate receptor alpha (FOLR1) and legumain (LGMN), which have both been previously described in uterine fluid and/or endometrium. In LFH, FOLR1 was around four times more abundant compared to HFH and 10 times more abundant when compared to MBD. FOLR1 may play a role in the transfer of folate to the embryo, as it is well known that folate is essential during pregnancy due to its importance for DNA synthesis (*171*). It has been found to be more abundant in uterine fluid compared to plasma on Day 7 of the estrous cycle in beef heifers (*151*), hinting at an active regulation of this protein in ULF by the endometrium. In the present study, LGMN was found to be 5.0 times higher in LFH compared to HFH and MBD. The protease LGMN has been found to be more abundant on Day 13 compared to Day 7 of the estrous cycle in bovine histotroph (*149*) and its mRNA expression in the bovine endometrium was upregulated in the endometrium in the luteal phase and therefore concluded that it is controlled by P4 (*168*). In addition, they reported lower abundance of LGMN in ULF in non-pregnant compared to pregnant cows together with retinol-binding protein (RBP) and tissue inhibitor of matrix metalloproteinase 2 (TIMP2), both of which have also been found to be around five to six-fold more abundant in LFH compared to HFH as well as MBD. TIMP2 was also detected on Day 18 in pregnant and non-pregnant heifers

by Ulbrich et al. (*172*), who suggested an involvement of TIMP2 in maternal recognition of pregnancy.

LGMN is, together with chromogranin A (CHGA), also assigned to the lysosome and lysosomal lumen. Although lysosomes are intracellular organelles, serving as the cell's digestive system, the GO term "lysosome" had the highest enrichment score in LFH compared to the two high fertility groups. Regarding the proteins assigned to this term, we found several proteins which were annotated as "extracellular region" or "extracellular space" or contained a signal peptide that allows the secretion through secretory vesicles (*173*), indicating that these proteins play a role in the uterine fluid. In addition to LGMN and CHGA, several cathepsins, e.g. CTSA, CTSL, CTSB and CTSZ, were among the lysosome related proteins in the GSEA and the DAVID GO analysis, which are also known to occur extracellularly. In a proteomic analysis of ULF performed by Forde et al. (*150*), the lysosome was also among the top KEGG pathways overrepresented in ULF on Day 16 in pregnant cows, comprising also legumain precursor as well as precursors of cathepsin B, D, S and Z. Besides their role in catabolism of intracellular proteins, the proteinases cathepsins are able to degrade proteins from the extracellular matrix and may regulate endometrial remodeling and conceptus implantation (*174, 175*).

Alterations of immune system-related proteins are associated with a low fertility index

Further evaluation of the set of abundance-altered proteins revealed that immune system-related GO terms, namely "immune response", "adaptive immune response", "innate immune response" and "complement and coagulation cascades" were enriched in LFH compared to HFH and MBD in both DAVID GO analysis and GSEA. Several studies have previously described that proteins associated with the immune system play a role in uterine fluid. In ewes, 22% of the identified proteins were related to the immune system and two of 15 abundance-altered proteins between pregnant and non-pregnant animals were members of the complement component system, which plays a role in embryonic as well as host protection (*144*). Moreover, Forde et al. (*150*) found that proteins in the ULF from Day 16 pregnant heifers were related with the GO terms "response to stimulus" and "complement and coagulation cascades" and concluded that this is related with the response to pregnancy recognition, as sufficient amounts of IFNT must be produced by about Day 16 to prevent luteolysis. Immune system-related proteins, e.g., lactotransferrin, have also been found to be increased in the uterus in ewes during the luteal phase of the estrous cycle (*145*). A study by

Faulkner et al (*151*), comparing uterine and plasma proteome of beef heifers on Day 7 of the estrous cycle, showed that predominant uterine proteins were also related to the immune system.

It is well known that regulation of immune system processes during the peri-implantation phase is a prerequisite for successful establishment of pregnancy. In human endometrial secretions prior to embryo transfer, Boomsma et al. (*176*) identified ten mediators of the immune system, among them four interleukins, macrophage inhibitory factor and tumor necrosis factor. Proteins involved in immune system-related processes were found to be more highly abundant in LFH compared to both HFH and MBD in our study, suggesting that animals with a low fertility index may suffer from a dysregulation of the defense response, possibly contributing to reduced fertility in this group.

Among the proteins associated with the immune system are those exhibiting extreme abundance alterations, such as lactotransferrin (LTF), chromogranin A (CHGA) or tubulointerstitial nephritis antigen-like 1 (TINAGL1). LTF exhibited the highest difference in abundance with an 83-fold increase in LFH compared to HFH. In addition, it was among the five most abundant proteins in all ULF samples. LTF, an extracellular protein that is found in exocrine fluids, is an iron-binding protein with antimicrobial activity involved in the host defense. It has been detected in several studies analyzing bovine (*151, 177*), ovine (*145, 147*) as well as equine ULF (*167*).

Similar to LTF, CHGA also has antimicrobial properties and is associated with immune system processes (*178*). It was 14-fold higher abundant in LFH compared to HFH and 17-fold increased compared to MBD. In addition to its antimicrobial function, CHGA has also been shown to play a role in regulating calcium and glucose metabolism (*179*). Using an LC-MS/MS-based proteomic approach, Mullen et al. (*149*) identified CHGA in bovine histotroph where it was found to be enriched on Day 13 compared to Day 7 of the estrous cycle, and hypothesized that CMGA in the uterus may also influence inflammatory pathways or regulate cell proliferation and metabolism at the embryo level.

TINAGL1 is another extracellular protein that plays a role in the immune response and which was significantly altered in our study. It was found to be 13 times more abundant in LFH compared to HFH and 14-fold higher compared to MBD. Forde et al. (*180*) have previously shown that TINAGL1 showed minimal endometrial gene expression from Day 7 to 13, when the uterus is not receptive, but increased on Day 16, especially in pregnant, but also in cyclic heifers (*180*). These authors concluded that endometrial TINALG1 plays a role

in implantation but is not directly involved in conceptus elongation. However, they failed to detect TINAGL1 protein in ULF.

Of interest, interferon-tau variant 3h (IFNT) and interferon tau-2 (IFNT2) were both approximately 2- to 3-fold more abundant in LFH compared to HFH and MBD. Interferon tau is well known to be the primary pregnancy recognition signal in cattle (reviewed by Hansen et al. (*181*)). IFNT is secreted by the mononuclear trophectoderm cells of the conceptus, beginning at the blastocyst stage, increases during trophoblast elongation and declines during the peri-attachment period (*182, 183*). The secretion of sufficient amounts of IFNT is crucial to suppress luteolysis and maintain CL function, which is required for P4 secretion and thus for growth and development of the conceptus (*184, 185*). It has been shown by microarray analyses that ISGs together with immune response-related genes were within the top up-regulated gene sets in Day 17 pregnant compared to non-pregnant cows (*186*). Successful establishment of pregnancy requires a balance of pro- and anti-inflammatory molecules to ensure functionality of the maternal immune system against pathogens and simultaneously preventing a rejection of the conceptus, which can be regarded as a semi-allograft. Accordingly, Bauersachs et al. (*161*) showed that transcript levels of genes involved in the modulation of the maternal immune system were elevated in endometrium samples from Day 18 pregnant compared to non-pregnant heifers. Among the mRNAs with higher abundance were also several that are induced by interferons. Thus, insufficient IFNT secretion and consequently compromised IFNT signaling are therefore likely to lead to deficiencies during pregnancy recognition and subsequent implantation of the conceptus into the uterus. Insufficient IFNT secretion might result from a decreased conceptus size or from impaired endometrial secretion.

In conclusion, results of this study demonstrate a major impact of the EBV for fertility on the quantitative protein profile of ULF. Most interestingly, differences in the genetic background of the two breeds studied – Montbéliarde and Holstein – are far less pronounced than the influence of the fertility status, since the vast majority of altered proteins was detected between low and high fertility groups, irrespective of breed. We found an increase of proteins related to metabolic processes, supporting the hypothesis that a disturbed metabolism in the uterus may affect reproductive success. Moreover, a large number of abundance alterations were found to be associated with the immune response in the low fertility group, suggesting an involvement of the immune system in the impaired fertility in such animals.

6 Side project B: Proteomic analysis of bovine oviduct fluid

Original Article: Influence of metabolic status and genetic merit for fertility on proteomic composition of bovine oviduct fluid

The full article is presented on the following pages and listed under the Pubmed ID 31347661. Supplementary information for this publication is accessible via the Biology of Reproduction homepage and in the Supplementary information.

Biology of Reproduction, 2019, 1–13
doi:10.1093/biolre/ioz142
Research Article
Advance Access Publication Date: 26 July 2019

OXFORD

Downloaded from https://academic.oup.com/biolreprod/advance-article-abstract/doi/10.1093/biolre/ioz142/5539041 by Universitaetsbibliothek Muenchen user on 17 October 2019

Research Article

Influence of metabolic status and genetic merit for fertility on proteomic composition of bovine oviduct fluid†

Katrin Gegenfurtner[1], Thomas Fröhlich[1], Miwako Kösters[1], Pascal Mermillod[2], Yann Locatelli[2], Sébastien Fritz[3], P. Salvetti[3], Niamh Forde[4], Patrick Lonergan[5], Eckhard Wolf[1,6] and Georg J. Arnold[1,*]

[1]Laboratory for Functional Genome Analysis (LAFUGA), Gene Center, LMU Munich, Munich, Germany [2]Institut National de Recherche Agronomique (INRA), UMR7247, Physiologie de la Reproduction et des Comportements, Nouzilly, France [3]Allice, Station de Phénotypage, Nouzilly, France [4]Division of Reproduction and Early Development, School of Medicine, University of Leeds, Leeds, UK [5]School of Agriculture and Food Science, University College Dublin, Dublin 4, Ireland [6]Chair for Molecular Animal Breeding and Biotechnology, Gene Center and Department of Veterinary Sciences, LMU Munich, Munich, Germany

***Correspondence:** Laboratory for Functional Genome Analysis (LAFUGA), Gene Center, LMU Munich, Munich, Germany. Tel: +4989218076825; E-mail: arnold@genzentrum.lmu.de

†**Grant Support:** This research was funded by the European Union Seventh Framework Programme FP7/2007-2013 under grant agreement no. 312097 ('FECUND').
‡**Conference Presentation:** Presented in part at the 5th International Conference on Analytical Proteomics, 3–6 July 2017, Caparica, Portugal, and the 44th IETS Annual Conference, 13–16 January 2018, Bangkok, Thailand.

Received 21 December 2018; Revised 3 April 2019; Accepted 22 July 2019

Abstract

The oviduct plays a crucial role in fertilization and early embryo development providing the microenvironment for oocyte, spermatozoa, and early embryo. Since dairy cow fertility declined steadily over the last decades, reasons for early embryonic loss have gained increasing interest. Analyzing two animal models, this study aimed to investigate the impact of genetic predisposition for fertility and of metabolic stress on the protein composition of oviduct fluid. A metabolic model comprised maiden Holstein heifers and postpartum lactating (Lact) and non-lactating (Dry) cows, while a genetic model consisted of heifers from the Montbéliarde breed and Holstein heifers with low- and high-fertility index. In a holistic proteomic analysis of oviduct fluid from all groups using nano-liquid chromatography tandem-mass spectrometry analysis and label-free quantification, we were able to identify 1976 proteins, among which 143 showed abundance alterations in the pairwise comparisons within both models. Most differentially abundant proteins were revealed between low fertility Holstein and Montbéliarde (52) in the genetic model and between lactating and maiden Holstein (19) in the metabolic model, demonstrating a substantial effect of genetic predisposition for fertility and metabolic stress on the oviduct fluid proteome. Functional classification of affected proteins revealed actin binding, translation, and immune system processes as prominent gene ontology (GO) clusters. Notably, Actin-related protein 2/3 complex subunit 1B and the three immune system-related proteins SERPIND1 protein, immunoglobulin kappa locus protein, and Alpha-1-acid glycoprotein were affected in both models, suggesting that abundance changes of immune-related proteins in oviduct fluid play an important role for early embryonic loss.

© The Author(s) 2019. Published by Oxford University Press on behalf of Society for the Study of Reproduction. All rights reserved. For permissions, please e-mail: journals.permissions@oup.com

Summary Sentence

Protein composition of oviduct fluid—the natural environment for the early embryo—depends on metabolic status and genetic predisposition of dairy cows, affecting, among others, proteins related to immune response.

Key words: domestic animal reproduction, early development, fallopian tubes, female reproductive tract, fertility, oviduct, proteomics, ruminants.

Introduction

The oviduct provides a unique environment in terms of metabolites, proteins, steroid hormones, and ions [1–5]. Several crucial steps for successful pregnancy establishment occur in the oviduct. Initially, the oviduct captures the oocyte at ovulation, transports, selects and stores the sperms, and regulates fertilization. Following fertilization, the first mitotic cleavage divisions also occur in the oviduct, the timing of which has consequences for the developmental potential of the embryo [6]. Furthermore, the switch from maternal to embryonic control of development, so-called embryonic genome activation [7, 8], occurs at the 8- to 16-cell stage in cattle between 3 and 4 days after fertilization when the embryo is still in the oviduct. Thus, there is a significant potential for the oviduct environment to influence the development of the embryo as it passes through its way to the uterus.

Indeed, significant evidence exists demonstrating a positive effect of oviduct secretions on the embryo. While it is possible to produce embryos in vitro, the quality of the embryos produced is significantly lower than those derived in vivo, as evidenced by differences in morphology, gene expression signatures, and cryotolerance [9, 10]. Developing in vitro produced embryos transiently in the sheep oviduct [11] or in vitro in the presence of bovine oviduct epithelial cells (BOEC) has been shown to improve their quality [12].

To understand how the oviduct fluid (OF) influences the gametes, the process of fertilization and the early embryonic development, insight into the proteomic profile of the OF is a prerequisite. The technical evolution of liquid chromatography tandem-mass spectrometry (LC-MS/MS)-based proteomics enables an increasingly comprehensive analysis of OF protein composition.

The bovine OF proteome has been analyzed in relation to the stage of the estrous cycle and the location relative to the corpus luteum (CL) [4]; differentially expressed proteins were mainly associated with cellular and metabolic processes. Another study analyzing the secretome of in vivo and in vitro cultured BOECs reported that the majority of secreted proteins are growth factors, metabolic regulators, enzymes, immune modulators, and extracellular matrix components [13]. Functional analysis of the proteins revealed an involvement in immune homeostasis, gamete maturation, fertilization, and the early embryonic development. In addition, several studies have been carried out showing that the composition of OF is dynamic and undergoes constant change depending on the stage of the cycle or the presence of gametes, zygotes, or early embryos [14–16]. A comprehensive overview of these studies was given by Maillo et al. [17]. However, data on the effects of lactation or genetic fertility index on the composition of OF are currently lacking.

The physiological changes associated with high milk production are related to poor reproductive efficiency in commercial dairy herds. Decreasing levels of glucose, insulin, and Insulin-like growth factor 1 (IGF1) or increasing levels of non-esterified fatty acids (NEFA) and ketone bodies circulating during nutrient partitioning are associated with low body condition score (BCS) and undoubtedly play a role in determining reproductive outcome. However, understanding the causes of infertility in dairy cattle is complex and may also be attributable to compromised oocyte quality and/or a suboptimal reproductive tract environment incapable of supporting normal embryo/conceptus development or a combination of both. Furthermore, genetic effects on physiological characteristics influencing fertility have been well described [18–20].

Interestingly, data from nonsurgical flushing of single-ovulating high-producing dairy cows indicate that about 50% of embryos degenerate by Day 7 after breeding, that is, shortly after leaving the oviduct [21, 22]. Furthermore, embryo development to Day 7 following endoscopic transfer of in vitro produced 3–4-cell embryos into the oviducts of postpartum lactating cows was compromised in comparison with that in the tract of nulliparous heifers [23]. More recently, age-matched postpartum primiparous dairy cows that were either milked post calving (i.e., lactating) or were dried off immediately at calving (i.e., non-lactating) were used to directly test the effects of lactation on postpartum fertility characteristics [24]. Consistent with the results of Rizos et al. [25], development to blastocyst was reduced after embryo transfer to the oviducts of lactating cows compared with non-lactating cows or heifers [24], suggesting an impaired oviduct environment due to the metabolic stress associated with lactation.

In this study, we hypothesized that differences in fertility are in part due to metabolic status (heifers vs. non-lactating vs. lactating cows) and genetic merit for fertility (high vs. low fertility heifers). Furthermore, we hypothesized that differences in the composition of OF are associated with a compromised ability to support early embryo development. We have previously characterized the metabolic status of age-matched postpartum primiparous dairy cows that were either lactating or non-lactating as well as a contemporaneous group of non-pregnant heifers [26]. Thus, two animal models were established, each comprising three groups of animals that differed on the one hand in their level of metabolic stress and on the other hand in their fertility index. In a subset of animals from each group, we collected OF on Day 3 of a synchronized estrous cycle and performed quantitative protein profiling using nano-LC-MS/MS in order to identify protein abundance changes associated with the reduced early embryo survival in lactating cows.

Materials and methods

All experimental procedures involving animals were sanctioned by the Institutional Animal Research Ethics Committee and were licensed in accordance with Statutory Instrument No. 543 of 2012 under Directive 2010/63/EU on the Protection of Animals used for Scientific Purposes.

Animals and oviduct fluid collection

Oviduct fluid from two different animal models was analyzed. The metabolic model, consisting of maiden Holstein (MH)-Friesian heifers and postpartum lactating (Lact) and non-lactating (Dry) Holstein-Friesian cows, has previously been described in detail

Downloaded from https://academic.oup.com/biolreprod/advance-article-abstract/doi/10.1093/biolre/ioz142/5539041 by Universitaetsbibliothek Muenchen user on 17 October 2019

[27]. In short, in-calf primiparous Holstein-Friesian heifers and non-pregnant Holstein-Friesian heifers with a similar economic breeding index (EBI = 140.6€ ± 20.4€) were enrolled into the study. At calving, cows were randomly assigned to one of the two groups, lactating or non-lactating. From calving, animals in the lactating group were milked twice a day (07:00 and 16:00 h), while those in the non-lactating group were dried off immediately after calving (i.e., never milked).

The genetic model comprised low fertility Holstein (LFH) heifers with an estimated breeding value (EBV) for heifer's fertility of −0.31 ± 0.24, high fertility Holstein (HFH) heifers with an EBV of +0.75 ± 0.18, and French Montbéliarde (MBD) heifers with an EBV for reproduction of +0.64 ± 0.20. The estrous cycles of all animals were synchronized using a controlled intravaginal drug device (PRID DELTA, Ceva Santé Animale, Libourne, France) containing 1.55 g of progesterone (P4) inserted for eight days. One day prior to PRID DELTA removal, each animal received a 2-ml intramuscular injection (i.m.) of a prostaglandin F2α analog (PG: Estrumate, MSD Santé Animale—Intervet, Beaucouzé, France; equivalent to 0.5 mg cloprosténol) to regress the endogenous CL. Animals were observed and monitored for estrus behavior (Day 0). All animals were slaughtered in a commercial abattoir on Day 3 after estrus. The oviducts were cleaned of surrounding tissues, separated at the isthmus/ampulla junction, and 500 µl of phosphate buffered saline (10 mM phosphate buffer, 2.7 mM potassium chloride, 137 mM sodium chloride, pH 7.4) was injected into the isthmic part of the oviduct. Oviduct fluid was then collected by gentle pressing of the oviduct. Oviductal cells were separated from the OF by centrifugation at 200*g* for 10 min and the supernatants were then centrifuged at 12 000*g* for 10 min. The remaining supernatants were collected and stored at −80 °C. Four biological replicates per group were analyzed for the genetic model and five for the metabolic model.

Sample preparation

Oviduct fluid samples were dried using a vacuum concentrator. Lyophilisates were redissolved in 8 M urea/0.4 M NH_4HCO_3 and ultrasonicated 12 times for 10 s (Bandelin Sonopuls UW3200, Bandelin, Berlin, Germany). Protein amounts were quantified using Pierce 660 nm Protein Assay (Thermo Scientific, Rockford, IL, USA). Samples were prepared for LC-MS/MS analysis by reduction of cysteine residues during 30 min of incubation in 5 mM dithiothreitol/0.4 M NH_4HCO_3 at 37 °C, followed by alkylation in 15 mM iodoacetamide/0.4 M NH_4HCO_3 for 30 min at room temperature in darkness. For enzymatic digestion, a Trypsin/Lysyl endopeptidase (Lys-C) mix (Mass Spec Grade, Promega) was added with a final protease to sample ratio (w/w) of 1:25 and incubated for 3 h at 37 °C to perform the Lys-C reaction. To facilitate trypsin digestion, samples were diluted to a final concentration of 1 M urea and incubated overnight at 37 °C. Formic acid (FA) was added to a final concentration of 0.6% and the solution subsequently dried using a vacuum concentrator.

Liquid chromatography tandem-mass spectrometry analysis

Digested protein samples were redissolved in 0.1% FA and separated using an EASY-nLC 1000 system (Thermo Scientific, Rockford, IL, USA), and a PepMap C18 column (500 mm × 75 µm, 2 µm bead size, Thermo Scientific) at a constant flow rate of 200 nl/min. The gradient consisted of a ramp to 25% B (100% acetonitrile, 0.1% FA) within 320 min and a second ramp to 50% B within 120 min in the case of the samples from the energy balance model. Samples from the genetic merit model were separated using a time-optimized gradient with a ramp to 25% B within 260 min and a second ramp to 50% B within 60 min. The chromatographic system was coupled online to an LTQ Orbitrap XL instrument (Thermo Scientific, Rockford, IL, USA) via liquid junction. The mass spectrometer was run in positive ion mode and the electrospray ionization was operated at a needle voltage of 1.9 kV. For data acquisition, collision-induced dissociation spectra were acquired using a collision energy of 35%. Acquisition cycles consisted of one full MS scan followed by five data dependent MS/MS scans.

Data processing

Spectral data (Thermo RAW files) were processed using MaxQuant version 1.5.2.8 and the implemented label-free quantification (LFQ) option [28]. For protein identification, MS/MS spectra were searched against the bovine UniProt database (July 2015) using the Andromeda search engine. The "match between runs" option was enabled with a match time window of 0.7 min and an alignment time window of 20 min. Unique and razor peptides were used for protein quantification. Trypsin and Lys-C were chosen as enzyme with maximum of two missed cleavages allowed. Carbamidomethylation was selected as fixed modification and oxidation (M) was used as variable modification. All other parameters were set according to MaxQuant default settings.

Further data analysis was performed using Perseus version 1.5.1.6. Label-free quantification intensities of precursor ions were log2 transformed and *t*-tests of pairwise comparisons between all groups within the metabolic and the genetic model were carried out. Proteins were considered as significantly altered in abundance with a *t*-test *P*-value of less than 0.05 and a log2-fold change of $>|0.6|$.

Venn diagrams, gene ontology, and gene set enrichment analysis

Venn diagrams were created using the freely accessible web application BioVenn provided on http://www.biovenn.nl/ [29]. Database for Annotation, Visualization and Integrated Discovery (DAVID) functional annotation clustering (https://david.ncifcrf.gov) was performed with all 143 proteins which exhibited significantly altered abundance for the GO terms "biological process," "molecular function," and "cellular component" using the integrated *Bos taurus* dataset as background [30–32]. Gene clusters of related biological functions showing an enrichment score above 1.3 were considered as relevant. Since in the metabolic model the overall number of proteins showing abundance alterations was not sufficiently large for meaningful annotation clustering, abundance-altered proteins from the metabolic model and the genetic model were pooled for this analysis.

Gene set enrichment analysis (GSEA) was carried out using the software GSEA v2.2.2 provided by the Broad Institute (http://software.broadinstitute.org/gsea/) [33, 34]. Label-free quantification intensities of all proteins identified in the two groups of the respective pairwise comparison were loaded into the GSEA software and the following parameters were set: number of permutations: 1000; collapse dataset to gene symbols: false; permutation type: gene set; max size: exclude larger sets: 500; and min size: exclude smaller sets: 5. As GSEA is based on LFQ values of the identified proteins, it is only applicable to pairwise comparisons and was therefore performed for all groups within each of the two models.

Downloaded from https://academic.oup.com/biolreprod/advance-article-abstract/doi/10.1093/biolre/ioz142/5539041 by Universitaetsbibliothek Muenchen user on 17 October 2019

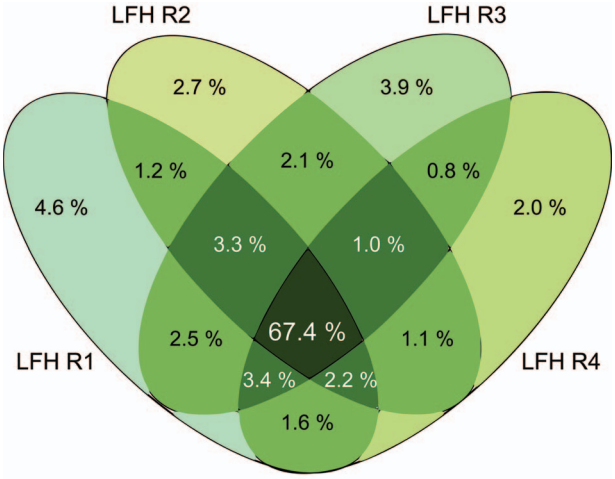

Figure 1. Venn Diagram showing the overlap of the quantified proteins within the four replicates of the LFH group. About 67.4% of all proteins were found in every replicate of the LFH group and less than 5% were detected exclusively in one replicate showing good conformance of the samples and the sample generation.

Among the databases provided by the Broad Institute, the following gene sets were chosen for analysis: c2.cp.kegg.v5.1.symbols.gmt [Curated]; c5.bp.v5.1.symbols.gmt [Gene ontology]; and c5.mf.v5.1.symbols.gmt [Gene ontology]. All other parameters were set to GSEA default values. Gene sets with a false discovery rate (FDR) *q*-value of less than 0.05 were considered as significant.

"Proteomaps" graphics were generated from log2-transformed LFQ values of all significantly altered proteins using the online tool Proteomaps (http://bionic-vis.biologie.uni-greifswald.de/) [35].

For prediction of signal peptide cleavage sites, FASTA sequences of the proteins of interest were submitted to the SignalP 4.1 server, accessible via http://www.cbs.dtu.dk/services/SignalP/. A default *D*-cutoff value of 0.45 was applied [36].

Results

A total of 1622 proteins (FDR < 1%, two individual peptides) were identified in the OF from the isthmus ipsilateral to the CL from all samples of the genetic model. To get insight into the reproducibility of the proteomic analysis as well as of the sample generation, we examined the distribution of the identified proteins within the four biological replicates of each group. As an example, a Venn diagram of the four replicates of the LFH group with the relative number of identified proteins is shown in Figure 1. In each of the four biological replicates, less than 5% of the proteins were detected exclusively in the respective sample. The vast majority (almost 87%) of all proteins was identified in at least two replicates, while 876 proteins (67.4%) were found in each replicate.

The Venn diagram in Figure 2A shows the distribution of the identified proteins among the three groups MBD, LFH, and HFH. A total of 1058 proteins (65.1%) were found in all three groups. Of the total proteins, 5.9% (95 proteins) were solely found in the HFH samples and 5.7% (92 proteins) solely in the LFH group, while the highest fraction of proteins identified exclusively in a single group (12.9%, 209 proteins) was detected in the MBD group. A principal component analysis (PCA) of all replicates of the genetic model is shown in Figure 3. The OF samples of the LFH group clustered separately from those of the HFH group. In contrast, the MBD samples showed a larger within group heterogeneity and partially overlap with the LFH group. A list of all identified proteins in the genetic model is provided in Supplementary Table S9.

From all OF samples taken from the isthmus ipsilateral to the CL in the metabolic model, 1572 proteins were identified in total, which are listed in Supplementary Table S8. The distribution of all proteins among the three groups of the metabolic model is shown in Figure 2B. A total of 1061 proteins (67.5%) were detected in all groups. The majority (74.9%) of the identified proteins were shared between at least two groups: 2.7% (42 proteins) were detected solely in the MH group and 4.8% (75 proteins) in the Dry group, while the Lact group showed the highest proportion (17.6%, 277 proteins).

To identify quantitative differences in the abundance of individual proteins, the LFQ values of the MaxQuant software were used. The total numbers of proteins showing abundance differences are depicted in Figure 4.

In the metabolic model, we found a total of 37 significantly (*P*-value < 0.05, log2-fold change $>|0.6|$) altered proteins in all, counting proteins altered in multiple comparisons only once, which corresponds to 2.4% of the identified proteins within this model. Regarding the three comparisons between Lact, Dry, and MH, we detected the highest number (19) of significantly altered proteins between MH and Lact. Comparing MH and Dry, 13 proteins differed in abundance and 12 proteins were changed between Lact and Dry.

Among the comparisons within the genetic model, in total 110 different proteins were significantly (*P*-value < 0.05, log2-fold change $>|0.6|$) altered in abundance in any of the pairwise comparisons (Figure 4). Most differences were detected between LFH and MBD (52), followed by HFH versus MBD (47) and LFH compared with HFH (37). For each of the six pairwise comparisons, proteins IDs, log2-fold changes, and *t*-test *P*-values are listed in Supplementary Tables S2–S7.

In general, for all pairwise comparisons, the number of proteins showing abundance alterations was higher in the genetic merit model than in the metabolic disturbance model. The comparisons in the genetic model as well as in the metabolic model are illustrated in the Volcano plots in Figure 5. Proteins are plotted by their *t*-test *P*-value and their log2-fold change.

Notably, we also found four proteins that were significantly altered in pairwise comparisons of the genetic as well as of the metabolic model, which are listed in Table 1.

For functional characterization of affected OF proteins, we performed a DAVID gene ontology analysis using the term "cellular component" as shown in Table 2. In addition to the GO terms "cell projection" and "non-membrane-bounded organelle", the cluster "extracellular region" was also enriched (enrichment score of 1.9).

To complement the results obtained by the DAVID GO cellular component analysis, a SignalP 4.1 analysis was performed for those proteins with altered abundance as well as the entire set of identified proteins. SignalP unveils proteins containing a signal peptide that allows the secretion by secretory vesicles via the endoplasmic reticulum and Golgi apparatus [37]. Analysis of all differentially abundant proteins in both the genetic and the metabolic model revealed that 22% of the proteins (31/143) contain a signal peptide and are therefore very likely to be secreted into the oviduct. These proteins are listed in Table 3. Regarding all identified proteins, 274 out of 1976 proteins were found to contain a signal peptide, corresponding to 14% of the proteins.

For a comprehensive analysis of the dataset, a GSEA was performed for every pairwise comparison within each model using the gene set databases KEGG (Kyoto Encyclopedia of Genes and

Downloaded from https://academic.oup.com/biolreprod/advance-article-abstract/doi/10.1093/biolre/ioz142/5539041 by Universitaetsbibliothek Muenchen user on 17 October 2019

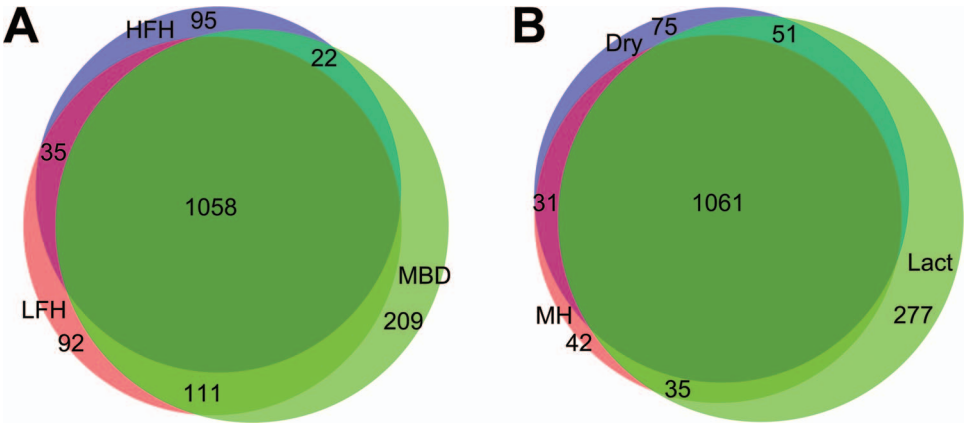

Figure 2. Venn diagrams of identified proteins from (A) the metabolic model and (B) the genetic model sorted by their corresponding groups. In both models, almost 1100 proteins were detected in all three groups. The highest number of proteins identified in only one of the groups was found in the lactating (metabolic model) and the MBD group (genetic model). The abundance of these proteins may have been below the detection limit and therefore they cannot be regarded as absent in the other groups.

Table 1. Proteins significantly altered in both the energy balance and the genetic model (see text for details).

UniProt accession	Gene name	Protein name	Comparison	Ratio	*P*-value
Q5GN72	AGP	Alpha-1-acid glycoprotein	Lact vs. MH	2.06	0.041
			LFH vs. MBD	0.29	0.031
F1MZ96	N/A	IGK protein	Dry vs. MH	1.97	0.044
			LFH vs. MBD	0.28	0.015
Q58CQ2	ARPC1B	Actin-related protein 2/3 complex subunit 1B	Lact vs. MH	1.65	0.042
			LFH vs. MBD	0.60	0.029
A6QPP2	SERPIND1	SERPIND1 protein	Lact vs. MH	1.91	0.004
			HFH vs. MBD	0.33	0.020
			LFH vs. MBD	0.33	0.029

MH: Maiden heifer; Lact: postpartum lactating cows; Dry: postpartum non-lactating cows; LFH: Low fertility heifer; HFH: High fertility heifer; and MBD: Montbéliarde heifer.

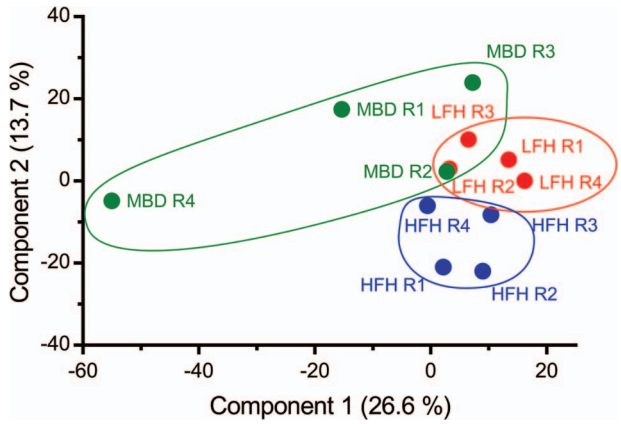

Figure 3. Principal component analysis of all biological replicates of the genetic model. In the genetic model, the PCA of all replicates of the three groups HFH, LFH, and MBD shows clear discrimination between the HFH and the LFH group.

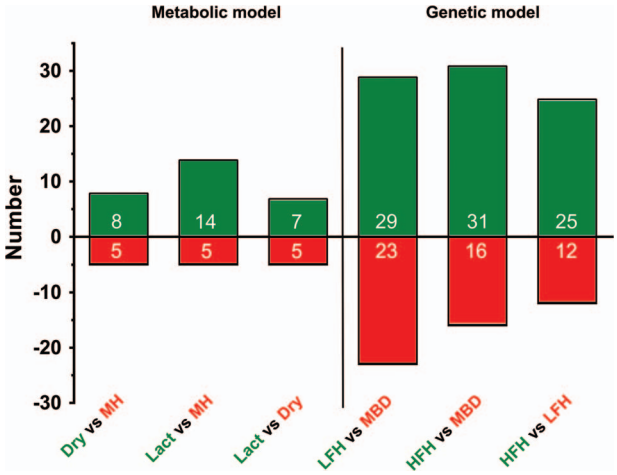

Figure 4. Number of differentially abundant proteins in each of the six pairwise comparisons. Green bars represent the number of proteins that are higher abundant in the group named first in the legend below the bar, while red bars show the number of proteins that are decreased in abundance compared with the second group.

Downloaded from https://academic.oup.com/biolreprod/advance-article-abstract/doi/10.1093/biolre/ioz142/5539041 by Universitaetsbibliothek Muenchen user on 17 October 2019

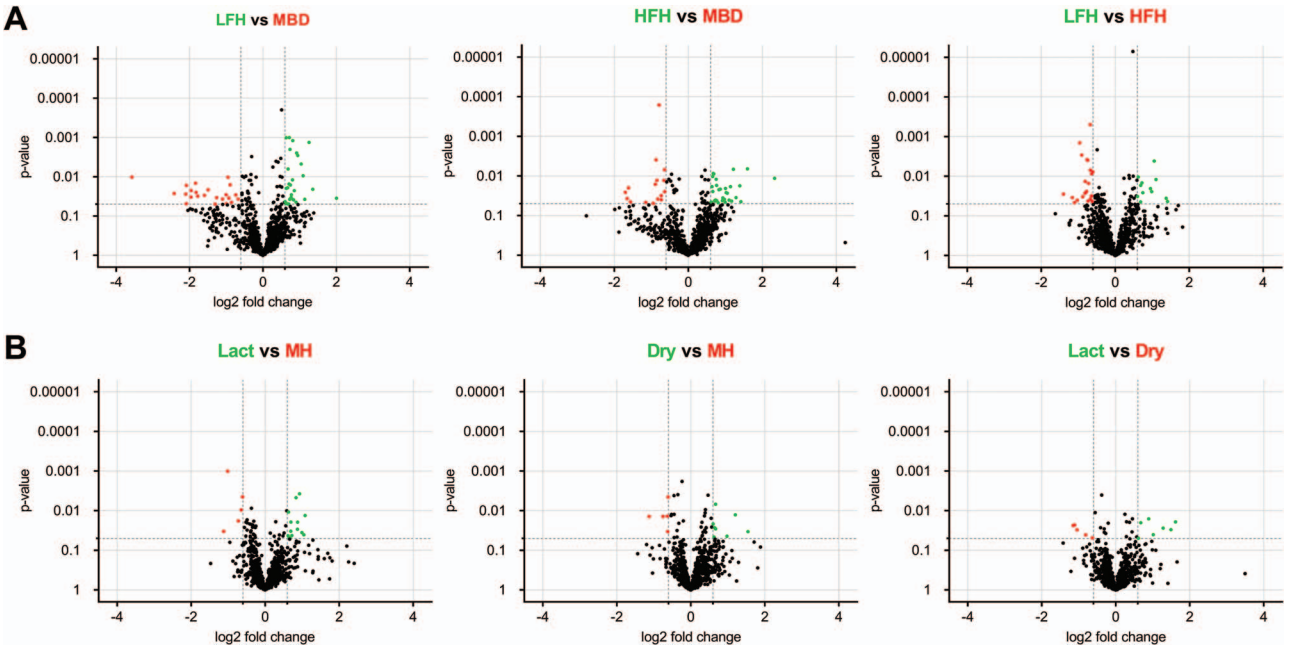

Figure 5. Volcano plots. Volcano plots of pairwise comparisons of (A) the genetic model and (B) the metabolic model. Red spots in the volcano plots represent proteins that show lower abundance in the group that is named first with a log2-fold change < -0.6 and a *t*-test *P*-value < 0.05. Green spots are assigned to proteins with a log2-fold change > 0.6 that are more abundant in the first group compared with the second group.

Table 2. Enriched annotation cluster from the DAVID GO analysis of abundance-altered proteins from both models according to the term "cellular component."

Annotation cluster 1 enrichment score: 3.23		Cell projection	
Term	%	*P*-value	Fold enrichment
GO:0042995~cell projection	9.2	2.02E-04	4.7
GO:0031252~cell leading edge	4.6	9.87E-04	11.0
GO:0001726~ruffle	3.7	1.05E-03	19.2
Annotation cluster 2 enrichment score: 2.57		Non-membrane-bounded organelle	
Term	%	*P*-value	Fold enrichment
GO:0005856~cytoskeleton	12.8	2.15E-03	2.6
GO:0043232~intracellular non-membrane-bounded organelle	19.3	3.01E-03	1.9
GO:0043228~non-membrane-bounded organelle	19.3	3.01E-03	1.9
Annotation cluster 3 enrichment score: 1.90		Extracellular region	
Term	%	*P*-value	Fold enrichment
GO:0042627~chylomicron	2.8	1.26E-03	52.8
GO:0034361~very-low-density lipoprotein particle	2.8	4.47E-03	28.8
GO:0034385~triglyceride-rich lipoprotein particle	2.8	4.47E-03	28.8
GO:0034364~high-density lipoprotein particle	2.8	9.46E-03	19.8
GO:0032994~protein-lipid complex	2.8	1.46E-02	15.8
GO:0034358~plasma lipoprotein particle	2.8	1.46E-02	15.8
GO:0005576~extracellular region	14.7	1.54E-02	1.9
GO:0044421~extracellular region part	7.3	1.01E-01	2.0
GO:0005615~extracellular space	5.5	1.03E-01	2.4

Downloaded from https://academic.oup.com/biolreprod/advance-article-abstract/doi/10.1093/biolre/ioz142/5539041 by Universitaetsbibliothek Muenchen user on 17 October 2019

Table 3. SignalP analysis – Proteins significantly altered in at least one pairwise comparison containing a signal peptide for active secretion.

Accession number	Gene name	Protein name
B0JYQ0	ALB	ALB protein
F1MLW7	LOC100297192	Uncharacterized protein, immunoglobulin light chain, lambda gene cluster, identity: 97%
G3N0S9	LOC515150	Apolipoprotein R
A5D7Q2	N/A	IgM precursor
V6F9A3	ApoC3	Apolipoprotein C-III
F1MZ96	N/A	IGK protein
Q29437	N/A	Primary amine oxidase, liver isozyme
Q5GN72	AGP	Alpha-1-acid glycoprotein
A6QPP2	SERPIND1	SERPIND1 protein
P02769	ALB	Serum albumin
Q2KIX7	N/A	Protein HP-25 homolog 1
P01045	KNG2	Kininogen-2
Q9GLX9	SPON1	Spondin-1
A6QP39	MSLN	MSLN protein
F2FB38	MUC16	Mucin-16
Q3ZCH5	AZGP1	Zinc-alpha-2-glycoprotein
P00978	AMBP	Protein AMBP
P12763	AHSG	Alpha-2-HS-glycoprotein
Q32PA9	FKBP2	Peptidyl-prolyl cis-trans isomerase FKBP2
Q28042	OVGP1	Oviduct-specific glycoprotein
P81644	APOA2	Apolipoprotein A-II
F1MVK1	N/A	Uncharacterized protein, complement C4-like isoform X3, identity: 93%
G3N1U4	SERPINA3–3	Serpin A3–3
F1N3Q7	APOA4	Apolipoprotein A-IV
F1 N036	DNAJC3	DnaJ homolog subfamily C member 3
F1MYN5	FBLN1	Fibulin-1
Q29RU4	C6	Complement component C6
Q28085	CFH	Complement factor H
Q2KJH6	SERPINH1	Serpin H1
Q3T083	SDF2L1	Stromal cell-derived factor 2-like protein 1
A4IF88	RCN1	RCN1 protein

Genomes) pathway and GO categories biological process and molecular function. Gene sets were considered as significantly enriched with a FDR *q*-value of less than 0.05. All significantly enriched gene sets of both animal models are listed in Table 4.

In the metabolic model, a lower number of significantly enriched gene sets were detected than in the genetic model. Comparing the Dry and Lact group, "KEGG proteasome" was enriched in Dry. In the comparison of the Dry versus MH groups, "KEGG complement and coagulation cascades" was overrepresented in Dry.

The vast majority of significantly enriched gene sets was found in the genetic merit model. Regarding MBD versus HFH, the KEGG pathways "Complement and coagulation cascades", "Systemic lupus erythematosus", and "Prion diseases" were more highly enriched in MBD than in HFH. In the comparison of LFH and HFH, "KEGG Ribosome" was enriched in LFH. In the comparison of LFH versus MBD, the gene sets "Structural constituent of ribosome" and "KEGG Ribosome" were enriched in LFH, whereas, for example, "KEGG complement and coagulation cascades", "KEGG systemic lupus erythematosus", and "immune response" were found to be more over-represented in the MBD group (Table 4).

The most frequently enriched gene set among all comparisons is the set "KEGG complement and coagulation cascades", which was significantly altered in the comparisons of MBD and HFH as well as MBD versus LFH and Dry compared with MH.

To gain further insight of the KEGG pathways, biological processes and molecular functions in which the significantly altered proteins are involved, and to validate the results obtained from the GSEA, we used DAVID to perform a gene ontology analysis [30, 31].

Functional annotation clustering of all proteins that were found to be significantly altered in the pairwise comparisons of the genetic and/or the metabolic model resulted in seven enriched clusters. These proteins were, for example, found to be assigned to the GO terms "actin binding", "lipid binding", "enzyme inhibitor activity", and "immune response". These findings are visualized in Figure 6A using Proteomaps. In more detail, Figure 6B shows the "Proteomaps" of proteins that were assigned to the gene sets "KEGG complement and coagulation cascades" and "immune response" as well as the DAVID GO cluster "immune response." An overview of significantly enriched annotation clusters (enrichment score greater than 1.3) is shown in Table 5. A complete list of GO terms in annotation clusters is available from Supplementary Table S1.

Discussion

The antagonistic relationship between single trait selection for increased milk yield and cow fertility has been well documented. Two

Downloaded from https://academic.oup.com/biolreprod/advance-article-abstract/doi/10.1093/biolre/ioz142/5539041 by Universitaetsbibliothek Muenchen user on 17 October 2019

Table 4. Results of the GSEA.

MBD > LFH	LFH > MBD
KEGG complement and coagulation cascades KEGG systemic lupus erythematosus Immune response Response to wounding Defense response Response to external stimulus	Structural constituent of ribosome KEGG ribosome
MBD > HFH	**LFH > HFH**
KEGG complement and coagulation cascades KEGG systemic lupus erythematosus KEGG prion diseases	KEGG ribosome
Dry > MH	**Dry > Lact**
KEGG complement and coagulation cascades	KEGG proteasome

MH: Maiden heifer; Lact: postpartum lactating cows; Dry: postpartum non-lactating cows; LFH: Low fertility heifer; HFH: High fertility heifer; and MBD: Montbéliarde heifer.

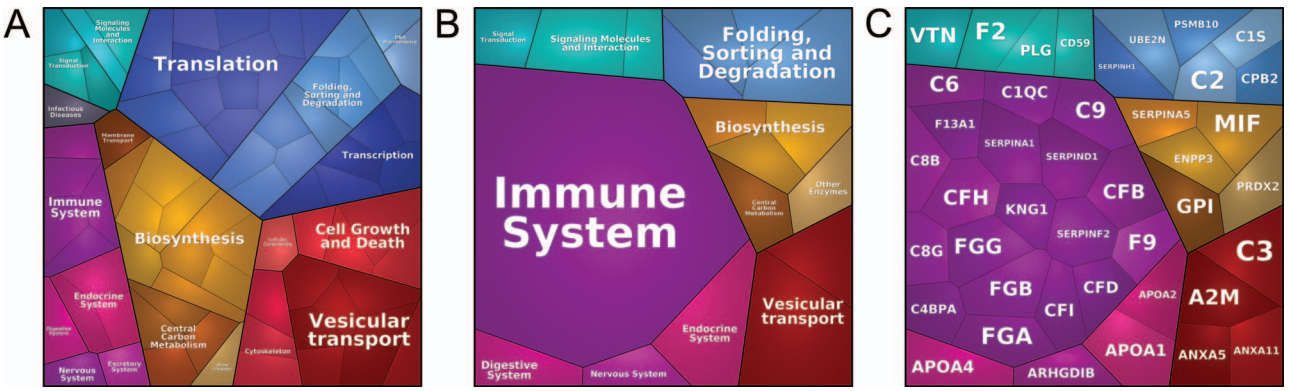

Figure 6. Visualization of affected biological processes. Proteomap visualization of proteins significantly altered in abundance and related biological processes from the genetic and the metabolic model (A). (B and C) Proteins related to "complement and coagulation cascades" and "immune response" in GSEA and DAVID GO analysis. The tiles of the Proteomap are arranged according to the hierarchical KEGG pathway maps. Related functional categories are arranged in adjacent regions and coded using similar colors. Areas of tiles represent protein abundances, weighted by protein size.

Table 5. Enriched annotation clusters from the DAVID GO analysis of abundance-altered proteins from both models according to the terms "biological process", "molecular function", and "KEGG pathways".

Annotation cluster	Cluster enrichment score	Cluster GO term
1	3.08	Cytoskeletal protein binding
2	2.71	Actin binding
3	2.47	Translation
4	1.90	Identical protein binding
5	1.69	Lipid binding
6	1.67	Enzyme inhibitor activity
7	1.39	Immune response

different animal models were established to study possible reasons for impaired reproductive performance in different reproductive organs and at several molecular levels. This study forms part of a larger study examining the impact of lactation on the cow metabolic status and follicular fluid metabolic profile [27], and on the conceptus [38] and endometrial [39] transcriptome.

Strategy and reproducibility of the proteomic analysis

For proteomic analysis, the straight-forward and frequently applied LFQ approach [28, 40] was chosen. To reduce undersampling, a common problem in complex samples, we used long (50 cm) separation columns in combination with long gradients. Even though the analysis of OF is challenging due to several high abundant proteins such as albumin and the oviduct-specific protein, such as Oviductal Glycoprotein 1 (OVGP1), we were able to identify more than 1500 proteins in each model. Other studies [4, 13, 41] achieved similar or lower numbers of identified proteins, leading us to the conclusion that the analytic depth of our dataset is reasonably high. To identify the overlap with previously identified proteins, we compared our dataset with the OF proteomes of the above-mentioned studies. Comparison of 1976 proteins from both models in our study to data in the literature revealed that 1101 proteins (56%) had already been

Downloaded from https://academic.oup.com/biolreprod/advance-article-abstract/doi/10.1093/biolre/ioz142/5539041 by Universitaetsbibliothek Muenchen user on 17 October 2019

reported to be present in bovine [4, 13] and equine [42] or ovine [41] OF. Thus, 875 novel proteins were identified in OF by our approach.

Since the genetic diversity between individual cows in each of the groups is considerably higher than in cell lines or inbred strains of laboratory animals frequently used for "omics" approaches, the reproducibility among different individuals of one group is especially challenging. A comparison of the qualitative results of the proteomic approach revealed a high level of consistency, with only 172 of a total of 1299 identified proteins detected exclusively in a single animal in the case of the LFH group (Figure 1). This underlines the quality of the OF samples as well as the proteomic approach, both indispensable for analytically meaningful proteomic results.

Comparing the identified proteins from the six different groups, we found an overlap of around two-thirds of the identified proteins in all three groups in the genetic as well as in the metabolic model. In a study of bovine OF by Lamy et al. [4], approximately 72% of proteins identified in the oviduct ipsilateral to the CL were common between four stages of the estrous cycle. However, in our study, we analyzed different metabolic stages and animals with a different genetic background. As shown in Figure 2, some proteins were detected in only one group, especially in MBD and Lact. However, it has to be considered that the abundance of these proteins may be below the detection limit in the other groups, and that proteins which were not identified should not be regarded as absent.

In order to gain a deeper understanding of the relevance of the abundance altered proteins, all proteins were classified according to their relative abundance based on LFQ intensities. Abundance is indicated as low, medium, or high with an LFQ intensity of <25%, 25–75%, or >75 of the maximum intensity, respectively. Abundance categories for each protein are listed in Supplementary Tables S2–S7. Interestingly, except for one protein, all significantly altered proteins in both the genetic and the metabolic model were either of medium or high abundance.

Origin of oviduct fluid proteins

Although several of the proteins significantly altered in abundance in our OF analysis have been reported in other studies of the OF proteome [4, 13, 41, 42], it is unclear whether these proteins have been actively secreted into the oviduct. Among the proteins that are altered in abundance, 22% contain a signal peptide that targets the protein for translocation across the endoplasmic reticulum [43]. Moreover, DAVID GO analysis according to the term "cellular component" showed that 14.7% of the abundance-altered proteins were associated with the term "extracellular region". Regarding the total set of identified proteins, 14% of the proteins were found to contain a signal peptide for secretion. This suggests that secreted proteins are predominantly affected by abundance alterations, indicating an active regulation of the levels of these proteins in the OF.

In a proteomic analysis of ewe cervix, uterus, and ewe cervix, uterus and oviduct fluid, Soleilhavoup et al. [41] also found 14% of the proteins to be classified as "secreted" in the GO analysis. Similar results have also been reported for bovine OF [4]. Contamination by intact cells was prevented in our study by using gentle flushing instead of squeezing the oviducts and by removal of cells and cell debris prior to sample processing. Therefore, proteins that were not found to be actively secreted are either non-canonically secreted, may derive from cells that have undergone cell death or may not be annotated as secreted in the database.

Alminana et al. [44] investigated the protein composition of extracellular vesicles (EV) obtained from in vivo- and in vitro-derived BOEC. They identified a set of proteins potentially important for gamete- and embryo-oviduct interactions and therefore suggested that EVs are a possible mechanism for the release of proteins into the oviduct and their transport to the embryo. Some of these proteins are also among the set of differentially abundant proteins in the present study, for example, DEAD-box helicase 17 (DDX17), OVGP1, GSN, STXBP1, or ANXA5, indicating that proteins identified in our study, which are not annotated as secreted could also derive from exosomes and microvesicles.

Metabolic stress as well as genetic predisposition affect the oviduct fluid proteome

The oviduct plays a key role in fertilization and early embryonic development and has gained increasing attention in the context of dairy cow infertility, since a considerable proportion of embryonic losses occurs prior to maternal recognition of pregnancy around Day 16 [45, 46]. Indeed, it has been reported that in high-producing dairy cows, up to 50% of embryos may be no longer viable by Day 7 [21]. Oviduct fluid provides the microenvironment for sperm, oocyte, and the early embryo and is composed mainly of proteins, lipids, and amino acids [47]. Forde et al. [27] analyzed animals from the same model as in the present study and demonstrated that lactation has a substantial impact on the metabolic status and the follicular fluid metabolomic profile of dairy cows. They reported an increase in concentrations of circulating NEFA and beta-hydroxybutyrate, as well as a decrease of insulin, IGF1, and glucose in postpartum lactating cows in comparison to nulliparous heifers. Overall, their data showed distinct changes in the metabolic status of lactating cows compared with non-lactating cows and heifers. In agreement with this finding, most of the 37 differentially abundant proteins were detected comparing Lact and MH followed by Dry versus MH. This is in accordance with Bauersachs et al. [39], analyzing differences in the endometrial transcriptome in the same metabolic model as used here. They found only minor differences in endometrial gene expression in non-lactating and lactating cows as opposed to heifers versus both postpartum groups. Among the comparisons within the metabolic model, seven proteins were significantly altered in abundance in more than one comparison. Three of these proteins were less abundant in the postpartum groups, Lact and Dry compared with MH: Prostaglandin reductase 1 (PTGR1), Elongation factor 1-beta (EEF1B), and Epoxide hydrolase 2 (EPHX2), which are all highly abundant in our data set. To our knowledge, a role of EEF1B in OF has not been described thus far. In contrast, EPHX2 was more expressed in the prepubertal compared with the postovulatory phase in a study analyzing the gene expression in porcine oviduct [48]. Epoxide hydrolase 2 binds to specific epoxides and converts them to the corresponding dihydrodiols. Prostaglandin reductase 1 catalyzes the conversion of leukotriene B4 into the biologically less active 12-oxo-leukotriene B4, which is the key step of the metabolic inactivation of leukotriene B4, and has previously been described to play a role in maternal recognition of pregnancy in a proteomic analysis of equine uterine fluid [49].

DEAD-box helicase 17 and Osteoclast-stimulating factor 1 (OSTF1), two proteins with high and medium abundance, respectively, were found to be significantly more abundant in Lact compared with MH and Dry. DEAD-box helicase 17 was around 1.6 times higher in Lact and is believed to be involved in embryogenesis, spermatogenesis, and cellular growth and division based on its distribution pattern [50, 51]. In addition, the protein has been identified in bovine oviductal EV [44]. OSTF1 is believed to induce

Downloaded from https://academic.oup.com/biolreprod/advance-article-abstract/doi/10.1093/biolre/ioz142/5539041 by Universitaetsbibliothek Muenchen user on 17 October 2019

bone resorption, but has only been described in the context of female mammalian reproduction in human and murine embryos in vitro in response to increasing ammonium concentrations [52].

As evident from Figure 4, a remarkably higher number of differentially abundant proteins was detected in the genetic model compared with the metabolic model. Among the genetic model, most abundance-altered proteins were detected between MBD and the two Holstein groups. Together with the lower number of differentially expressed proteins in the metabolic model, this leads to the assumption that genetic differences are prevalent regarding the protein composition of the OF. Nevertheless, between LFH and HFH, differing only in their EBV for fertility, 37 proteins were found to be altered in abundance. Principal component analysis of the samples of the genetic model also showed a clear separation between the two Holstein groups at the proteome level. Previous studies also comparing Holstein dairy cows with a similar genetic merit for milk production but with a negative or positive EBV for reproduction showed a distinct effect of the genetic merit for fertility traits on the reproductive efficiency. Cows with a good genetic merit for reproduction had higher postpartum BCSs, circulating concentrations of insulin and insulin-like growth factor I, and reduced calving to conception intervals [19]. Moreover, it has been shown that the EBV for fertility also has an influence on follicular fluid and serum concentrations of amino acids as well as on fatty acids concentrations in non-pregnant cows [20]. One of the proteins significantly higher (2.6-fold) in HFH compared with LFH is oviduct-specific glycoprotein (OVGP), which is one of the most abundant proteins in OF and has been discussed in several studies and reviews [17, 47]. For instance, an OVGP1-heparin complex has been reported to be involved in zona pellucida modification prior to fertilization that affects sperm binding and contributes to the regulation of polyspermy in pig [53, 54]. Oviduct-specific glycoprotein was also described to interact with spermatozoa [55] in the bovine and to promote sperm capacitation [56], viability, and motility [57]. Moreover, the addition of OVGP leads to increased embryo development in vitro in pigs [58] and goats [17, 59]. An increase of OVGP1 in the HFH group may therefore contribute to an improved fertility compared with those with a lower genetic merit for reproduction.

A substantial proportion of affected proteins is assigned to "Complement and coagulation cascades" and "Immune system" processes

Functional classification of abundance-altered proteins was performed using DAVID GO analysis in addition to GSEA. As shown in Table 4, significantly enriched gene sets in these comparisons are mainly related to the KEGG pathway "Complement and coagulation cascades", Moreover, DAVID GO functional annotation revealed a significant enrichment of the cluster "Immune response", which is in accordance to previous studies showing that the oviduct plays a vital role in the regulation of immunological processes. As comprehensively reviewed [60, 61], the oviduct contains a unique immune system able to distinguish among pathogens, allogeneic sperm, and the semi-allogeneic embryo, which is a crucial premise for successful fertilization and early embryo survival. Proteins involved in the gene sets and GO cluster related to immune response are graphically illustrated in Figure 6B and C. In the pairwise comparison of MBD and LFH, we found the macrophage migration inhibitory factor (MIF) to be more highly abundant in LFH. Migration inhibitory factor is involved in cell-mediated immunity, immunoregulation, and inflammation and plays a role in the regulation of macrophage function in host defense [62]. Migration inhibitory factor mRNA and protein expression was increased during the postovulatory phase compared with estrus and the luteal phase in Japanese black heifers [63]. Migration inhibitory factor has been reported to be secreted into the oviduct [13] and was also identified in the ewe OF [41]; however, its role in early embryogenesis remains unclear.

In addition to MIF, several immunoglobulins were found to be significantly altered comparing MBD and LFH, but with higher abundance in MBD. Basic Local Alignment Search Tool (BLAST) search (https://blast.ncbi.nlm.nih.gov/Blast.cgi) of the sequences of uncharacterized proteins with the UniProt accession numbers F1MLW7, A5D7Q2, G5E604, and G3N0V0 showed 97–100% identity with immunoglobulin light chain, lambda gene cluster, IgM precursor, immunoglobulin light chain variable region, and secreted immunoglobulin gamma2 heavy chain constant region, respectively. Immunoglobulins are well known to be among the major components of OF [64, 65], which is in agreement as the significantly altered proteins were also highly abundant in our study.

Another protein related to immune response is the "deleted in malignant brain tumors 1" (DMBT1) protein with a 2.9-fold increase in Dry compared with MH. Deleted in malignant brain tumors 1 was also 4.6-fold higher in Lact compared with MH (P = 0.08). It has been shown to bind surfactant protein D and is suggested to play a role in the interaction of tumor cells and the immune system. In equine and porcine, DMBT1 was found to be expressed by oviduct epithelial cells. Moreover, preincubation of oocytes with recombinant DMBT1 increased the monospermic fertilization rate, which was also observed by IVF under supplementation of oviductal fluid [66]. Ambruosi et al. [66] therefore suggest that DMBT1 acts as a bridge between oocytes and sperm cells or oocytes and oviductal cells and mediates their interaction by linking other associated proteins. Moreover, the *DMBT1* gene has previously been detected among a set of genes with up-regulated expression in endometria from Day 19 pregnant heifers of the same animal model as in our study compared with pregnant non-lactating and lactating dairy cows [39].

Additionally, two proteins of the complement cascade, Complement component C6 and Complement factor H (CFH) were found to be significantly altered in pairwise comparisons. Both were found to be 2.2-fold higher in Dry compared with Lact and have previously been identified in OF in cattle and ewe [13, 41]. C6 is part of the membrane attack complex that can be incorporated into the cell membrane and cause cell lysis, while CFH has been described to play a role in the regulation of complement activation. In a study by Maillo et al. [67] examining the effect of multiple embryos on the transcriptome of the bovine oviduct, most of the downregulated genes in pregnant heifers were related with the complement system, inflammation, or major histocompatibility complex.

Interestingly, abundance alterations of proteins related to immune response were only found in comparisons within the metabolic model and comparing the Holstein groups to MBD, but not between LFH and HFH. Moreover, all of the proteins discussed above exhibited high abundance, that is, a LFQ intensity above 75% of the maximum intensity. Our data suggest that differences in the immune response of the OF are therefore related to different breeds or changes in the metabolic status, but may not be linked with the EBV for fertility. Moreover, we found that some of the proteins related to immune response in the metabolic model were higher in Dry and Lact than in MH (SERPIND1 protein, APOA2, APOA4, and DMBT1) but none was higher in MH compared with

Downloaded from https://academic.oup.com/biolreprod/advance-article-abstract/doi/10.1093/biolre/ioz142/5539041 by Universitaetsbibliothek Muenchen user on 17 October 2019

the postpartum groups. This suggests that metabolic stress leads to an enhancement of proteins involved in immune system processes.

Proteins commonly affected in the metabolic as well as in the genetic model

Despite the higher number of altered proteins in the genetic model compared with the metabolic model, the question remains whether all of these proteins are related to fertility. Therefore, we investigated the overlap of both models to identify proteins that are affected by the metabolic status as well as the genetic merit for fertility. Interestingly, a set of four proteins were found to be altered in abundance in both models. One of these proteins is Actin-related protein 2/3 complex subunit 1B (ARPC1B), which was 1.7-fold higher in Lact compared with MH and also 1.7-fold increased in MBD compared with LFH. Actin-related protein 2/3 complex subunit 1B functions as a subunit of the human Arp2/3 complex involved in the control of actin polymerization in cells [68] and has also been identified in bovine OF [13]. The functional role of ARPC1B in the OF remains unclear.

An uncharacterized protein with the UniProt accession number F1MZ96 was also found in both models. It was 2.0-fold higher in Dry compared with MH and showed a 3.6-fold increase in MBD compared with LFH. Basic Local Alignment Search Tool search of the protein sequence resulted in a 98% overlap with IGK protein (immunoglobulin kappa locus), suggesting that this protein may also be involved in the immune response.

Alpha-1-acid glycoprotein (AGP), an acute phase plasma protein, proved to be 2.1-fold increased in Lact compared with MH and 3.4-fold increased in MBD versus LFH. Kowsar et al. (2014) suggested a secretion of AGP by BOEC to regulate antimicrobial processes [69]. Moreover, they hypothesized that oviductal AGP could regulate the expression of Tumor necrosis factor (TNFA), a pro-inflammatory cytokine, by the BOEC. A study by Liu et al. (2014) found evidence that locally produced AGP may be involved in protecting sperm from phagocytosis by polymorphonuclear neutrophils in the bovine oviduct [70].

Abundance of SERPIND1, which was also associated with the previously discussed DAVID GO term “immune response”, was altered in three comparisons. It was around three times higher in MBD compared with both Holstein groups and 1.9-fold increased in Lact compared with MH. SERPIND1 was identified among a set of inhibitors of acrosomal and other lysosomal proteases like α-1-antiproteinase/antitrypsin and different other serpins in bovine OF [13].

It should be noted that all proteins showing abundance alterations in both models were more abundant in MBD than in the Holstein groups and also more abundant in the postpartum groups Dry and Lact compared with MH. Except for ARPC1B, all of these proteins were found to contain a signal peptide for active secretion and have an immune system-related function, although AGP and IGK protein were not included in the annotation cluster “immune response”. This is consistent with the results discussed above indicating that proteins related to immune response were not altered in abundance in the comparison of LFH and HFH and are therefore not affected by the EBV for fertility. Of interest, these proteins were all highly abundant, indicating that the concentrations of the respective proteins have a physiological effect in the OF. Moreover, this adds to our finding that metabolic stress results in an increase of proteins that play a role in defense response, as these proteins were less abundant in MH than in the other groups of the metabolic model.

In summary, we were able to show that the genetic predisposition for fertility and breed have a strong impact on the OF proteome, while the impact of metabolic stress was lower, suggesting a robustness of the oviduct environment. The remarkably high fraction of immune response-related proteins suggests that reduced reproductive success in both models may be triggered by alterations of the immune system components in the microenvironment for the gametes and the early embryo.

Supplementry data

Supplementary data are available at *BIOLRE* online.

Acknowledgment

We wish to acknowledge the help of staff at ALLICE, INRA, and NUID UCD for their assistance in sample collection.

References

1. Hugentobler SA, Diskin MG, Leese HJ, Humpherson PG, Watson T, Sreenan JM, Morris DG. Amino acids in oviduct and uterine fluid and blood plasma during the estrous cycle in the bovine. *Mol Reprod Dev* 2007; **74**:445–454.
2. Hugentobler SA, Humpherson PG, Leese HJ, Sreenan JM, Morris DG. Energy substrates in bovine oviduct and uterine fluid and blood plasma during the oestrous cycle. *Mol Reprod Dev* 2008; **75**:496–503.
3. Hugentobler SA, Morris DG, Sreenan JM, Diskin MG. Ion concentrations in oviduct and uterine fluid and blood serum during the estrous cycle in the bovine. *Theriogenology* 2007; **68**:538–548.
4. Lamy J, Labas V, Harichaux G, Tsikis G, Mermillod P, Saint-Dizier M. Regulation of the bovine oviductal fluid proteome. *Reproduction* 2016; **152**:629–644.
5. Lamy J, Liere P, Pianos A, Aprahamian F, Mermillod P, Saint-Dizier M. Steroid hormones in bovine oviductal fluid during the estrous cycle. *Theriogenology* 2016; **86**:1409–1420.
6. Lonergan P, Khatir H, Piumi F, Rieger D, Humblot P, Boland MP. Effect of time interval from insemination to first cleavage on the developmental characteristics, sex ratio and pregnancy rate after transfer of bovine embryos. *J Reprod Fertil* 1999; **117**:159–167.
7. Memili E, Dominko T, First NL. Onset of transcription in bovine oocytes and preimplantation embryos. *Mol Reprod Dev* 1998; **51**:36–41.
8. Graf A, Krebs S, Zakhartchenko V, Schwalb B, Blum H, Wolf E. Fine mapping of genome activation in bovine embryos by RNA sequencing. *Proc Natl Acad Sci USA* 2014; **111**:4139–4144.
9. Rizos D, Fair T, Papadopoulos S, Boland MP, Lonergan P. Developmental, qualitative, and ultrastructural differences between ovine and bovine embryos produced in vivo or in vitro. *Mol Reprod Dev* 2002; **62**:320–327.
10. Enright BP, Lonergan P, Dinnyes A, Fair T, Ward FA, Yang X, Boland MP. Culture of in vitro produced bovine zygotes in vitro vs in vivo: implications for early embryo development and quality. *Theriogenology* 2000; **54**:659–673.
11. Lazzari G, Colleoni S, Lagutina I, Crotti G, Turini P, Tessaro I, Brunetti D, Duchi R, Galli C. Short-term and long-term effects of embryo culture in the surrogate sheep oviduct versus in vitro culture for different domestic species. *Theriogenology* 2010; **73**:748–757.
12. Cordova A, Perreau C, Uzbekova S, Ponsart C, Locatelli Y, Mermillod P. Development rate and gene expression of IVP bovine embryos cocultured with bovine oviduct epithelial cells at early or late stage of preimplantation development. *Theriogenology* 2014; **81**:1163–1173.
13. Pillai VV, Weber DM, Phinney BS, Selvaraj V. Profiling of proteins secreted in the bovine oviduct reveals diverse functions of this luminal microenvironment. *PLoS One* 2017; **12**:e0188105.

Downloaded from https://academic.oup.com/biolreprod/advance-article-abstract/doi/10.1093/biolre/ioz142/5539041 by Universitaetsbibliothek Muenchen user on 17 October 2019

14. Mondejar I, Martinez-Martinez I, Aviles M, Coy P. Identification of potential oviductal factors responsible for zona pellucida hardening and monospermy during fertilization in mammals. *Biol Reprod* 2013; **89**:67.
15. Georgiou AS, Sostaric E, Wong CH, Snijders AP, Wright PC, Moore HD, Fazeli A. Gametes alter the oviductal secretory proteome. *Mol Cell Proteomics* 2005; **4**:1785–1796.
16. Seytanoglu A, Georgiou AS, Sostaric E, Watson PF, Holt WV, Fazeli A. Oviductal cell proteome alterations during the reproductive cycle in pigs. *J Proteome Res* 2008; **7**:2825–2833.
17. Maillo V, Sanchez-Calabuig MJ, Lopera-Vasquez R, Hamdi M, Gutierrez-Adan A, Lonergan P, Rizos D. Oviductal response to gametes and early embryos in mammals. *Reproduction* 2016; **152**:R127–R141.
18. Butler WR. Nutritional interactions with reproductive performance in dairy cattle. *Anim Reprod Sci* 2000; **60–61**:449–457.
19. Cummins SB, Lonergan P, Evans AC, Berry DP, Evans RD, Butler ST. Genetic merit for fertility traits in Holstein cows: I. Production characteristics and reproductive efficiency in a pasture-based system. *J Dairy Sci* 2012; **95**:1310–1322.
20. Moore SG, O'Gorman A, Brennan L, Fair T, Butler ST. Follicular fluid and serum metabolites in Holstein cows are predictive of genetic merit for fertility. *Reprod Fertil Dev* 2017; **29**:658–669.
21. Sartori R, Bastos MR, Wiltbank MC. Factors affecting fertilisation and early embryo quality in single- and superovulated dairy cattle. *Reprod Fertil Dev* 2010; **22**:151–158.
22. Wiltbank MC, Baez GM, Garcia-Guerra A, Toledo MZ, Monteiro PL, Melo LF, Ochoa JC, Santos JE, Sartori R. Pivotal periods for pregnancy loss during the first trimester of gestation in lactating dairy cows. *Theriogenology* 2016; **86**:239–253.
23. Rizos D, Ramirez MA, Pintado B, Lonergan P, Gutierrez-Adan A. Culture of bovine embryos in intermediate host oviducts with emphasis on the isolated mouse oviduct. *Theriogenology* 2010; **73**:777–785.
24. Maillo V, Rizos D, Besenfelder U, Havlicek V, Kelly AK, Garrett M, Lonergan P. Influence of lactation on metabolic characteristics and embryo development in postpartum Holstein dairy cows. *J Dairy Sci* 2012; **95**:3865–3876.
25. Rizos D, Carter F, Besenfelder U, Havlicek V, Lonergan P. Contribution of the female reproductive tract to low fertility in postpartum lactating dairy cows. *J Dairy Sci* 2010; **93**:1022–1029.
26. Forde N, O'Gorman A, Whelan H, Duffy P, O'Hara L, Kelly AK, Havlicek V, Besenfelder U, Brennan L, Lonergan P. Lactation-induced changes in metabolic status and follicular-fluid metabolomic profile in postpartum dairy cows. *Reprod Fertil Dev* 2015.
27. Forde N, O'Gorman A, Whelan H, Duffy P, O'Hara L, Kelly AK, Havlicek V, Besenfelder U, Brennan L, Lonergan P. Lactation-induced changes in metabolic status and follicular-fluid metabolomic profile in postpartum dairy cows. *Reprod Fertil Dev* 2016; **28**:1882–1892.
28. Cox J, Mann M. MaxQuant enables high peptide identification rates, individualized p.p.b.-range mass accuracies and proteome-wide protein quantification. *Nat Biotechnol* 2008; **26**:1367–1372.
29. Hulsen T, de Vlieg J, Alkema W. BioVenn – a web application for the comparison and visualization of biological lists using area-proportional Venn diagrams. *BMC Genomics* 2008; **9**:1–6.
30. Huang D W, Sherman BT, Lempicki RA. Bioinformatics enrichment tools: paths toward the comprehensive functional analysis of large gene lists. *Nucleic Acids Res* 2009; **37**:1–13.
31. Huang D W, Sherman BT, Lempicki RA. Systematic and integrative analysis of large gene lists using DAVID bioinformatics resources. *Nat Protoc* 2009; **4**:44–57.
32. Ashburner M, Ball CA, Blake JA, Botstein D, Butler H, Cherry JM, Davis AP, Dolinski K, Dwight SS, Eppig JT, Harris MA, Hill DP et al. Gene ontology: tool for the unification of biology. The Gene Ontology Consortium. *Nat Genet* 2000; **25**:25–29.
33. Mootha VK, Lindgren CM, Eriksson KF, Subramanian A, Sihag S, Lehar J, Puigserver P, Carlsson E, Ridderstrale M, Laurila E, Houstis N, Daly MJ et al. PGC-1alpha-responsive genes involved in oxidative phosphorylation are coordinately downregulated in human diabetes. *Nat Genet* 2003; **34**:267–273.
34. Subramanian A, Tamayo P, Mootha VK, Mukherjee S, Ebert BL, Gillette MA, Paulovich A, Pomeroy SL, Golub TR, Lander ES, Mesirov JP. Gene set enrichment analysis: a knowledge-based approach for interpreting genome-wide expression profiles. *Proc Natl Acad Sci USA* 2005; **102**:15545–15550.
35. Liebermeister W, Noor E, Flamholz A, Davidi D, Bernhardt J, Milo R. Visual account of protein investment in cellular functions. *Proc Natl Acad Sci USA* 2014; **111**:8488–8493.
36. Petersen TN, Brunak S, von Heijne G, Nielsen H. SignalP 4.0: discriminating signal peptides from transmembrane regions. *Nat Methods* 2011; **8**:785–786.
37. Emanuelsson O, Brunak S, von Heijne G, Nielsen H. Locating proteins in the cell using TargetP, SignalP and related tools. *Nat Protoc* 2007; **2**:953–971.
38. Forde N, Simintiras CA, Sturmey RG, Graf A, Wolf E, Blum H, Lonergan P. Effect of lactation on conceptus-maternal interactions at the initiation of implantation in cattle: I. Effects on the conceptus transcriptome and amino acid composition of the uterine luminal fluid. *Biol Reprod* 2017; **97**:798–809.
39. Bauersachs S, Simintiras CA, Sturmey RG, Krebs S, Bick J, Blum H, Wolf E, Lonergan P, Forde N. Effect of metabolic status on conceptus-maternal interactions on day 19 in dairy cattle: II. Effects on the endometrial transcriptome. *Biol Reprod* 2017; **97**:413–425.
40. Cox J, Hein MY, Luber CA, Paron I, Nagaraj N, Mann M. Accurate proteome-wide label-free quantification by delayed normalization and maximal peptide ratio extraction, termed MaxLFQ. *Mol Cell Proteomics* 2014; **13**:2513–2526.
41. Soleilhavoup C, Riou C, Tsikis G, Labas V, Harichaux G, Kohnke P, Reynaud K, de Graaf SP, Gerard N, Druart X. Proteomes of the female genital tract during the oestrous cycle. *Mol Cell Proteomics* 2016; **15**:93–108.
42. Smits K, Nelis H, Van Steendam K, Govaere J, Roels K, Ververs C, Leemans B, Wydooghe E, Deforce D, Van Soom A. Proteome of equine oviducal fluid: effects of ovulation and pregnancy. *Reprod Fertil Dev* 2017; **29**:1085–1095.
43. von Heijne G. The signal peptide. *J Membr Biol* 1990; **115**:195–201.
44. Alminana C, Corbin E, Tsikis G, Alcantara-Neto AS, Labas V, Reynaud K, Galio L, Uzbekov R, Garanina AS, Druart X, Mermillod P. Oviduct extracellular vesicles protein content and their role during oviduct-embryo cross-talk. *Reproduction* 2017; **154**:153–168.
45. Besenfelder U, Havlicek V, Brem G. Role of the oviduct in early embryo development. *Reprod Domest Anim* 2012; **47** (Suppl 4):156–163.
46. Berg DK, van Leeuwen J, Beaumont S, Berg M, Pfeffer PL. Embryo loss in cattle between Days 7 and 16 of pregnancy. *Theriogenology* 2010; **73**:250–260.
47. Aviles M, Gutierrez-Adan A, Coy P. Oviductal secretions: will they be key factors for the future ARTs? *Mol Hum Reprod* 2010; **16**: 896–906.
48. Acuna OS, Aviles M, Lopez-Ubeda R, Guillen-Martinez A, Soriano-Ubeda C, Torrecillas A, Coy P, Izquierdo-Rico MJ. Differential gene expression in porcine oviduct during the oestrous cycle. *Reprod Fertil Dev* 2017; **29**:2387–2399.
49. Smits K, Willems S, Van Steendam K, Van De Velde M, De Lange V, Ververs C, Roels K, Govaere J, Van Nieuwerburgh F, Peelman L, Deforce D, Van Soom A. Proteins involved in embryo-maternal interaction around the signalling of maternal recognition of pregnancy in the horse. *Sci Rep* 2018; **8**:5249.
50. Schmid SR, Linder P. D-E-A-D protein family of putative RNA helicases. *Mol Microbiol* 1992; **6**:283–291.
51. Resource Coordinators NCBI. Database resources of the National Center for Biotechnology Information. *Nucleic acids research* 2016; **44**:D7–D19.
52. Gardner DK, Hamilton R, McCallie B, Schoolcraft WB, Katz-Jaffe MG. Human and mouse embryonic development, metabolism and gene expression are altered by an ammonium gradient in vitro. *Reproduction* 2013; **146**:49–61.

Downloaded from https://academic.oup.com/biolreprod/advance-article-abstract/doi/10.1093/biolre/ioz142/5539041 by Universitaetsbibliothek Muenchen user on 17 October 2019

53. Ghersevich S, Massa E, Zumoffen C. Oviductal secretion and gamete interaction. *Reproduction* 2015; **149**:R1–R14.
54. Coy P, Canovas S, Mondejar I, Saavedra MD, Romar R, Grullon L, Matas C, Aviles M. Oviduct-specific glycoprotein and heparin modulate sperm-zona pellucida interaction during fertilization and contribute to the control of polyspermy. *Proc Natl Acad Sci USA* 2008; **105**:15809–15814.
55. Lamy J, Nogues P, Combes-Soia L, Tsikis G, Labas V, Mermillod P, Druart X, Saint-Dizier M. Identification by proteomics of oviductal sperm-interacting proteins. *Reproduction* 2018; **155**: 457–466.
56. King RS, Killian GJ. Purification of bovine estrus-associated protein and localization of binding on sperm. *Biol Reprod* 1994; **51**: 34–42.
57. Abe H, Sendai Y, Satoh T, Hoshi H. Bovine oviduct-specific glycoprotein: a potent factor for maintenance of viability and motility of bovine spermatozoa in vitro. *Mol Reprod Dev* 1995; **42**: 226–232.
58. McCauley TC, Buhi WC, Wu GM, Mao J, Caamano JN, Didion BA, Day BN. Oviduct-specific glycoprotein modulates sperm-zona binding and improves efficiency of porcine fertilization in vitro. *Biol Reprod* 2003; **69**:828–834.
59. Pradeep MA, Jagadeesh J, De AK, Kaushik JK, Malakar D, Kumar S, Dang AK, Das SK, Mohanty AK. Purification, sequence characterization and effect of goat oviduct-specific glycoprotein on in vitro embryo development. *Theriogenology* 2011; **75**:1005–1015.
60. Girardi G. Complement inhibition keeps mothers calm and avoids fetal rejection. *Immunol Invest* 2008; **37**:645–659.
61. Marey MA, Yousef MS, Kowsar R, Hambruch N, Shimizu T, Pfarrer C, Miyamoto A. Local immune system in oviduct physiology and pathophysiology: attack or tolerance? *Domest Anim Endocrinol* 2016; **56** (Suppl):S204–211.
62. Calandra T, Spiegel LA, Metz CN, Bucala R. Macrophage migration inhibitory factor is a critical mediator of the activation of immune cells by exotoxins of Gram-positive bacteria. *Proc Natl Acad Sci USA* 1998; **95**:11383–11388.
63. Nahar A, Kadokawa H. Expression of macrophage migration inhibitory factor (MIF) in bovine oviducts is higher in the postovulatory phase than during the oestrus and luteal phase. *Reprod Fertil Dev* 2017; **29**:1521–1529.
64. Buhi WC, Alvarez IM, Kouba AJ. Secreted proteins of the oviduct. *Cells Tissues Organs* 2000; **166**:165–179.
65. Leese HJ. The formation and function of oviduct fluid. *J Reprod Fertil* 1988; **82**:843–856.
66. Ambruosi B, Accogli G, Douet C, Canepa S, Pascal G, Monget P, Moros Nicolas C, Holmskov U, Mollenhauer J, Robbe-Masselot C, Vidal O, Desantis S et al. Deleted in malignant brain tumor 1 is secreted in the oviduct and involved in the mechanism of fertilization in equine and porcine species. *Reproduction* 2013; **146**:119–133.
67. Maillo V, Gaora PO, Forde N, Besenfelder U, Havlicek V, Burns GW, Spencer TE, Gutierrez-Adan A, Lonergan P, Rizos D. Oviduct-embryo interactions in cattle: two-way traffic or a one-way street? *Biol Reprod* 2015; **92**:144.
68. Mullins RD, Heuser JA, Pollard TD. The interaction of Arp2/3 complex with actin: Nucleation, high affinity pointed end capping, and formation of branching networks of filaments. *Proc Natl Acad Sci USA* 1998; **95**:6181–6186.
69. Kowsar R, Hambruch N, Marey MA, Liu J, Shimizu T, Pfarrer C, Miyamoto A. Evidence for a novel, local acute-phase response in the bovine oviduct: progesterone and lipopolysaccharide up-regulate alpha 1-acid-glycoprotein expression in epithelial cells in vitro. *Mol Reprod Dev* 2014; **81**:861–870.
70. Liu J, Marey MA, Kowsar R, Hambruch N, Shimizu T, Haneda S, Matsui M, Sasaki M, Hayakawa H, Pfarrer C, Miyamoto A. An acute-phase protein as a regulator of sperm survival in the bovine oviduct: alpha 1-acid-glycoprotein impairs neutrophil phagocytosis of sperm in vitro. *J Reprod Dev* 2014; **60**:342–348.

Downloaded from https://academic.oup.com/biolreprod/advance-article-abstract/doi/10.1093/biolre/ioz142/5539041 by Universitaetsbibliothek Muenchen user on 17 October 2019

7 References

1. I. Gordon, *Laboratory Production of Cattle Embryos*. (CABI, 2003).

2. P. Lonergan, N. Forde, Maternal-embryo interaction leading up to the initiation of implantation of pregnancy in cattle. *Animal* **8 Suppl 1**, 64-69 (2014).

3. A. J. Watson, L. C. Barcroft, Regulation of blastocyst formation. *Front Biosci* **6**, D708-730 (2001).

4. P. Lonergan, T. Fair, N. Forde, D. Rizos, Embryo development in dairy cattle. *Theriogenology* **86**, 270-277 (2016).

5. A. J. Wilcox, D. D. Baird, C. R. Weinberg, Time of Implantation of the Conceptus and Loss of Pregnancy. *New England Journal of Medicine* **340**, 1796-1799 (1999).

6. T. Fair, P. Hyttel, T. Greve, Bovine oocyte diameter in relation to maturational competence and transcriptional activity. *Molecular reproduction and development* **42**, 437-442 (1995).

7. M. A. Crowe, M. G. Diskin, E. J. Williams, Parturition to resumption of ovarian cyclicity: comparative aspects of beef and dairy cows. *Animal* **8 Suppl 1**, 40-53 (2014).

8. A. Sen, F. Caiazza, Oocyte maturation: a story of arrest and release. *Front Biosci (Schol Ed)* **5**, 451-477 (2013).

9. R. P. Norris *et al.*, Cyclic GMP from the surrounding somatic cells regulates cyclic AMP and meiosis in the mouse oocyte. *Development* **136**, 1869-1878 (2009).

10. S. Vaccari, J. L. Weeks, 2nd, M. Hsieh, F. S. Menniti, M. Conti, Cyclic GMP signaling is involved in the luteinizing hormone-dependent meiotic maturation of mouse oocytes. *Biology of reproduction* **81**, 595-604 (2009).

11. P. Lonergan, T. Fair, Maturation of Oocytes in Vitro. *Annu Rev Anim Biosci* **4**, 255-268 (2016).

12. G. Pincus, E. V. Enzmann, The Comparative Behavior of Mammalian Eggs in Vivo and in Vitro : I. The Activation of Ovarian Eggs. *The Journal of experimental medicine* **62**, 665-675 (1935).

13. R. Moor, Y. Dai, Maturation of pig oocytes in vivo and in vitro. *Reprod Suppl* **58**, 91-104 (2001).

14. K. Coenen, L. Massicotte, M. A. Sirard, Study of newly synthesized proteins during bovine oocyte maturation in vitro using image analysis of two-dimensional gel electrophoresis. *Molecular reproduction and development* **67**, 313-322 (2004).

15. E. M. Ferreira *et al.*, Cytoplasmic maturation of bovine oocytes: structural and biochemical modifications and acquisition of developmental competence. *Theriogenology* **71**, 836-848 (2009).

16. P. Hyttel, T. Greve, H. Callesen, Ultrastructural aspects of oocyte maturation and fertilization in cattle. *J Reprod Fertil Suppl* **38**, 35-47 (1989).

17. D. Adhikari, K. Liu, The regulation of maturation promoting factor during prophase I arrest and meiotic entry in mammalian oocytes. *Molecular and cellular endocrinology* **382**, 480-487 (2014).

18. C. Anderiesz *et al.*, Effect of recombinant human gonadotrophins on human, bovine and murine oocyte meiosis, fertilization and embryonic development in vitro. *Human reproduction* **15**, 1140-1148 (2000).

19. Y. H. Choi, E. M. Carnevale, G. E. Seidel, E. L. Squires, Effects of gonadotropins on bovine oocytes matured in TCM-199. *Theriogenology* **56**, 661-670 (2001).

20. A. I. Younis, B. G. Brackett, R. A. Fayrer-Hosken, Influence of serum and hormones on bovine oocyte maturation and fertilization in vitro. *Gamete Res* **23**, 189-201 (1989).

21. D. Rizos, F. Ward, P. Duffy, M. P. Boland, P. Lonergan, Consequences of bovine oocyte maturation, fertilization or early embryo development in vitro versus in vivo: implications for blastocyst yield and blastocyst quality. *Molecular reproduction and development* **61**, 234-248 (2002).

22. D. Tesfaye *et al.*, Suppression of connexin 43 and E-cadherin transcripts in in vitro derived bovine embryos following culture in vitro or in vivo in the homologous bovine oviduct. *Molecular reproduction and development* **74**, 978-988 (2007).

23. S. J. Dieleman *et al.*, Effects of in vivo prematuration and in vivo final maturation on developmental capacity and quality of pre-implantation embryos. *Theriogenology* **57**, 5-20 (2002).

24. C. E. Farin *et al.*, The role of transcription in EGF- and FSH-mediated oocyte maturation in vitro. *Anim Reprod Sci* **98**, 97-112 (2007).

25. T. A. Brevini, F. Cillo, S. Antonini, V. Tosetti, F. Gandolfi, Temporal and spatial control of gene expression in early embryos of farm animals. *Reproduction, fertility, and development* **19**, 35-42 (2007).

26. A. Graf *et al.*, Fine mapping of genome activation in bovine embryos by RNA sequencing. *Proceedings of the National Academy of Sciences of the United States of America* **111**, 4139-4144 (2014).

27. E. Memili, N. L. First, Zygotic and embryonic gene expression in cow: a review of timing and mechanisms of early gene expression as compared with other species. *Zygote* **8**, 87-96 (2000).

28. S. Mamo *et al.*, Sequential analysis of global gene expression profiles in immature and in vitro matured bovine oocytes: potential molecular markers of oocyte maturation. *BMC Genomics* **12**, 151 (2011).

29. N. Crozet, J. Kanka, J. Motlik, J. Fulka, Nucleolar fine structure and RNA synthesis in bovine oocytes from antral follicles. *Gamete Research* **14**, 65-73 (1986).

30. X. S. Cui *et al.*, Maternal gene transcription in mouse oocytes: genes implicated in oocyte maturation and fertilization. *The Journal of reproduction and development* **53**, 405-418 (2007).

31. S. Assou *et al.*, The human cumulus--oocyte complex gene-expression profile. *Human reproduction* **21**, 1705-1719 (2006).

32. A. Thelie *et al.*, Regulation of bovine oocyte-specific transcripts during in vitro oocyte maturation and after maternal-embryonic transition analyzed using a transcriptomic approach. *Molecular reproduction and development* **76**, 773-782 (2009).

33. Y. Q. Su *et al.*, Selective degradation of transcripts during meiotic maturation of mouse oocytes. *Developmental biology* **302**, 104-117 (2007).

34. E. Memili, T. Dominko, N. L. First, Onset of transcription in bovine oocytes and preimplantation embryos. *Molecular reproduction and development* **51**, 36-41 (1998).

35. M. T. Moura, R. V. de Sousa, L. de Oliveira Leme, R. Rumpf, Analysis of actinomycin D treated cattle oocytes and their use for somatic cell nuclear transfer. *Anim Reprod Sci* **109**, 40-49 (2008).

36. Y. J. Menezo, F. Herubel, Mouse and bovine models for human IVF. *Reproductive biomedicine online* **4**, 170-175 (2002).

37. M. Mihm, A. C. Evans, Mechanisms for dominant follicle selection in monovulatory species: a comparison of morphological, endocrine and intraovarian events in cows, mares and women. *Reproduction in domestic animals = Zuchthygiene* **43 Suppl 2**, 48-56 (2008).

38. T. Fair, F. Carter, S. Park, A. C. O. Evans, P. Lonergan, Global gene expression analysis during bovine oocyte in vitro maturation. *Theriogenology* **68**, S91-S97 (2007).

39. M. G. Katz-Jaffe, B. R. McCallie, K. A. Preis, J. Filipovits, D. K. Gardner, Transcriptome analysis of in vivo and in vitro matured bovine MII oocytes. *Theriogenology* **71**, 939-946 (2009).

40. P. R. Adona *et al.*, In vitro maturation alters gene expression in bovine oocytes. *Zygote* **24**, 624-633 (2016).

41. L. Nemcova *et al.*, Detection of genes associated with developmental competence of bovine oocytes. *Animal Reproduction Science* **166**, 58-71 (2016).

42. F. H. Biase *et al.*, Messenger RNAs in metaphase II oocytes correlate with successful embryo development to the blastocyst stage. *Zygote* **22**, 69-79 (2012).

43. C. Vigneault, C. Gravel, M. Vallee, S. McGraw, M. A. Sirard, Unveiling the bovine embryo transcriptome during the maternal-to-embryonic transition. *Reproduction* **137**, 245-257 (2009).

44. A. Thelie *et al.*, Differential regulation of abundance and deadenylation of maternal transcripts during bovine oocyte maturation in vitro and in vivo. *BMC Dev Biol* **7**, 125 (2007).

45. J. Kim *et al.*, Identification of maturation and protein synthesis related proteins from porcine oocytes during in vitro maturation. *Proteome Sci* **9**, 28 (2011).

46. J. D. Richter, Translational control during early development. *BioEssays : news and reviews in molecular, cellular and developmental biology* **13**, 179-183 (1991).

47. N. T. Snider, M. B. Omary, Post-translational modifications of intermediate filament proteins: mechanisms and functions. *Nature reviews. Molecular cell biology* **15**, 163-177 (2014).

48. B. Schwanhausser *et al.*, Global quantification of mammalian gene expression control. *Nature* **473**, 337-342 (2011).

49. L. Anderson, J. Seilhamer, A comparison of selected mRNA and protein abundances in human liver. *Electrophoresis* **18**, 533-537 (1997).

50. R. N. Hayes, M. L. Gross, Collision-induced dissociation. *Methods Enzymol* **193**, 237-263 (1990).

51. S. A. McLuckey, Principles of collisional activation in analytical mass spectrometry. *J Am Soc Mass Spectrom* **3**, 599-614 (1992).

52. S. E. Ong, M. Mann, Stable isotope labeling by amino acids in cell culture for quantitative proteomics. *Methods Mol Biol* **359**, 37-52 (2007).

53. S. P. Gygi *et al.*, Quantitative analysis of complex protein mixtures using isotope-coded affinity tags. *Nature biotechnology* **17**, 994-999 (1999).

54. A. Thompson *et al.*, Tandem Mass Tags: A Novel Quantification Strategy for Comparative Analysis of Complex Protein Mixtures by MS/MS. *Analytical chemistry* **75**, 1895-1904 (2003).

55. P. L. Ross *et al.*, Multiplexed protein quantitation in Saccharomyces cerevisiae using amine-reactive isobaric tagging reagents. *Molecular & cellular proteomics : MCP* **3**, 1154-1169 (2004).

56. J. Cox, M. Mann, MaxQuant enables high peptide identification rates, individualized p.p.b.-range mass accuracies and proteome-wide protein quantification. *Nature biotechnology* **26**, 1367-1372 (2008).

57. P. C. Carvalho, J. Hewel, V. C. Barbosa, J. R. Yates, 3rd, Identifying differences in protein expression levels by spectral counting and feature selection. *Genet Mol Res* **7**, 342-356 (2008).

58. M. Ma *et al.*, Protein expression profile of the mouse metaphase-II oocyte. *Journal of proteome research* **7**, 4821-4830 (2008).

59. A. M. Vitale *et al.*, Proteomic profiling of murine oocyte maturation. *Molecular reproduction and development* **74**, 608-616 (2007).

60. P. Zhang *et al.*, Proteomic-based identification of maternal proteins in mature mouse oocytes. *BMC Genomics* **10**, 348 (2009).

61. B. Wang, M. J. Pfeiffer, H. C. Drexler, G. Fuellen, M. Boiani, Proteomic Analysis of Mouse Oocytes Identifies PRMT7 as a Reprogramming Factor that Replaces SOX2 in the Induction of Pluripotent Stem Cells. *Journal of proteome research* **15**, 2407-2421 (2016).

62. S. Wang *et al.*, Proteome of mouse oocytes at different developmental stages. *Proceedings of the National Academy of Sciences of the United States of America* **107**, 17639-17644 (2010).

63. M. J. Pfeiffer *et al.*, Proteomic analysis of mouse oocytes reveals 28 candidate factors of the "reprogrammome". *Journal of proteome research* **10**, 2140-2153 (2011).

64. M. J. Pfeiffer *et al.*, Differences in embryo quality are associated with differences in oocyte composition: a proteomic study in inbred mice. *Proteomics* **15**, 675-687 (2015).

65. I. Virant-Klun, S. Leicht, C. Hughes, J. Krijgsveld, Identification of Maturation-Specific Proteins by Single-Cell Proteomics of Human Oocytes. *Molecular & cellular proteomics : MCP* **15**, 2616-2627 (2016).

66. Z. Ellederova *et al.*, Protein patterns of pig oocytes during in vitro maturation. *Biology of reproduction* **71**, 1533-1539 (2004).

67. A. Susor *et al.*, Proteomic analysis of porcine oocytes during in vitro maturation reveals essential role for the ubiquitin C-terminal hydrolase-L1. *Reproduction* **134**, 559-568 (2007).

68. D. R. Deutsch *et al.*, Stage-specific proteome signatures in early bovine embryo development. *Journal of proteome research* **13**, 4363-4376 (2014).

69. F. J. Berendt *et al.*, Highly sensitive saturation labeling reveals changes in abundance of cell cycle-associated proteins and redox enzyme variants during oocyte maturation in vitro. *Proteomics* **9**, 550-564 (2009).

70. D. Peddinti, E. Memili, S. C. Burgess, Proteomics-based systems biology modeling of bovine germinal vesicle stage oocyte and cumulus cell interaction. *PloS one* **5**, e11240 (2010).

71. L. Chen *et al.*, Comparative Proteomic Analysis of Buffalo Oocytes Matured in vitro Using iTRAQ Technique. *Sci Rep* **6**, 31795 (2016).

72. T. Turan *et al.*, Results with EMA/CO (etoposide, methotrexate, actinomycin D, cyclophosphamide, vincristine) chemotherapy in gestational trophoblastic neoplasia. *International journal of gynecological cancer : official journal of the International Gynecological Cancer Society* **16**, 1432-1438 (2006).

73. G. J. D'Angio *et al.*, The treatment of Wilms' tumor: results of the Second National Wilms' Tumor Study. *Cancer* **47**, 2302-2311 (1981).

74. S. Farber, Chemotherapy in the treatment of leukemia and Wilms' tumor. *Jama* **198**, 826-836 (1966).

75. R. P. Perry, D. E. Kelley, Inhibition of RNA synthesis by actinomycin D: characteristic dose-response of different RNA species. *Journal of cellular physiology* **76**, 127-139 (1970).

76. H. M. Sobell, Actinomycin and DNA transcription. *Proceedings of the National Academy of Sciences of the United States of America* **82**, 5328-5331 (1985).

77. S. Kamitori, F. Takusagawa, Crystal structure of the 2:1 complex between d(GAAGCTTC) and the anticancer drug actinomycin D. *Journal of Molecular Biology* **225**, 445-456 (1992).

78. H. M. Sobell, S. C. Jain, Stereochemistry of actinomycin binding to DNA: II. Detailed molecular model of actinomycin-DNA complex and its implications. *Journal of Molecular Biology* **68**, 21-34 (1972).

79. O. Bensaude, Inhibiting eukaryotic transcription: Which compound to choose? How to evaluate its activity? *Transcription* **2**, 103-108 (2011).

80. X. S. Liu, C. Ma, A.-W. Hamam, X. J. Liu, Transcription-dependent and transcription-independent functions of the classical progesterone receptor in Xenopus ovaries. *Developmental biology* **283**, 180-190 (2005).

81. S. Tyanova *et al.*, The Perseus computational platform for comprehensive analysis of (prote)omics data. *Nature methods* **13**, 731 (2016).

82. T. Hulsen, J. de Vlieg, W. Alkema, BioVenn – a web application for the comparison and visualization of biological lists using area-proportional Venn diagrams. *BMC Genomics* **9**, 1-6 (2008).

83. W. Huang da, B. T. Sherman, R. A. Lempicki, Bioinformatics enrichment tools: paths toward the comprehensive functional analysis of large gene lists. *Nucleic Acids Res* **37**, 1-13 (2009).

84. W. Huang da, B. T. Sherman, R. A. Lempicki, Systematic and integrative analysis of large gene lists using DAVID bioinformatics resources. *Nature protocols* **4**, 44-57 (2009).

85. M. Ashburner *et al.*, Gene ontology: tool for the unification of biology. The Gene Ontology Consortium. *Nature genetics* **25**, 25-29 (2000).

86. V. K. Mootha *et al.*, PGC-1alpha-responsive genes involved in oxidative phosphorylation are coordinately downregulated in human diabetes. *Nature genetics* **34**, 267-273 (2003).

87. A. Subramanian *et al.*, Gene set enrichment analysis: a knowledge-based approach for interpreting genome-wide expression profiles. *Proceedings of the National Academy of Sciences of the United States of America* **102**, 15545-15550 (2005).

88. F. Supek, M. Bosnjak, N. Skunca, T. Smuc, REVIGO summarizes and visualizes long lists of gene ontology terms. *PloS one* **6**, e21800 (2011).

89. D. Szklarczyk *et al.*, STRING v11: protein-protein association networks with increased coverage, supporting functional discovery in genome-wide experimental datasets. *Nucleic Acids Res* **47**, D607-d613 (2019).

90. G. Bindea, J. Galon, B. Mlecnik, CluePedia Cytoscape plugin: pathway insights using integrated experimental and in silico data. *Bioinformatics* **29**, 661-663 (2013).

91. G. Bindea *et al.*, ClueGO: a Cytoscape plug-in to decipher functionally grouped gene ontology and pathway annotation networks. *Bioinformatics* **25**, 1091-1093 (2009).

92. P. Shannon *et al.*, Cytoscape: a software environment for integrated models of biomolecular interaction networks. *Genome research* **13**, 2498-2504 (2003).

93. S. Tsukamoto *et al.*, Functional analysis of lysosomes during mouse preimplantation embryo development. *The Journal of reproduction and development* **59**, 33-39 (2013).

94. J. P. Luzio, P. R. Pryor, N. A. Bright, Lysosomes: fusion and function. *Nature reviews. Molecular cell biology* **8**, 622-632 (2007).

95. S. G. Burgess *et al.*, Aurora-A-Dependent Control of TACC3 Influences the Rate of Mitotic Spindle Assembly. *PLoS genetics* **11**, e1005345 (2015).

96. A. S. Nikonova, I. Astsaturov, I. G. Serebriiskii, R. L. Dunbrack, Jr., E. A. Golemis, Aurora A kinase (AURKA) in normal and pathological cell division. *Cellular and molecular life sciences : CMLS* **70**, 661-687 (2013).

97. K. Kinoshita *et al.*, Aurora A phosphorylation of TACC3/maskin is required for centrosome-dependent microtubule assembly in mitosis. *The Journal of cell biology* **170**, 1047-1055 (2005).

98. C. P. De Souza, K. A. Ellem, B. G. Gabrielli, Centrosomal and cytoplasmic Cdc2/cyclin B1 activation precedes nuclear mitotic events. *Exp Cell Res* **257**, 11-21 (2000).

99. J. Yu, N. B. Hecht, R. M. Schultz, Expression of MSY2 in mouse oocytes and preimplantation embryos. *Biology of reproduction* **65**, 1260-1270 (2001).

100. C. Vigneault, S. McGraw, M. A. Sirard, Spatiotemporal expression of transcriptional regulators in concert with the maternal-to-embryonic transition during bovine in vitro embryogenesis. *Reproduction* **137**, 13-21 (2009).

101. S. Medvedev, H. Pan, R. M. Schultz, Absence of MSY2 in mouse oocytes perturbs oocyte growth and maturation, RNA stability, and the transcriptome. *Biology of reproduction* **85**, 575-583 (2011).

102. Y. Akiyama *et al.*, Novel oral controlled-release microspheres using polyglycerol esters of fatty acids. *Journal of controlled release : official journal of the Controlled Release Society* **26**, 1-10 (1993).

103. X. Wu *et al.*, Zygote arrest 1 (Zar1) is a novel maternal-effect gene critical for the oocyte-to-embryo transition. *Nature genetics* **33**, 187-191 (2003).

104. T. Hamatani, M. G. Carter, A. A. Sharov, M. S. Ko, Dynamics of global gene expression changes during mouse preimplantation development. *Dev Cell* **6**, 117-131 (2004).

105. S. Rana, P. B. Maples, N. Senzer, J. Nemunaitis, Stathmin 1: a novel therapeutic target for anticancer activity. *Expert review of anticancer therapy* **8**, 1461-1470 (2008).

106. J. Koppel *et al.*, Cellular and subcellular localization of stathmin during oocyte and preimplantation embryo development. *Molecular reproduction and development* **53**, 306-317 (1999).

107. B. Xie *et al.*, Cloning of Porcine Pituitary Tumor Transforming Gene 1 and Its Expression in Porcine Oocytes and Embryos. *PloS one* **11**, e0153189-e0153189 (2016).

108. D. Adhikari *et al.*, Inhibitory phosphorylation of Cdk1 mediates prolonged prophase I arrest in female germ cells and is essential for female reproductive lifespan. *Cell research* **26**, 1212-1225 (2016).

109. D. Adhikari *et al.*, Cdk1, but not Cdk2, is the sole Cdk that is essential and sufficient to drive resumption of meiosis in mouse oocytes. *Human molecular genetics* **21**, 2476-2484 (2012).

110. A. A. Challa, B. Stefanovic, A novel role of vimentin filaments: binding and stabilization of collagen mRNAs. *Molecular and cellular biology* **31**, 3773-3789 (2011).

111. C. Payne, V. Rawe, J. Ramalho-Santos, C. Simerly, G. Schatten, Preferentially localized dynein and perinuclear dynactin associate with nuclear pore complex proteins to mediate genomic union during mammalian fertilization. *Journal of cell science* **116**, 4727-4738 (2003).

112. S. Hafidh, V. Capkova, D. Honys, Safe keeping the message: mRNP complexes tweaking after transcription. *Advances in experimental medicine and biology* **722**, 118-136 (2011).

113. M. C. MacNicol, A. M. MacNicol, Developmental timing of mRNA translation--integration of distinct regulatory elements. *Molecular reproduction and development* **77**, 662-669 (2010).

114. O. Guzeloglu-Kayisli *et al.*, Human embryonic poly(A)-binding protein (EPAB) alternative splicing is differentially regulated in human oocytes and embryos. *Molecular human reproduction* **20**, 59-65 (2014).

115. U. Eichenlaub-Ritter, M. Peschke, Expression in in-vivo and in-vitro growing and maturing oocytes: focus on regulation of expression at the translational level. *Human reproduction update* **8**, 21-41 (2002).

116. A. C. Evans *et al.*, Use of microarray technology to profile gene expression patterns important for reproduction in cattle. *Reproduction in domestic animals = Zuchthygiene* **43 Suppl 2**, 359-367 (2008).

117. S. G. Szeto, E. C. Williams, A. D. Rudner, J. M. Lee, Phosphorylation of filamin A by Cdk1 regulates filamin A localization and daughter cell separation. *Exp Cell Res* **330**, 248-266 (2015).

118. H. Wang *et al.*, Filamin A is required for spindle migration and asymmetric division in mouse oocytes. *Faseb j* **31**, 3677-3688 (2017).

119. D. Simaite *et al.*, Recessive mutations in PCBD1 cause a new type of early-onset diabetes. *Diabetes* **63**, 3557-3564 (2014).

120. Y. Y. Cao *et al.*, Fast clinical molecular diagnosis of hyperphenylalaninemia using next-generation sequencing-based on a custom AmpliSeq panel and Ion Torrent PGM sequencing. *Molecular genetics and metabolism* **113**, 261-266 (2014).

121. M. Hochstrasser, Ubiquitin-dependent protein degradation. *Annual review of genetics* **30**, 405-439 (1996).

122. Y. Pomerantz, N. Dekel, Molecular participants in regulation of the meiotic cell cycle in mammalian oocytes. *Reproduction, fertility, and development* **25**, 484-494 (2013).

123. M. Glotzer, A. W. Murray, M. W. Kirschner, Cyclin is degraded by the ubiquitin pathway. *Nature* **349**, 132-138 (1991).

124. A. W. Murray, M. J. Solomon, M. W. Kirschner, The role of cyclin synthesis and degradation in the control of maturation promoting factor activity. *Nature* **339**, 280-286 (1989).

125. J. E. Holt, K. T. Jones, Control of homologous chromosome division in the mammalian oocyte. *Molecular human reproduction* **15**, 139-147 (2009).

126. L. J. Huo *et al.*, Ubiquitin-proteasome pathway modulates mouse oocyte meiotic maturation and fertilization via regulation of MAPK cascade and cyclin B1 degradation. *Mech Dev* **121**, 1275-1287 (2004).

127. L. B. Josefsberg, D. Galiani, A. Dantes, A. Amsterdam, N. Dekel, The proteasome is involved in the first metaphase-to-anaphase transition of meiosis in rat oocytes. *Biology of reproduction* **62**, 1270-1277 (2000).

128. R. Sartori, M. R. Bastos, M. C. Wiltbank, Factors affecting fertilisation and early embryo quality in single- and superovulated dairy cattle. *Reproduction, fertility, and development* **22**, 151-158 (2010).

129. M. C. Wiltbank *et al.*, Pivotal periods for pregnancy loss during the first trimester of gestation in lactating dairy cows. *Theriogenology* **86**, 239-253 (2016).

130. M. C. Lucy, Reproductive loss in high-producing dairy cattle: where will it end? *Journal of dairy science* **84**, 1277-1293 (2001).

131. D. P. Berry, E. Wall, J. E. Pryce, Genetics and genomics of reproductive performance in dairy and beef cattle. *Animal* **8 Suppl 1**, 105-121 (2014).

132. R. Rearte *et al.*, Effect of milk production on reproductive performance in dairy herds. *Journal of dairy science* **101**, 7575-7584 (2018).

133. M. C. Lucy, Symposium review: Selection for fertility in the modern dairy cow-Current status and future direction for genetic selection. *Journal of dairy science* **102**, 3706-3721 (2019).

134. J. B. Cole, P. M. VanRaden, Symposium review: Possibilities in an age of genomics: The future of selection indices. *Journal of dairy science* **101**, 3686-3701 (2018).

135. P. D. Carvalho, V. G. Santos, J. O. Giordano, M. C. Wiltbank, P. M. Fricke, Development of fertility programs to achieve high 21-day pregnancy rates in high-producing dairy cows. *Theriogenology* **114**, 165-172 (2018).

136. S. B. Cummins *et al.*, Genetic merit for fertility traits in Holstein cows: I. Production characteristics and reproductive efficiency in a pasture-based system. *Journal of dairy science* **95**, 1310-1322 (2012).

137. S. T. Butler, Genetic control of reproduction in dairy cows. *Reproduction, fertility, and development* **26**, 1-11 (2013).

138. S. G. Moore, T. Fair, P. Lonergan, S. T. Butler, Genetic merit for fertility traits in Holstein cows: IV. Transition period, uterine health, and resumption of cyclicity. *Journal of dairy science* **97**, 2740-2752 (2014).

139. S. B. Cummins, P. Lonergan, A. C. Evans, S. T. Butler, Genetic merit for fertility traits in Holstein cows: II. Ovarian follicular and corpus luteum dynamics, reproductive hormones, and estrus behavior. *Journal of dairy science* **95**, 3698-3710 (2012).

140. S. G. Moore, S. Scully, J. A. Browne, T. Fair, S. T. Butler, Genetic merit for fertility traits in Holstein cows: V. Factors affecting circulating progesterone concentrations. *Journal of dairy science* **97**, 5543-5557 (2014).

141. S. G. Moore *et al.*, Differentially Expressed Genes in Endometrium and Corpus Luteum of Holstein Cows Selected for High and Low Fertility Are Enriched for Sequence Variants Associated with Fertility. *Biology of reproduction* **94**, 19 (2016).

142. T. E. Spencer, C. A. Gray, Sheep uterine gland knockout (UGKO) model. *Methods Mol Med* **121**, 85-94 (2006).

143. H. C. Fitzgerald *et al.*, Idiopathic infertility in women is associated with distinct changes in proliferative phase uterine fluid proteins. *Biology of reproduction* **98**, 752-764 (2018).

144. J. M. Koch, J. Ramadoss, R. R. Magness, Proteomic profile of uterine luminal fluid from early pregnant ewes. *Journal of proteome research* **9**, 3878-3885 (2010).

145. C. Soleilhavoup *et al.*, Proteomes of the Female Genital Tract During the Oestrous Cycle. *Molecular & cellular proteomics : MCP* **15**, 93-108 (2016).

146. K. Brooks, G. W. Burns, J. G. Moraes, T. E. Spencer, Analysis of the Uterine Epithelial and Conceptus Transcriptome and Luminal Fluid Proteome During the Peri-Implantation Period of Pregnancy in Sheep. *Biology of reproduction* **95**, 88 (2016).

147. J. J. Romero, B. E. Liebig, C. D. Broeckling, J. E. Prenni, T. R. Hansen, Pregnancy-induced changes in metabolome and proteome in ovine uterine flushings. *Biology of reproduction* **97**, 273-287 (2017).

148. S. Faulkner, G. Elia, O. B. P, M. Dunn, D. Morris, Composition of the bovine uterine proteome is associated with stage of cycle and concentration of systemic progesterone. *Proteomics* **13**, 3333-3353 (2013).

149. M. P. Mullen *et al.*, Proteomic characterization of histotroph during the preimplantation phase of the estrous cycle in cattle. *Journal of proteome research* **11**, 3004-3018 (2012).

150. N. Forde *et al.*, Proteomic analysis of uterine fluid during the pre-implantation period of pregnancy in cattle. *Reproduction* **147**, 575-587 (2014).

151. S. Faulkner *et al.*, A comparison of the bovine uterine and plasma proteome using iTRAQ proteomics. *Proteomics* **12**, 2014-2023 (2012).

152. W. Liebermeister *et al.*, Visual account of protein investment in cellular functions. *Proceedings of the National Academy of Sciences of the United States of America* **111**, 8488-8493 (2014).

153. J. Casado-Vela *et al.*, Comprehensive proteomic analysis of human endometrial fluid aspirate. *Journal of proteome research* **8**, 4622-4632 (2009).

154. J. Cox *et al.*, Accurate proteome-wide label-free quantification by delayed normalization and maximal peptide ratio extraction, termed MaxLFQ. *Molecular & cellular proteomics : MCP* **13**, 2513-2526 (2014).

155. S. B. Cummins, S. M. Waters, A. C. Evans, P. Lonergan, S. T. Butler, Genetic merit for fertility traits in Holstein cows: III. Hepatic expression of somatotropic axis genes during pregnancy and lactation. *Journal of dairy science* **95**, 3711-3721 (2012).

156. K. Gegenfurtner *et al.*, Influence of metabolic status and genetic merit for fertility on proteomic composition of bovine oviduct fluid†. *Biology of reproduction*, (2019).

157. K. Smits *et al.*, Proteins involved in embryo-maternal interaction around the signalling of maternal recognition of pregnancy in the horse. *Sci Rep* **8**, 5249 (2018).

158. N. Forde, P. Lonergan, Transcriptomic analysis of the bovine endometrium: What is required to establish uterine receptivity to implantation in cattle? *The Journal of reproduction and development* **58**, 189-195 (2012).

159. S. Bauersachs, E. Wolf, Transcriptome analyses of bovine, porcine and equine endometrium during the pre-implantation phase. *Anim Reprod Sci* **134**, 84-94 (2012).

160. O. Sandra, G. Charpigny, L. Galio, I. Hue, Preattachment Embryos of Domestic Animals: Insights into Development and Paracrine Secretions. *Annu Rev Anim Biosci* **5**, 205-228 (2017).

161. S. Bauersachs *et al.*, Embryo-induced transcriptome changes in bovine endometrium reveal species-specific and common molecular markers of uterine receptivity. *Reproduction* **132**, 319-331 (2006).

162. C. Klein *et al.*, Monozygotic twin model reveals novel embryo-induced transcriptome changes of bovine endometrium in the preattachment period. *Biology of reproduction* **74**, 253-264 (2006).

163. B. M. Jalali, P. Likszo, A. Andronowska, D. J. Skarzynski, Alterations in the distribution of actin and its binding proteins in the porcine endometrium during early pregnancy: Possible role in epithelial remodeling and embryo adhesion. *Theriogenology* **116**, 17-27 (2018).

164. C. B. Steinhauser *et al.*, Fructose Synthesis and Transport at the Uterine-Placental Interface of Pigs: Cell-Specific Localization of SLC2A5, SLC2A8, and Components of the Polyol Pathway1. *Biology of reproduction* **95**, (2016).

165. C. A. Simintiras *et al.*, Biochemical characterization of progesterone-induced alterations in bovine uterine fluid amino acid and carbohydrate composition during the conceptus elongation windowdagger. *Biology of reproduction* **100**, 672-685 (2019).

166. M. Clemente *et al.*, Progesterone and conceptus elongation in cattle: a direct effect on the embryo or an indirect effect via the endometrium? *Reproduction* **138**, 507-517 (2009).

167. K. Smits *et al.*, Proteome of equine oviducal fluid: effects of ovulation and pregnancy. *Reproduction, fertility, and development* **29**, 1085-1095 (2017).

168. A. M. Ledgard, R. S. Lee, A. J. Peterson, Bovine endometrial legumain and TIMP-2 regulation in response to presence of a conceptus. *Molecular reproduction and development* **76**, 65-74 (2009).

169. D. Morris, M. Diskin, Effect of progesterone on embryo survival. *Animal* **2**, 1112-1119 (2008).

170. N. K. Khurana, H. Niemann, Energy metabolism in preimplantation bovine embryos derived in vitro or in vivo. *Biology of reproduction* **62**, 847-856 (2000).

171. S. J. James, B. J. Miller, D. R. Cross, L. J. McGarrity, S. M. Morris, The essentiality of folate for the maintenance of deoxynucleotide precursor pools, DNA synthesis, and cell cycle progression in PHA-stimulated lymphocytes. *Environ Health Perspect* **101 Suppl 5**, 173-178 (1993).

172. S. E. Ulbrich *et al.*, Bovine endometrial metallopeptidases MMP14 and MMP2 and the metallopeptidase inhibitor TIMP2 participate in maternal preparation of pregnancy. *Molecular and cellular endocrinology* **332**, 48-57 (2011).

173. O. Emanuelsson, S. Brunak, G. von Heijne, H. Nielsen, Locating proteins in the cell using TargetP, SignalP and related tools. *Nature protocols* **2**, 953-971 (2007).

174. G. Song *et al.*, Cathepsin B, cathepsin L, and cystatin C in the porcine uterus and placenta: potential roles in endometrial/placental remodeling and in fluid-phase transport of proteins secreted by uterine epithelia across placental areolae. *Biology of reproduction* **82**, 854-864 (2010).

175. G. Song, T. E. Spencer, F. W. Bazer, Cathepsins in the ovine uterus: regulation by pregnancy, progesterone, and interferon tau. *Endocrinology* **146**, 4825-4833 (2005).

176. C. M. Boomsma *et al.*, Endometrial secretion analysis identifies a cytokine profile predictive of pregnancy in IVF. *Human reproduction* **24**, 1427-1435 (2009).

177. M. Munoz *et al.*, Proteome of the early embryo-maternal dialogue in the cattle uterus. *Journal of proteome research* **11**, 751-766 (2012).

178. P. Shooshtarizadeh *et al.*, The antimicrobial peptides derived from chromogranin/secretogranin family, new actors of innate immunity. *Regul Pept* **165**, 102-110 (2010).

179. K. B. Helle, A. Corti, M. H. Metz-Boutigue, B. Tota, The endocrine role for chromogranin A: a prohormone for peptides with regulatory properties. *Cellular and molecular life sciences : CMLS* **64**, 2863-2886 (2007).

180. N. Forde *et al.*, Alterations in expression of endometrial genes coding for proteins secreted into the uterine lumen during conceptus elongation in cattle. *BMC Genomics* **14**, 321 (2013).

181. T. R. Hansen, L. D. P. Sinedino, T. E. Spencer, Paracrine and endocrine actions of interferon tau (IFNT). *Reproduction* **154**, F45-F59 (2017).

182. R. M. Roberts, T. Ezashi, C. S. Rosenfeld, A. D. Ealy, H. M. Kubisch, Evolution of the interferon tau genes and their promoters, and maternal-trophoblast interactions in control of their expression. *Reprod Suppl* **61**, 239-251 (2003).

183. M. Guillomot *et al.*, Cellular localization of an embryonic interferon, ovine trophoblastin and its mRNA in sheep embryos during early pregnancy. *Biol Cell* **68**, 205-211 (1990).

184. T. E. Spencer, F. W. Bazer, Biology of progesterone action during pregnancy recognition and maintenance of pregnancy. *Front Biosci* **7**, d1879-1898 (2002).

185. T. E. Spencer, T. L. Ott, F. W. Bazer, tau-Interferon: pregnancy recognition signal in ruminants. *Proc Soc Exp Biol Med* **213**, 215-229 (1996).

186. C. G. Walker *et al.*, Modulation of the maternal immune system by the pre-implantation embryo. *BMC Genomics* **11**, 474 (2010).

8 Appendix

8.1 Abbreviations

ActD	Actinomycin D
CC	Cumulus cell
CID	Collision-induced dissociation
CL	Corpus luteum
COC	Cumulus-oocyte-complex
DAVID	Database for annotation, visualization and integrated discovery
DIGE	Difference gel electrophoresis
DMSO	Dimethyl sulfoxide
DTT	Dithiothreitol
EBV	Estimated breeding value
ECS	Estrous cow serum
EGA	Embryonic genome activation
FA	Formic acid
FDR	False discovery rate
FECUND	Fundamental cattle reproduction study
FSH	Follicle-stimulating hormone
GO	Gene ontology
GSEA	Gene set enrichment analysis
GV	Germinal vesicle
GVBD	Germinal vesicle breakdown
HFH	High fertility Holstein heifers
IAA	Iodoacetamide
ICAT	Isotope-coded affinity tag
iTRAQ	Isobaric tags for relative and absolute quantitation
IVF	*in vitro* fertilization
IVM	*in vitro* maturation
IVP	*in vitro* production
KEGG	Kyoto encyclopedia of genes and genomes
LC	Liquid chromatography
LFH	Low fertility Holstein heifers
LFQ	Label-free quantification
LH	Luteinizing hormone
MALDI-TOF	Matrix-assisted laser desorption/ionization time of flight
MBD	Montbéliarde
MH	Maiden heifer

MII	Metaphase II
MII AD	Actinomycin D-treated metaphase II oocytes
MS	Mass spectrometer
OF	Oviduct fluid
PAGE	Polyacrylamide gel electrophoresis
PBS	Phosphate-buffered saline
PVP	Polyvinylpyrrolidone
REVIGO	Reduce and visualize gene ontology
SILAC	Stable isotope labelling by amino acids in cell culture
TCEP	Tris-(2-carboxyethyl)-phosphine
TCM	Tissue culture medium
TMT	Tandem mass tag
ULF	Uterine luminal fluid
UTP	Uridine-5'-triphosphate
ZP	Zona pellucida

8.2 Supplementary

The following Supplementary tables for all projects are available on the compact disc appended to this dissertation.

8.2.1 Supplementary tables Main project

Supplementary table 1: Full list of proteins identified in GV, MII and MII AD oocytes in all replicates with corresponding LFQ intensity values.

Supplementary tables 2 to 7: Significantly altered proteins in the comparison of GV and MII (2), GV and MII AD (3) and MII and MII AD (4) oocytes; proteins with significantly lower (5) or higher (6) abundance in both MII control and MII ActD-treated compared to GV oocytes; proteins significantly altered in opposite directions in MII and MII AD compared to GV oocytes (7).

Supplementary tables 8 to 12: Enriched biological processes for proteins higher or lower abundant in both MII and MII AD compared to GV according to STRING analysis (8); significantly enriched GO terms in the comparison of GV and MII (9), GV and MII AD (10) and MII and MII AD (11); Significantly enriched GO terms for proteins with higher abundance in MII compared to GV, which are not enriched in MII AD compared to GV (12).

Supplementary tables 13 to 15: Significantly enriched gene sets in the comparison of GV and MI (13), GV and MII AD (14) and MII and MII AD (15).

8.2.2 Supplementary tables Side project A

Supplementary table 1: Full list of proteins identified in ULF in all groups and replicates with corresponding LFQ intensity values.

Supplementary tables 2 to 4: Significantly altered proteins in the comparison of LFH and HFH (2), LFH and MBD (3) and HFH and MBD (4).

Supplementary tables 5 to 7: Significantly enriched gene sets in the comparison of LFH and HFH (5), LFH and MBD (6) and HFH and MBD (7).

Supplementary tables 8 to 10: Significantly enriched GO terms in the comparison of LFH and HFH (8), LFH and MBD (9) and HFH and MBD (10).

8.2.3 Supplementary tables Side project B

Supplementary table 1: List of annotation clusters and GO terms of abundance-altered proteins from both models according to the terms “biological process”, “molecular function” and “KEGG pathways.

Supplementary tables 2 to 7: Significantly altered proteins in the pairwise comparisons of the groups of the metabolic model and the genetic model.

Supplementary table 8: Full list of all identified proteins from the metabolic model with their respective LFQ intensities and their relative abundance.

Supplementary table 9: Full list of all identified proteins from the genetic merit model with their respective LFQ intensities and their relative abundance.

8.3 List of publications and conference contributions

8.3.1 Articles

Influence of metabolic status and genetic merit for fertility on proteomic composition of bovine oviduct fluid

Gegenfurtner, K., Fröhlich T., Kösters M., Mermillod P, Locatelli Y., Fritz S, Salvetti P., Forde N., Lonergan P., Wolf E., Arnold G.J.; Biol Reprod, 2019

Genetic merit for fertility alters the bovine uterine luminal fluid proteome

Gegenfurtner, K., Fröhlich T., Flenkenthaler F., Kösters M., Fritz S., Desnoes O., Le Bourhis D., Salvetti P., Sandra O., Charpigny G., Mermillod P., Lonergan P., Wolf E., Arnold G.J.; Biol Reprod, in press

8.3.2 Scientific talk

V International Conference on Analytical Proteomics, July 3 – 6, 2017, Caparica, Portugal

Influence of Metabolic Status and Genetic Predisposition on Proteomic Composition of Bovine Oviduct Fluids

8.3.3 Poster presentations

50. Jahrestagung Physiologie & Pathologie der Fortpflanzung und gleichzeitig 42. Veterinär-Humanmedizinische Gemeinschaftstagung, February 15 – 12, 2017, Martinsried, Germany

Der Einfluss des metabolischen Status und des Zuchtwerts für Fruchtbarkeit auf die Proteomzusammensetzung von boviner Oviduktflüssigkeit

Meyer K., Fröhlich T., Kösters M., Riedel E., Fritz S., Salvetti P., Forde N., Lonergan P-, Wolf E. and Arnold G.J.

V International Conference on Analytical Proteomics, July 3 – 6, 2017, Caparica, Portugal

Influence of Metabolic Status and Genetic Predisposition on Proteomic Composition of Bovine Oviduct Fluids

Meyer K., Fröhlich T., Kösters M., Fritz S., Salvetti P., Forde N., Lonergan P-, Wolf E. and Arnold G.J.

16th Human Proteome Organisation World Congress, September 17 – 21, 2017, Dublin, Ireland

Proteomic Analysis of the Impact of Metabolic Status and Genetic Predisposition on Oviduct Fluid Composition

Meyer K., Fröhlich T., Kösters M., Fritz S., Salvetti P., Forde N., Lonergan P-, Wolf E. and Arnold G.J.

44th Annual Conference of the IETS, January 13-16, 2018, Bangkok, Thailand

Influence of Metabolic Status and Genetic Merit for Fertility on Proteomic Composition of Bovine Uterine Luminal Fluid

Gegenfurtner K., Fröhlich T, Kösters M., Fritz S., Salvetti P., Forde N., Lonergan P-, Wolf E. and Arnold G.J.

8.3.4 Awards and travel grants

Poster award and travel grant: V International Conference on Analytical Proteomics, July 3 – 6, 2017, Caparica, Portugal

Influence of Metabolic Status and Genetic Predisposition on Proteomic Composition of Bovine Oviduct Fluids

Meyer K., Fröhlich T., Kösters M., Fritz S., Salvetti P., Forde N., Lonergan P-, Wolf E. and Arnold G.J.

Travel grant of the DGPF for 16th Human Proteome Organisation World Congress, September 17 – 21, 2017, Dublin, Ireland

Proteomic Analysis of the Impact of Metabolic Status and Genetic Predisposition on Oviduct Fluid Composition

Meyer K., Fröhlich T., Kösters M., Fritz S., Salvetti P., Forde N., Lonergan P-, Wolf E. and Arnold G.J.

8.4 Acknowledgments

Zunächst möchte ich mich herzlichst bei Herrn Dr. Georg Arnold und Herrn Dr. Thomas Fröhlich bedanken, die es mir ermöglicht haben, an dieser Arbeit zu forschen und mich mit zahlreichen Ideen und ihrem wissenschaftlichen Input und den konstruktiven Diskussionen unterstüzt haben. Außerdem möchte ich mich für die Möglichkeit bedanken, meinen Horizont auf zahlreichen Kongressen erweitern zu dürfen und für die immer angenehme Arbeitsatmosphäre in der Gruppe.

Mein herzlichster Dank gilt außerdem Frau Prof. Dr. Angelika Vollmar für die Betreuung meiner Doktorarbeit und für die Unterstützung bei allen Anliegen rund um die Promotion.

Desweiteren danke ich Herrn Prof. Dr. Eckhard Wolf für die Bereitschaft das Zweitgutachten für diese Dissertation anzufertigen und für die Hilfe und die schnellen Korrekturen bei allen Publikationen.

Ebenfalls möchte ich der Prüfungskommission, bestehend aus Frau Prof. Dr- Angelika Vollmar, Herrn Prof. Dr. Eckhard Wolf, Herrn Prof Dr. Franz Paintner, Herrn Prof. Dr. Wolfgang Frieß, Herrn Prof. Dr. Franz Bracher und Herrn PD Dr. Maik Dahlhoff für die Bereitschaft meine Arbeit zu bewerten danken.

Ein großer Dank geht auch an die Kooperationspartner innerhalb des FECUND-Projektes, dem Team von ALLICE/INRA und der School of Agriculture and Food, UCD, insbesondere Herrn Prof. Dr. Pat Lonergan für die gute Zusammenarbeit.

Vielen Dank auch an Erika und Kilian vom Moorversuchsgut Oberschleißheim, die mir bei Fragen zur IVP geholfen und die Medien zur Verfügung gestellt haben.

Ich möchte mich außerdem herzlich bei der AG Fröhlich und der AG Wolf bedanken. Vielen Dank an Miwako für die Hilfe bei allen praktischen Fragen, sowie Daniela für die Einführung in die IVP. Außerdem danke ich Lena und Eva und vor allem Jan, Max und Sepp für die schöne Zeit und die vielen über die Arbeit hinausgehenden Ausflüge. Mein besonderer Dank geht außerdem an Klaus und Flo, die mich auch in anstrengenden Phasen aufgemuntert und mit ihrer guten Laune angesteckt haben.

Besonderer Dank geht an meine Freunde und meine Familie. Danke, dass ihr mich in allen Phasen der Arbeit unterstützt habt. Ich danke meinen Geschwistern Simon und Lisa für ihre Unterstützung nicht nur während der Doktorarbeit. Vor allem meinen Eltern möchte ich für ihre Hilfe zu jeder Zeit danken, ohne die diese Arbeit nur schwer möglich gewesen wäre.

Zu guter Letzt danke ich meinem Mann Flo für unsere großartige Zeit zusammen. Vielen Dank, dass du mich auch in den stressigsten Phasen unseres Studiums und der Dokorarbeit unterstützt hast und ich mich immer auf dich verlassen kann.